74-63

1974

VOLUME I

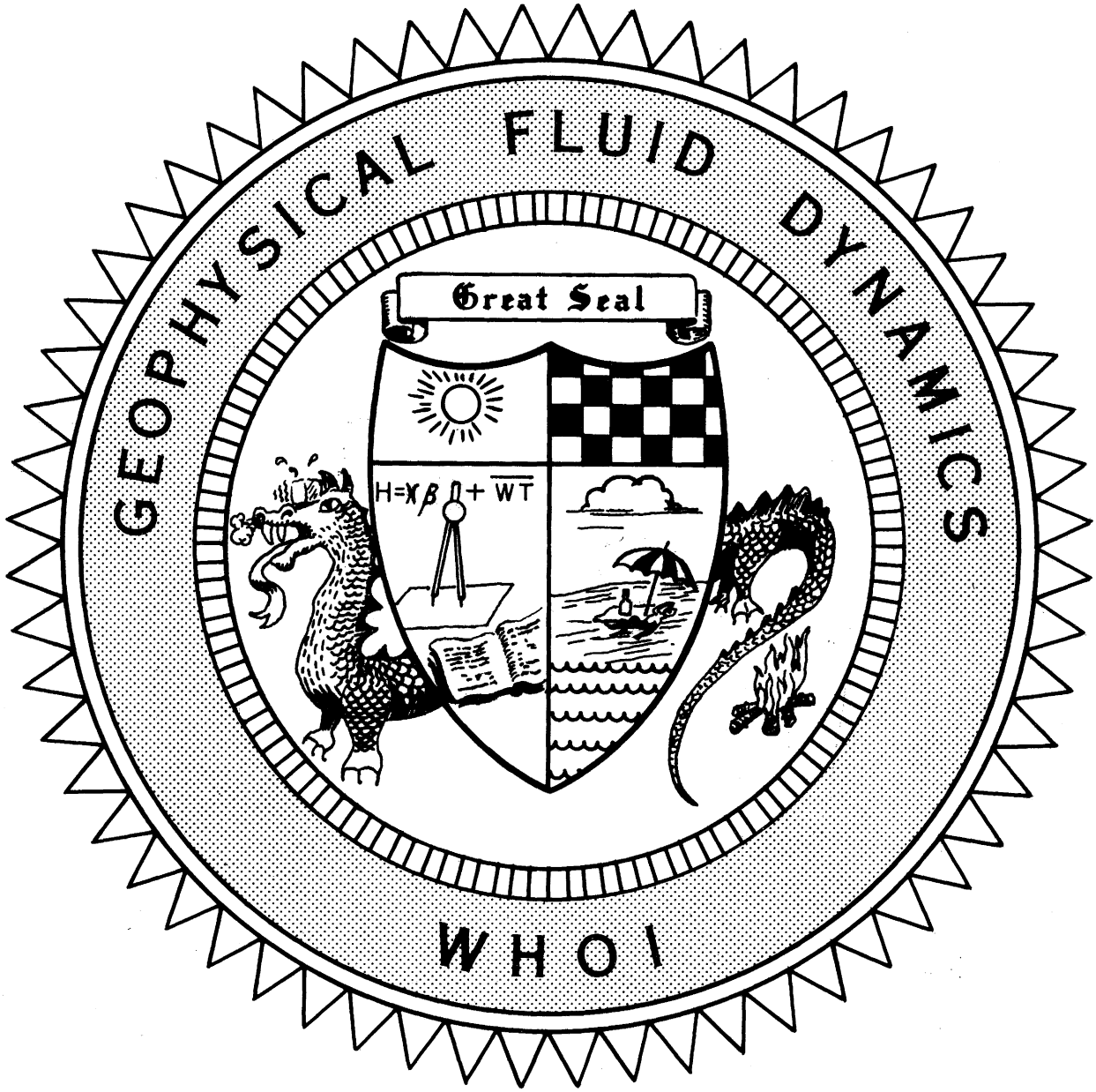

COURSE LECTURES

SEMINARS

ABSTRACTS

Notes on the 1974

Summer Study Program

in

GEOPHYSICAL FLUID DYNAMICS

at

THE WOODS HOLE OCEANOGRAPHIC INSTITUTION

Reference No. 74-63

Contents of the Volumes

Participants and Staff Members

Anderson, James	Stevens Institute
Bennett, John	NOAA, Rockville, Maryland
Bryan, Kirk	Princeton University
Busse, Friedrich H.	University of California at Los Angeles
Howard, Louis N.	Massachusetts Institute of Technology
Kamenkovitch, Vladmir M.	Institute of Oceanology, Moscow, U.S.S.R.
Keller, Joseph B.	Courant Institute of Mathematical Sciences, N.Y.U.
Luyten, James R.	Woods Hole Oceanographic Institution
Malkus, Willem V.R.	Massachusetts Institute of Technology
Needler, George	Bedford Institute, Dartmouth, Nova Scotia
Niiler, Pearn P.	Nova University
Rhines, Peter B.	Woods Hole Oceanographic Institution
Spiegel, Edward A.	Columbia University
Stern, Melvin E.	University of Rhode Island
Turner, J. Stewart	University of Cambridge, England
Veronis, George	Yale University
Welander, Pierre	University of Washington
Whitehead, John A.	Woods Hole Oceanographic Institution

Fellows

Armi, Laurence D.	Fluid Mechanics	Univ.of Calif. at Berkeley
Brink, Kenneth H.	G.F.D. & Phys.Oceanog.	Yale University
Buckley, Joseph R.	Phys.Oceanography	Univ.of British Columbia,Vancouver
Cane, Mark A.	Meteorology	Mass. Institute of Technology
Clarke, Allan J.	Appl.Math.& Oceanog.	Univ. of Cambridge, England
Hall, Robert E.	Physics	Univ.of Calif. at San Diego
Kennett, Rosemary G.	Fluid Dynamics	Calif. Inst. of Technology
Koenigsberg, Mark	Appl. Mathematics	Mass. Institute of Technology
Taylor, Karl	Geophysics	Yale University
Willebrand, Jürgen	Physics	Univ.of Kiel, Fed.Rep., Germany

Editor's Preface

This year the central topic was the general circulation of the oceans. Some of the basic ideas used in wind-driven and thermohaline studies were presented in the introductory course of lectures and simple models that have guided our thinking in the development of the topic were discussed. As part of the introductory lectures Peter Niiler developed a model of the mixed layer, exploring the reasoning and the parameterization behind the theories of this important boundary region at the surface of the ocean. Dennis Moore gave a careful account of transient flows in equatorial regions and showed how dynamical conditions on the eastern and western boundaries are satisfied by a superposition of planetary, Kelvin and Yanai waves. Peter Rhines concluded the series with a discussion of topographically induced low frequency motions. At the request of the students Joseph B. Keller gave a lecture on "Solution of Partial Differential Equations by Ray Theory".

As in years past notes of the lectures were taken by the students and are recorded in this first volume of the yearly report together with abstracts of the seminars by invited staff. For the most part the reports reflect the students' understanding and interpretation of the material.

Mary C. Thayer has assembled and typed all of the lectures. We are all especially grateful for her continued dedication and determination to keep the program running smoothly.

The National Science Foundation has supported the program and the Woods Hole Oceanographic Institution has made available to us its many facilities. We are thankful to these two institutions for their encouragement and support.

George Veronis

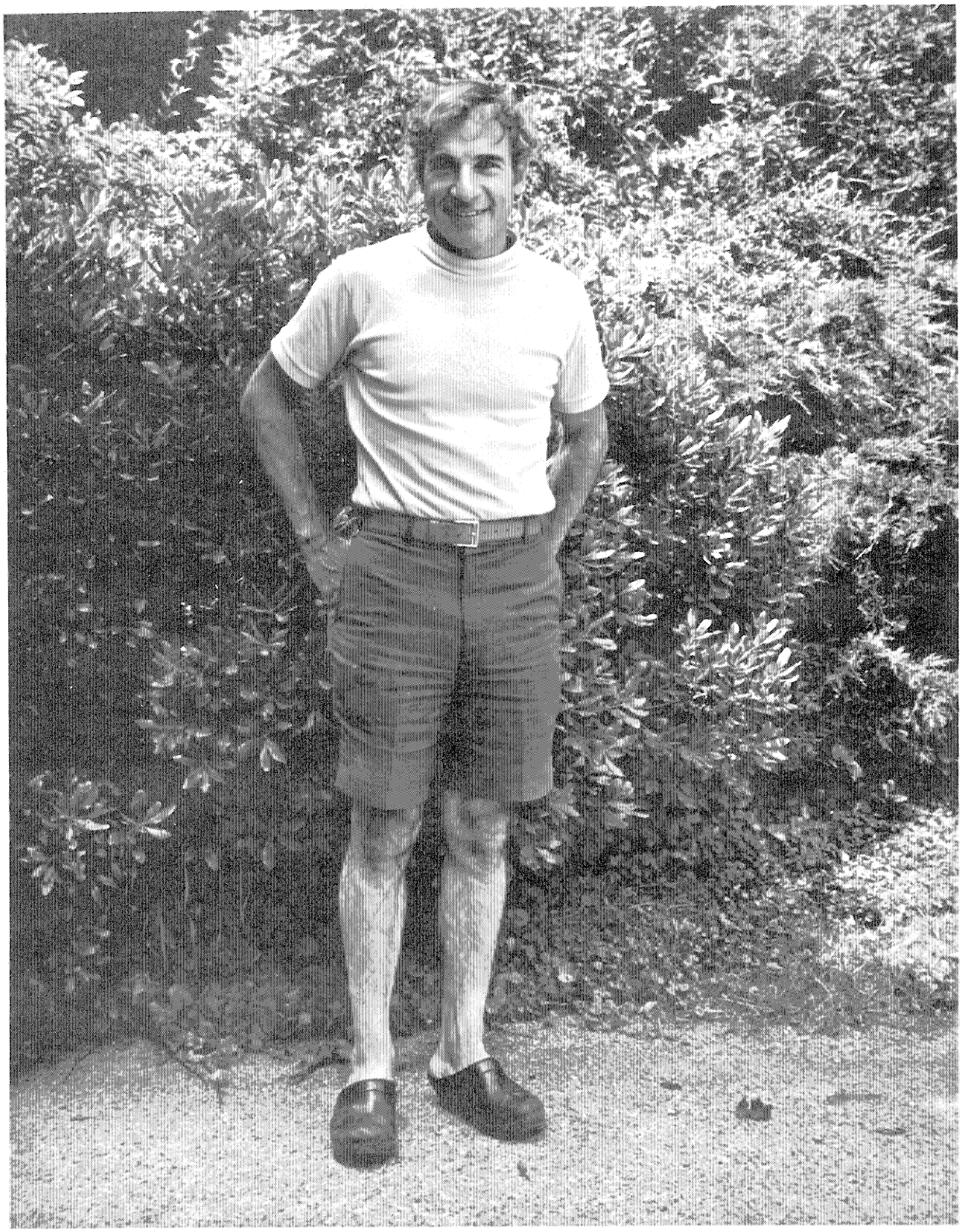

"Gorgeous George". 1974 Director and Lecturer.

CONTENTS OF VOLUME I

COURSE LECTURES

by

George Veronis
Yale University

LARGE SCALE OCEAN CIRCULATION

SEMINARS and ABSTRACTS

CONTENTS OF VOLUME I (continued)

CONTENTS OF VOLUME I (continued)

COURSE LECTURES

by

George Veronis
Yale University

LARGE SCALE OCEAN CIRCULATION

Lecture #1.

The large scale circulation of the oceans contains motions with horizontal scales from about 100 km to global scale. It may be separated into a mean pattern and transient motions with a time scale of the order of one month. In the following only the mean flow is considered.

The main driving forces are:

(1) Horizontal differences in heating and cooling at the sea surface from Pole to Equator. The scale is $\sim$ R (radius of Earth).

(2) Wind stress at the surface, with a horizontal distribution according to atmospheric circulation. The scale is somewhat, though not by an order of magnitude, smaller than R.

(3) Differences in evaporation minus precipitation, with scales less than or equal to those of wind. This force is not usually taken into account, its influence being about 10% of that of wind. Locally, it might be a more efficient mechanism (especially in the equatorial regions).

(4) Several oscillating driving mechanisms which are usually neglected are due to fluctuations, e.g. diurnal heating and cooling, tides. By the nonlinearity of the equations of motion these fluctuations produce a small but nonvanishing contribution to the mean motion.

(5) The horizontal gradients of water density due to convection. This mechanism is important, but has not yet been considered much.

The scales of motion are not always the same as the scales of the driving forces. Consider the abyssal circulation, which is driven mainly by heating and cooling, since wind stress and evaporation minus precipitation act only in shallow layers near the surface. Due to topography, the cooling in in the northern parts of the oceans is not of the same importance in the different oceans, the strongest cooling being in the North Atlantic. Since the oceans are connected, deep water may move from the North Atlantic to the other oceans. The horizontal scale of the abyssal circulation is therefore global, $>$ R.

The horizontal distribution of potential density at the ocean floor, referred to a level of 4 km depth, shows small but characteristic gradients in the north-south direction, and also around the Antarctic continent. The density differences are typically of the order 10^{-4} cgs units. For the maps the reader is referred to Lynn and Reid (1968). Similar features are found in the distribution of salinity and potential temperature, all indicating that the most important cooling and sinking takes place in the North Atlantic. However, if one chooses the sea surface rather than 4 km depth as a reference level, this feature completely vanishes, and no significant large scale differences are found. The reason for this different behavior is the dependence of the coefficients in the equation of state on temperature, salinity and pressure (see Veronis, 1973). It is important to remember that the potential density at surface reference level is not dynamically significant for the abyssal circulation.

From vertical profiles along a north-south line in the Atlantic Ocean nearly parallel to the east coast of America it turns out that in the Atlantic Ocean several masses of water have to be distinguished:

(a) Antarctic Bottom Water (AABW), which is formed in the Ross Sea. The AABW has the lowest temperature found in the ocean (-1.39°C).

(b) North Atlantic Deep Water (NADW), formed by cooling and sinking in a region south of Greenland.

(c) Antarctic Intermediate Water (AIW), formed at latitudes between 55° and 60°S. The AIW is colder, but less salty and less dense, than the NADW.

Several tracers may be used to detect these structures, e.g., salinity, oxygen, silica, suspended particulate matter. None of these is a completely conservative quantity, each showing characteristic deviations from the above-mentioned structure due to sources and sinks.

Salinity:

An intermediate maximum occurs, which is due to the Mediterranean outflow. The distribution near the surface shows the influence of the wind stress pattern; and also differences in evaporation minus precipitation.

Oxygen:

The main sink is biological comsumption, the source being at the surface. It is remarkable that the oxygen distribution shows not only the large scale structure but also considerable smaller scales, e.g., the Equatorial Undercurrent.

The sources for silica and suspended particulate matter are mainly at the bottom.

The wind stress pattern corresponds highly to the observed currents at the surface. It is interesting, however, that there are cases in which the density near the surface is not correlated to the wind, whereas the density at a greater depth is. The reason for this is not yet well understood.

Reference

Lynn, R.J. and J.L.Reid 1968 Characteristics and circulation of deep and abyssal waters. Deep-Sea Res. 15: 577-598.

Notes submitted by
Jürgen Willebrand

Lecture #2.

1. Equations of motion

Consider the equations of motion for an inviscid fluid, namely

$$\frac{d\underset{\sim}{v}}{dt} = \frac{1}{\rho}\nabla p - \nabla\phi + \text{ frictional forces,} \qquad (2.1)$$

$$\frac{d\rho}{dt} + \rho\nabla\cdot\underset{\sim}{v} = 0 \qquad (2.2)$$

where $$\frac{d}{dt} \equiv \frac{\partial}{\partial t} + \underset{\sim}{v}\cdot\nabla$$

and $-\nabla\phi$ is the body force, such as the gravitational force. The frictional forces are omitted in this lecture. To these equations must be added an energy equation, property (e.g. salinity) conservation laws and an equation of state which, for the ocean, is generally

$$\rho = \rho(p, T, S)$$

where S is the salinity. We now transform to a coordinate system rotating with the earth. Then (2.1) becomes

$$\frac{d\underset{\sim}{v}}{dt} + 2\underset{\sim}{\Omega} \wedge \underset{\sim}{v} = -\frac{1}{\rho}\nabla p - \nabla\Phi \tag{2.3}$$

where

$$\Phi \equiv \phi + \frac{1}{2}\Omega^2 R^2$$

and R is the magnitude of the component of $\underset{\sim}{r}$ perpendicular to the rotation axis.

2. Conservation of potential vorticity (Ertel, 1942)

Equation (2.3) may be written as:

$$\frac{\partial \underset{\sim}{v}}{\partial t} + (\nabla \wedge \underset{\sim}{v}) \wedge \underset{\sim}{v} + \nabla\left(\frac{1}{2}\underset{\sim}{v}\cdot\underset{\sim}{v}\right) + 2\underset{\sim}{\Omega} \wedge \underset{\sim}{v} = -\frac{1}{\rho}\nabla p - \nabla\Phi \,. \tag{2.4}$$

Consider a system governed by (2.4) and (2.2) with

$$\rho = \rho(s, p)$$

where s is some state property that is conserved, so that

$$\frac{ds}{dt} \equiv \frac{\partial s}{\partial t} + \underset{\sim}{v}\cdot\nabla s = 0. \tag{2.5}$$

Taking the curl of (2.4) gives the vorticity equation:

$$\frac{d\underset{\sim}{\omega}}{dt} - \underset{\sim}{\omega}\cdot\nabla\underset{\sim}{v} + \underset{\sim}{\omega}\nabla\cdot\underset{\sim}{v} = -\nabla\left(\frac{1}{\rho}\right) \wedge \nabla p$$

where

$$\underset{\sim}{\omega} = 2\underset{\sim}{\Omega} + \nabla \wedge \underset{\sim}{v} \,.$$

Eliminating $\nabla\cdot\underset{\sim}{v}$ from (2.2) and (2.4) gives

$$\frac{d}{dt}\left(\frac{\underset{\sim}{\omega}}{\rho}\right) - \frac{\underset{\sim}{\omega}\cdot\nabla\underset{\sim}{v}}{\rho} = \frac{\nabla\rho \wedge \nabla p}{\rho^3} \,. \tag{2.6}$$

The gradient of (2.5) gives

$$\frac{d}{dt}\nabla s + \nabla\underset{\sim}{v}\cdot\nabla s = 0 \,. \tag{2.7}$$

Adding the scalar product of (2.6) with ∇s to the scalar product of (2.7) with $\underset{\sim}{\omega}/\rho$ gives:

$$\frac{d}{dt}\left(\frac{\nabla s\cdot\underset{\sim}{\omega}}{\rho}\right) = 0.$$

$\nabla s\cdot\underset{\sim}{\omega}/\rho$ is called the potential vorticity.

3. Approximation of the earth by a sphere

The earth's shape is approximately that of an oblate spheroid, whose ellipticity is estimated to be 1/298. Since the oceans have an average depth

of 4 km which is small in comparison with the earth's radius of 66,000 km., the equilibrium shape of the earth is taken to be spherical. This produces an error of $3e/2 \simeq 1/200$ in the equations. (For justification, see Veronis (1973)).

4. Approximation of neglecting $2\Omega\cos\phi$ term (Phillips, 1966)

We use the equation of motion in the form:

$$\frac{\partial \underset{\sim}{v}}{\partial t} = \underset{\sim}{F} - \underset{\sim}{g} - \nabla\left(\tfrac{1}{2}\underset{\sim}{v}\cdot\underset{\sim}{v}\right) + \underset{\sim}{v}\wedge(\nabla\wedge\underset{\sim}{v}) - 2\,\underset{\sim}{\Omega}\wedge\underset{\sim}{v} \tag{2.8}$$

where $\underset{\sim}{F}$ denotes the frictional forces and the pressure gradient. We use spherical coordinates (r, λ, φ) where λ and φ denote the longitude and latitude respectively (with scale factors $h_\lambda = r\cos\varphi$, $h_\varphi = r$ and $h_r = 1$). This gives the exact angular momentum balance:

$$\frac{d}{dt}\left[r\cos\varphi\,(u + 2\Omega r\cos\varphi)\right] = r\cos\varphi\,F_\lambda .$$

The shallow system approximation is to introduce into all curvilinear operators the approximate scale factors:

$$h'_\lambda = a\cos\varphi, \quad h'_\varphi = Ra .$$

If (u, v, w) now denotes the eastward, northward and upward velocities, the components of the approximation to (2.8) are:

$$\frac{du}{dt} = F_\lambda + \left(2\Omega + \frac{u}{a\cos\varphi}\right)v\sin\varphi,$$

$$\frac{dv}{dt} = F_\varphi - \left(2\Omega + \frac{u}{a\cos\varphi}\right)u\sin\varphi,$$

$$\frac{dw}{dt} = F_z - g .$$

This gives the approximate angular momentum balance:

$$\frac{d}{dt}\left[a\cos\varphi\,(u + 2\Omega r\cos\varphi)\right] = a\cos\varphi\,F_\lambda .$$

We note that shallowness is not sufficient for the horizontal component of the Coriolis term to be neglected since stratification is necessary. A second argument for its neglect is now given (Veronis, 1973). The potential vorticity in spherical coordinates is

$$\begin{aligned}\frac{\nabla s\cdot\omega}{\rho} = {} & \frac{1}{\rho}\left\{\frac{1}{r\cos\varphi}\left[\frac{\partial v}{\partial r\lambda} - \frac{\partial}{\partial\varphi}\left(u\cos\varphi\right)\right] + 2\Omega\sin\varphi\right\}\frac{\partial s}{\partial r} + \\ & + \frac{1}{\rho}\left\{\frac{1}{r\cos\varphi}\left[\frac{\partial}{\partial r}(ru\cos\varphi) - \frac{\partial w}{\partial\lambda}\right] - 2\Omega\cos\varphi\right\}\frac{1}{r}\frac{\partial s}{\partial\varphi} + \\ & + \frac{1}{\rho}\left\{\frac{1}{r}\frac{\partial w}{\partial\varphi} - \frac{1}{r}\frac{\partial}{\partial r}(rv)\right\}\frac{1}{r\cos\varphi}\frac{\partial s}{\partial\lambda} .\end{aligned}$$

The horizontal component of the Coriolis term thus provides a negligible contribution to the potential vorticity in comparison with the vertical component when

$$2\Omega\cos\varphi\,\frac{1}{r}\,\frac{ds}{d\varphi} \ll 2\Omega\sin\varphi\,\frac{\partial s}{\partial r},$$

that is, when

$$L_z/L_H \ll \tan\varphi$$

where L_z and L_H are typical vertical and horizontal lengths respectively. For motions away from the Equator with scales $L_z < 1$ km and $L_H > 100$ km, say, then the horizontal component of the Coriolis term may be neglected.

5. Boussinesq Approximation (Malkus, 1964 G.F.D. Lectures)

We write the equation of motion as

$$\rho\left(\frac{d\underset{\sim}{v}}{dt} + 2\underset{\sim}{\Omega}\wedge\underset{\sim}{v}\right) = -\nabla p - \rho\,\underset{\sim}{g}. \tag{2.9}$$

For the ocean ρ varies between 1.02 and 1.07 gm cm^{-3} and hence is nearly constant. We approximate (2.9) by replacing ρ by the mean density, ρ_m, on the left-hand side, giving

$$\rho_m\left(\frac{d\underset{\sim}{v}}{dt} + 2\underset{\sim}{\Omega}\wedge\underset{\sim}{v}\right) = -\nabla p - \rho\,\underset{\sim}{g}.$$

The reference system, denoted by (ρ_a, p_a, T_a), is adiabatic and hydrostatically balanced, so that

$$\nabla p_a = -\underset{\sim}{g}\,\rho_a.$$

The salinity is taken to be constant (usually 34.85 parts/1000), so that

$$\rho_a = \rho_a(p_a, T_a).$$

The First Law of Thermodynamics gives:

$$\delta Q = T\,d\eta = C_p\,dT + T\left(\frac{\partial\eta}{\partial p}\right)_T dp$$

where η is the specific entropy and C_p is the specific heat at constant pressure, so that, for an adiabatic process,

$$\frac{dT_a}{dz} = -\frac{T}{C_p}\left(\frac{\partial\eta}{\partial p}\right)_T\frac{dp_a}{dz} = \frac{g\rho_a T_a}{C_p}\left(\frac{\partial\eta}{\partial p}\right)_T = -\frac{g\rho_a T_a}{C_p}\left(\frac{\partial v}{\partial T}\right)_p$$

where v is the specific volume. If $\alpha = v^{-1}\left(\partial v/\partial T\right)_p$ denotes the coefficient of thermal expansion, this becomes

$$\frac{\partial T_a}{\partial z} = -\frac{g\alpha T_a}{C_p}$$

For the ocean a typical value of the adiabatic temperature gradient, $\partial T_a/\partial z$, is -0.1^{o}km. Now suppose that

$$p = p_a + \tilde{p}, \quad \rho = \rho_a + \tilde{\rho}, \quad T = T_a + \theta.$$

Then the equation of motion is approximated by

$$\rho_m\left[\frac{d\underset{\sim}{v}}{dt} + 2\underset{\sim}{\Omega}\wedge\underset{\sim}{v}\right] = -\nabla\tilde{p} - \underset{\sim}{g}\tilde{\rho}.$$

Suppose now that

$$\rho = \rho(\theta, S, p)$$

where S is the salinity. The equation of state is linearized about the adiabatic reference state, so that

$$\tilde{\rho} = \rho - \rho_a = \left(\frac{\partial\rho}{\partial T}\right)_{p,S}\theta + \left(\frac{\partial\rho}{\partial s}\right)_{p,T}\tilde{S} + \left(\frac{\partial\rho}{\partial p}\right)_{T,s}\tilde{p} + \ldots$$

and thus

$$\frac{\tilde{\rho}}{\rho_a} \approx \frac{\tilde{\rho}}{\rho_m} = -\alpha\theta + \gamma\tilde{S} + K\tilde{p}$$

where

$$\alpha = \frac{1}{\rho_a}\left(\frac{\partial\rho}{\partial T}\right)_{p,S}, \quad \gamma = \frac{1}{\rho_a}\left(\frac{\partial\rho}{\partial s}\right)_{p,T}, \quad K = \frac{1}{\rho_a}\left(\frac{\partial\rho}{\partial p}\right)_{T,S}$$

Now $|g K\tilde{p}| << |d\tilde{p}|dz|$, so the equation of motion is finally approximated as

$$\rho_m\left(\frac{d\underset{\sim}{v}}{dt} + 2\underset{\sim}{\Omega}\wedge\underset{\sim}{v}\right) = -\nabla\tilde{p} + \underset{\sim}{g}\alpha\theta - \underset{\sim}{g}\gamma\tilde{S} \qquad (2.10)$$

Now consider the equation of continuity, (2.2). As above, the term $(\underset{\sim}{v}\cdot\nabla)\rho$ is much smaller than $\rho\nabla\cdot\underset{\sim}{v}$ and is thus neglected. For motions with characteristic time scales >> periods of acoustic waves, the term $\partial\rho/\partial t$ may be neglected and hence the continuity equation is approximated by

$$\nabla\cdot\underset{\sim}{v} = 0$$

The system is completed with the equations:

$$\frac{d\theta}{dt} = 0, \qquad \frac{d\tilde{S}}{dt} = 0.$$

It is noted that the use of $\tilde{\rho}$ instead of ρ can lead to difficulties (Veronis, 1973) which are best avoided by letting α and γ be functions of z in (2.10).

Notes submitted by
Rosemary G. Kennett

Lecture #3.

Scaling of the Equations of Motion

The equations of motion in spherical coordinates will be scaled for large scale motions. Cases for which the resulting scaled equations do not apply will violate some or one of the scaling assumptions.

With the Boussinesq assumption and after taking out the adiabatic field, the equations of motion in spherical coordinates become:

$$\frac{du}{dt} + \frac{uw}{r} - \frac{uv\tan\phi}{r} + 2\Omega\cos\phi\, w - 2\Omega\sin\phi\, v = -\frac{1}{\rho_n r}\frac{\partial \tilde{p}}{\partial \lambda}$$

$$\frac{dv}{dt} + \frac{vw}{r} + \frac{u^2\tan\phi}{r} + 2\Omega\sin\phi = -\frac{1}{\rho_m r}\frac{\partial \tilde{p}}{\partial \phi}$$

$$\frac{dw}{dt} - \frac{u^2+v^2}{r} - 2\Omega\cos\phi\, u = -\frac{1}{\rho_m}\frac{\partial \tilde{p}}{\partial r} - g\frac{\tilde{\rho}}{\rho_m}$$

$$\frac{d\tilde{\rho}}{dt} = 0$$

$$\frac{1}{r\cos\phi}\frac{\partial u}{\partial \lambda} + \frac{1}{r}\frac{\partial v}{\partial \phi} - \frac{v}{r}\tan\phi + \frac{\partial w}{\partial r} + \frac{2w}{r} = 0$$

with the definition: $\frac{d}{dt} = \frac{\partial}{\partial t} + \frac{u}{r\cos\phi}\frac{\partial}{\partial \lambda} + \frac{v}{r}\frac{\partial}{\partial u} + w\frac{\partial}{\partial r}$.

For the purpose of scaling, the variables and operators will be denoted as follows:

$$\frac{\partial}{\partial t} = \tau\Omega\delta_t,\ \frac{1}{a\cos\phi}\frac{\partial}{\partial \lambda} = \frac{1}{L}\delta_\lambda,\ \frac{1}{a}\frac{\partial}{\partial \phi} = \frac{1}{L}\delta_\phi,\ \frac{\partial}{\partial r} = \frac{1}{H}\delta_z,$$

$$u = Vu',\ v = Vv',\ w = Ww',\ \tilde{\rho} = (\Delta\rho)\rho,\quad \tilde{p} = (\Delta p)p$$

where the δ operators, prime quantities, ρ, and p are nondimensional and assumed of order one. Note that τ is a nondimensional factor in the time scaling and the different scaling for horizontal and vertical motions. Since: $r = a(1 + z/a)$ and, $z \leq H$, and $H/a < .001$: take $r \approx a$. Substitution then yields (dropping primes):

$$\tau\delta_t u + R\left[\underline{v}\cdot\nabla u + \eta\mu uw - \eta uv\tan\phi\right] + 2\mu\cos\phi\, w - 2\sin\phi\, v = -P\delta_\lambda p$$

$$\tau\delta_t v + R\left[\underline{v}\cdot\nabla v + \eta\mu vw + \eta u^2\tan\phi\right] + 2\sin\phi\, u = -P\delta_\phi p$$

$$\epsilon\mu\left[\tau\delta_t w + R(\underline{v}\cdot\nabla w - \eta u^2 - \eta v^2)\right] - 2\epsilon\cos\phi\, u = -P\delta_z p - Q\rho$$

$$\delta_\lambda u + \delta_\phi v - \eta v\tan\phi + 2\eta\mu w + \frac{\mu}{\epsilon}\delta_z w = 0$$

$$\tilde{\tau}\delta_t\rho + R\underline{v}\cdot\nabla\rho = 0$$

with the definition $\underline{v}\cdot\nabla = u\delta_\lambda + v\delta_\phi + \frac{\mu}{\epsilon}w\delta_z$.

The nondimensional parameters which appear are as follows:

$R = \frac{V}{\Omega L}$, the Rossby number which is a measure of the nonlinearity of the system

$\mu = \frac{W}{V}$, the ratio of vertical to horizontal velocity

$\epsilon = \frac{H}{L}$, the ratio of vertical to horizontal length scales

$\eta = \frac{L}{a}$, the ratio of the horizontal length scale to the earth's radius

$Q = \frac{gH}{V\Omega L} \frac{\Delta\rho}{\rho_m}$, a ratio of frequencies squared

and $P = \Delta P / \Omega V L \rho_m$, a scaling of the pressure differences with rotational forces.

Two assertions are now made: The first is that $\epsilon << 1$; the second is that $\frac{\mu}{\epsilon} \leq 1$, or the vertical divergence is upper bounded by each horizontal divergence, $W \leq V \frac{H}{L}$. Formally, take $\frac{\mu}{\epsilon} = 1$.
The following result:

1. From the vertical equation of motion we get hydrostatic balance: $P \sim Q$ and $\Delta P \sim g \Delta \rho H$.

2. $\underline{V} \cdot \nabla = u \delta_\lambda + v \delta_\phi + w \delta_z$. The vertical convection is the same magnitude as the horizontal convection.

3. All metric terms involving w are at most $O(\epsilon)$.

4. The horizontal component of the Coriolis terms is $O(\epsilon)$.

With the ordering by Coriolis acceleration implied in scaling the pressure and with the restriction P = Q = 1, the equations, to $O(\epsilon)$, are:

$$\tau \delta_t u + R(\underline{V} \cdot \nabla u - \eta u v \tan\phi) - 2 \sin\phi v = -\delta_\lambda p$$

$$\tau \delta_t v + R(\underline{V} \cdot \nabla v - \eta u^2 \tan\phi) + 2 \sin\phi u = -\delta_\phi p$$

$$\delta_z p = -\rho$$

$$\tau \delta_t \rho + R \underline{V} \cdot \nabla \rho = 0$$

$$\delta_\lambda u + \delta_\phi v - \eta v \tan\phi + \delta_z w = 0$$

Three additional scalings of these equations are now considered.

Small scale motions: $\eta = \frac{L}{a} \ll 1$.

Swallow eddies are an example of this class of motions; typical magnitudes are

$$L \sim 10^2 \text{km.} \qquad H \sim 10^5 \text{cm.} \qquad V \leq 10^2 \text{cm/sec.}$$

$$\tau \leq 10^{-1}.$$

The nondimensional parameters associated with the upper limit have the values

$$Q \sim P \sim 1, \qquad R \sim 10^{-1}, \qquad \eta = 10^{-2}$$

To avoid the complication of the spherical character of the earth an expansion is made about some latitude, ϕ_0 .

$$\phi = \phi_0 + \phi' = \phi_0 + (y/a) = \phi_0 + \eta y$$

Then expanding $\sin\phi$ and $\cos\phi$ about ϕ_0 yields

$$\sin\phi = \sin\phi_0 \left(1 + \eta y' \cot\phi + \dots\right)$$

$$\cos\phi = \cos\phi_0 \left(1 - \eta y' \tan\phi + \dots\right)$$

we can write

$$\frac{1}{a\cos\phi}\frac{\partial}{\partial\lambda} \simeq \frac{1+\eta y'\tan\phi_0}{a\cos\phi_0}\frac{\partial}{\partial\lambda} \equiv \left(1+\eta y'\tan\phi_0\right)\frac{\partial}{\partial x'}$$

$$\therefore \delta_\lambda \equiv \left(1+\eta y'\tan\phi_0\right)\frac{\partial}{\partial x'}$$

$$\frac{1}{a}\frac{\partial}{\partial\phi'} \equiv \frac{1}{L}\frac{\partial}{\partial y'}; \quad \partial_y = \frac{\partial}{\partial y'}, \quad \partial_z = \frac{\partial}{\partial z}, \quad \delta_t = \frac{\partial}{\partial t}$$

To lowest order in η the equations of motion are:

$$\tau\frac{\partial u}{\partial t} + R\underline{v}\cdot\nabla u - fv = -\frac{\partial p}{\partial x}$$

$$\tau\frac{\partial v}{\partial t} + R\underline{v}\cdot\nabla v + fu = -\frac{\partial p}{\partial y}$$

$$\frac{\partial p}{\partial z} = -\rho$$

$$\tau\frac{\partial \rho}{\partial t} + R\underline{v}\cdot\nabla\rho = 0$$

$$\frac{\partial u}{\partial x} + \frac{\partial v}{\partial y} + \frac{\partial w}{\partial z} = 0$$

where $f = 2\sin\phi_0 = \text{const.}$ (traditionally $f = 2\Omega\sin\phi_0$)

This set of equations is called an f-plane system.

Intermediate scale motions $\eta < 1$.

Wind-driven gyres are an example of this class of motions. As for small scale motions (f-plane), expand ϕ about some latitude ϕ_0. Compare the terms $\delta_\phi v$ and $\eta v \tan\phi$ in the continuity equation

$$\delta_\phi v = \frac{\partial v}{\partial y}, \quad \eta v \tan\phi = \eta \tan\phi_0 v + \frac{\eta^2 y' v}{\cos^2\phi_0} + \cdots$$

The conditions $\eta < 1$ and $\phi_0 < 45^\circ$ (strictly $\phi_0 << 45^\circ$) imply that the metric term may be neglected to lowest order. With the Coriolis parameter written as

$$2\sin\phi\, v = 2\sin\phi_0 v\left(1 + \eta y' \cot\phi_0 + \cdots\right)$$

The system of equations is the same as for the f-plane system with:

$$f = 2\sin\phi_0 + 2\eta\cos\phi_0\, y' \equiv f_0 + \beta y'$$

where $\beta = 2\frac{L}{a}\cos\phi_0$ (traditionally $\beta = \frac{2\Omega\cos\phi_0}{a}$).

This set of equations is called a β-plane system. Note that toward the poles in the continuity equation the spherical effects are no longer small compared with the variation of the Coriolis parameter, and the β-plane system must be used with caution.

Global scale motions: $\eta \sim 1$.

The global circulation is an example of this class; typical magnitudes are:

$$L \sim a = 6.4 \times 10^8 \text{cm}, \quad V \sim 1 \text{ cm/sec} \quad \text{and} \quad R = 10^{-5}$$

For very long-period motions, take $\tau = 0$. The use of R = 0 simplifies the equations of motion to:

$$L\sin\phi\, v = \frac{1}{\cos\phi}\frac{\partial p}{\partial \lambda}$$

$$L\sin\phi\, u = -\frac{\partial p}{\partial \phi}$$

$$\frac{\partial p}{\partial z} = -\rho g$$

$$\frac{d\rho}{dt} = 0 \left(\frac{d}{dt} \equiv \underset{\sim}{v}\cdot\nabla\right)$$

$$\frac{1}{\cos\phi}\left[\frac{\partial u}{\partial \lambda} + \frac{\partial}{\partial \phi}(v\cos\phi)\right] + \frac{\partial w}{\partial z} = 0$$

Notes submitted by
Laurence D. Armi

Lecture #4.

In the last lecture, sets of working equations were presented for large scale oceanic flows under various circumstances. Today's lecture deals with preliminary discussions of two important phenomena related to these equations, and then progresses to a global circulation calculation.

1) The phenomena

A) Geostrophic flow

This is a process fundamental to one understanding of many oceanographic phenomena which arises from the balance of Coriolis and pressure gradient accelerations which were derived in the last lecture. A simple thought experiment is given as a means of demonstrating geostrophy in a conceptually simple situation.

Consider a cylindrical tank containing homogeneous fluid rotating about its axis with angular velocity Ω . The system is at a state of rigid-body rotation. This is system Number One.

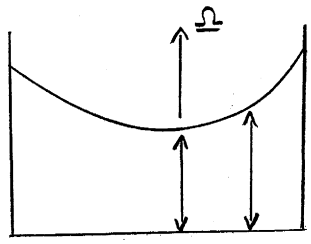

The relevent equations are:

$$\frac{1}{\rho}\frac{\partial p_1}{\partial z} = -g$$

$$\frac{1}{\rho}\frac{\partial p_1}{\partial r} = \Omega^2 r,$$

which yield: $h_1(r) = h_0 + \frac{\Omega^2 r^2}{2g}$.

Now consider system Number Two, which is identical except that it has angular velocity $\Omega + \Delta\Omega$.

$$\frac{1}{\rho}\frac{\partial p_2}{\partial z} = -g$$

$$\frac{1}{\rho}\frac{\partial p_2}{\partial r} = (\Omega + \Delta\Omega)^2 r$$

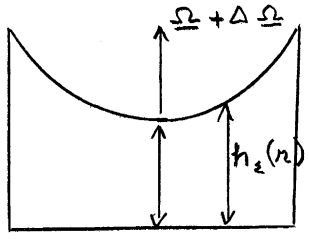

$$h_2(r) = h_{02} + \frac{\Omega^2 r^2}{2g}$$

Our third system is this: the tank and all the fluid in it rotates at angular velocity Ω , except for an annulus of fluid which is, by some means, kept at angular velocity $\Omega + \Delta\Omega$. We have

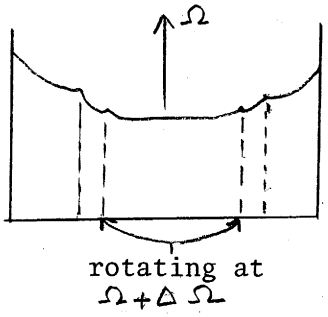

The relative velocity in the annulus is the difference in some sense between the above two systems. We define

$$\Delta p = p' = p_2 - p_1$$

and subtract the horizontal momentum equations of the above two systems.

$$\frac{1}{\rho}\frac{\partial}{\partial r}(\Delta p) = 2\Omega\Delta\Omega r + (\Delta\Omega)^2 r$$

Now if

$$\Delta\Omega \ll \Omega \quad \text{(thus drop the } (\Delta\Omega)^2 \text{ term)}$$

and we say

$$\Delta\Omega r = v',$$

we obtain

$$\frac{1}{\rho}\frac{\partial p'}{\partial r} = 2\Omega v',$$

which is the geostrophic balance. We see this is a situation where the pressure gradients are compensated by a normal flow. In Cartesian coordinates it becomes:

$$\frac{1}{\rho}\frac{\partial p}{\partial x} = 2\Omega v$$

$$\frac{1}{\rho}\frac{\partial p}{\partial y} = -2\Omega u$$

An immediate result of geostrophy is the thermal wind equations. If we write the equations for the ocean:

$$f\rho v = \frac{1}{a\cos\phi}\frac{\partial p}{\partial \lambda}$$

$$f\rho u = -\frac{1}{a}\frac{\partial p}{\partial \phi}$$

$$\frac{\partial p}{\partial z} = -g\rho$$

(where $f = 2\Omega\sin\phi$), we readily obtain:

$$f\frac{\partial}{\partial z}(\rho v) = -\frac{g}{a\cos\phi}\frac{\partial \rho}{\partial \lambda}$$

$$f\frac{\partial}{\partial z}(\rho u) = \frac{g}{a}\frac{\partial \rho}{\partial \phi}.$$

These equations are extensively used in observational oceanography for obtaining vertical velocity profiles, to within a constant added term, from hydrographic data.

An example of their use is motivated by John Bennett's talk. Consider Lake Ontario where warming occurs preferentially on the edges at any given level:

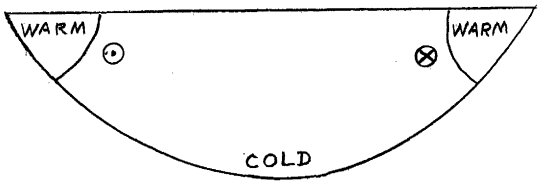

⊗ flow into page

⊙ flow out of the page

B) Ekman layers

Consider a system infinite in x and y, with fluid in the lower half plane. A stress acts on the surface, $z = 0$, in the x direction (the orientation does not matter). Finally, we assume the flow is steady, and that the density is constant (these two assumptions are not necessary). We have the boundary condition:

$$\nu \left(\frac{\partial u}{\partial z}\right)_{z=0} = \tau = \text{constant, and } \left(\frac{\partial v}{\partial z}\right)_{z=0} = 0$$

and the equations:

$$-2\Omega v = \nu \frac{\partial^2 u}{\partial z^2}$$

$$2\Omega u = \nu \frac{\partial^2 v}{\partial z^2}$$

$$\frac{\partial w}{\partial z} = 0$$

thus $w = \text{constant} = 0$,

since $w = 0$ at the surface. We also specify that the velocities, u and v, vanish at great depth. Now define

$$\phi = u + i v,$$

so, by solving,

$$\phi = \phi_0 e^{\sqrt{2}\, i z/\delta},$$

where

$$\delta = \sqrt{\frac{\nu}{\Omega}}$$

is the Ekman depth, an internal scale of the system. By using the stress boundary conditions we get

$$u' = \frac{\tau}{2\sqrt{\nu\Omega}} e^{z/\delta}\left(\cos z/\delta + \sin z/\delta\right)$$

$$v = \frac{\tau}{2\sqrt{\nu\Omega}} e^{z/\delta}\left(\sin z/\delta - \cos z/\delta\right).$$

We see that

$$(u)_{z=0} = -(v)_{z=0} = \frac{\tau}{2\sqrt{\nu\Omega}},$$

so that the surface velocity is directed 45° to the right of the applied stress.

This Ekman phenomenon is important in understanding frictional interactions in rotating systems, although it is not always applicable in exactly the form derived here. For the ocean, we would have predicted a very thin layer using molecular viscosity. A more-often-used approach is to use an eddy viscosity for ν, but this is messy and not constant with depth. To handle this, consider:

$$-2\Omega v = \frac{\partial}{\partial z}\tau^x$$

$$2\Omega u = \frac{\partial}{\partial z}\tau^y,$$

and define

$$\int_{-\infty}^{0} v\, dz \equiv V$$

$$\int_{-\infty}^{0} u\, dz \equiv U$$

$$2\Omega V = \tau_o^x$$

$$2\Omega U = 0$$

where $\tau_o^y = 0$.

From this we readily see that the depth-integrated transport goes off at 90° to the right of the applied stress.

We have one note to add on scales. In the last lecture, we assumed:

$$\epsilon = \frac{H}{L} \ll 1.$$

We now have a vague (due to turbulent viscosity) Ekman depth, which assumes:

$$\frac{\delta}{H} \ll 1,$$

so we must have

$$\frac{\delta}{L} \ll 1$$

also.

Now consider an upper layer of the ocean. We have a diagram where solid arrows are applied stresses and double arrows represent transports. We draw in Ekman transports as our above results indicate them.

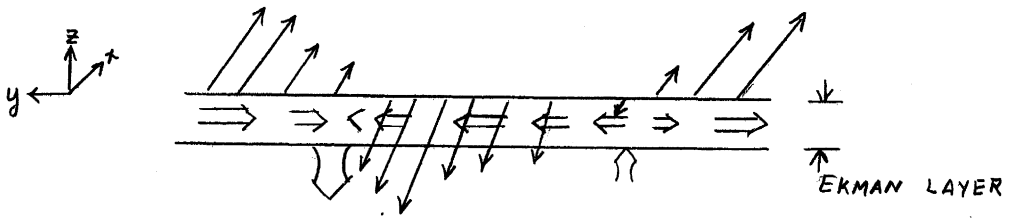

The curved double arrows represent the vertical transports into or out of the Ekman layer demanded by mass conservation. These can be derived by means of integrating the continuity equation:

$$\int_{-\infty}^{0} \frac{\partial w}{\partial z}\, dz = -w\Big|_{z=-\infty} = -\int_{-\infty}^{0} \left(\frac{\partial u}{\partial x} + \frac{\partial v}{\partial y}\right) dz.$$

It thus becomes clear that the Ekman layer provides a vertical velocity condition on the top of the interior region of the fluid.

II) A global scale ocean circulation calculation - the thermocline.

The discussion is based on a 1971 paper by Welander (J.Mar.Res., 29: 60-68), where he studies an inviscid, non-conducting, steady system. The working equations, with the Boussinesq approximation already made are:

$$\rho\left(\underline{v}\cdot\nabla\underline{v} + 2\underline{\Omega}\times\underline{v}\right) = -\nabla p - \rho\nabla\Phi \qquad (1)$$

$$\nabla\cdot\underline{v} = 0 \qquad (2)$$

$$\underline{v}\cdot\nabla\rho = 0 \qquad (3)$$

The potential vorticity of the system,

$$P = \frac{(2\underline{\Omega} + \nabla\times\underline{v})\cdot\nabla\rho}{\rho}$$

is conserved along a stream line. The ρ in the denominator is not really needed, since it is conserved along a stream line by Eq. (3). We also derive:

$$\underline{v}\cdot\nabla\left(\rho\frac{\underline{v}\cdot\underline{v}}{2} + p + \rho\phi\right) = \underline{v}\cdot\nabla B = 0,$$

which states that the Bernoulli function, B, is conserved along a stream line. Thus we have three conserved quantities: ρ , P and B.

Now, we can consider a stream line as an intersection of two surfaces in space:

$$\psi = \text{const.} \qquad \text{and} \qquad \lambda = \text{const.}$$

thus

$$\rho = \rho(\psi, \lambda), \quad P = P(\psi, \lambda) \text{ and } B = B(\psi, \lambda)$$

From this it is clear that

$$P = F(B, \rho),$$

a very general result which is about as much as can be said from what we know here.

Now we restrict our attention to (slow) oceanic flow below the Ekman frictional layer. That is:

$$R << 1,$$

so that:

$$\rho f \hat{k} \times \underline{v} = -\nabla p - \underline{g}\rho$$
$$\nabla \cdot \underline{v} = 0$$
$$\underline{v} \cdot \nabla \rho = 0$$

We then derive:

$$P = 2\Omega \sin\phi \frac{\partial \rho}{\partial z}$$
$$B = p + \rho g z.$$

What is left to work with is this:

$$\sin\phi \frac{\partial \rho}{\partial z} = F(\rho, p + \rho g z)$$
$$\frac{\partial p}{\partial z} = -g\rho.$$

In order to get a solution now, we need ρ_o and p_o (ρ and p defined on some surface) and a form for F.

As a special case, we consider

$$P = a\rho - bB + c.$$

We readily derive

$$\sin\phi \frac{\partial^2 \rho}{\partial z^2} = (a - bgz) \frac{\partial \rho}{\partial z},$$

which leads to

$$\frac{\partial \rho}{\partial z} = C_1(\lambda, \phi) e^{(az - bgz^2/2)/\sin\phi}$$

and

$$\rho = \rho_o(\lambda, \phi) + C(\lambda, \phi) \int_0^z e^{-(\zeta + z_0)^2/D\sin\phi} d\zeta.$$

The constants are:

$$z_0 = \frac{a}{bg}$$

$$D = \frac{2}{bg}$$

$$C = C_1 e^{a^2/2bg}$$

Now we are in a position to look at the nature of the solution. There are two vertical scales:

1) $z_0 = \frac{a}{bg}$

If $\frac{a}{b} > 0$, the density profile is exponential-like.

If $\frac{a}{b} < 0$, the density profile will have an inflection point at z_0 .

2) $z = -\sqrt{D \sin\phi}$

We need to have $\frac{\sin\phi}{b} > 0$, and then there will be an appropriate decay at depth.

This scale , z , represents a thermocline thickness.

Welander, in his paper, used data assembled by Reid for the South Pacific to get $\rho_0(\lambda, \phi)$, and $C(\lambda, \phi)$, as well as the scale depths.

The results are sketched here. The qualitative agreement with observed data appears reasonable, and it does show a bunching of constant-density lines near the equator similar to the observed. The breakdown of the general agreement in the southern part of the ocean is no surprise, as it is due to the circumpolar current which is not accounted for in the model.

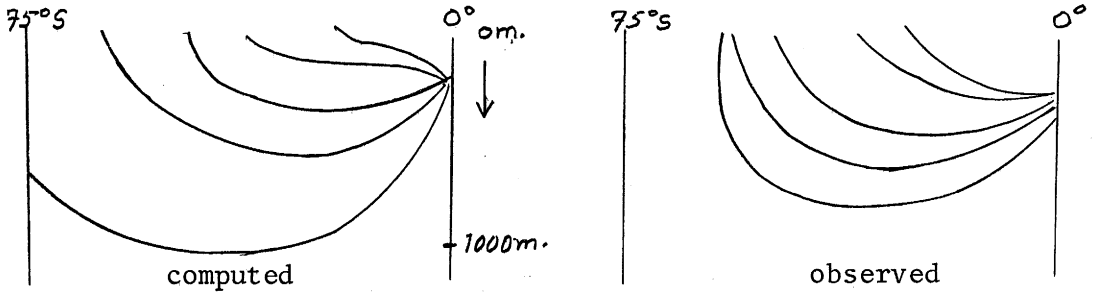

It is possible to compute a velocity structure according to this model, since along the plane where ρ_0 , and C are calculated we have

$$\sin\phi \left(\frac{\partial \rho}{\partial z}\right)_0 = a\rho_0 - bp_0 + C ,$$

and p_0 can be calculated, leading to a velocity structure. Welander did not do this.

Notes submitted by
Kenneth H. Brink

Lecture #5. Analysis of a Diffusive Thermocline Model

The main difference between this model and the ideal fluid model of Welander (1971a) is in the introduction of diffusive processes. The aim is to determine the role of these processes in the maintenance of the thermocline. This model, however, does not provide a severe test as will be shown later.

The basic equations are:

$$f\,\underset{\sim}{k} \times \underset{\sim}{v} = -\nabla P - g\rho\,\underset{\sim}{k} \tag{1}$$

$$\nabla \cdot \underset{\sim}{v} = 0 \tag{2}$$

$$\underset{\sim}{v} \cdot \nabla \rho = k\rho_{zz} \tag{3}$$

$$\text{where } P = \frac{p}{\rho_m}, \quad \rho = \frac{\tilde{\rho}}{\rho_m} \tag{4}$$

Vertical diffusion in this system is introduced by Eq.3. Horizontal diffusion is ignored. The justification for this is that the sea surface is heated and the heat so introduced is carried downward by turbulent transport. Thus, at least in the thermocline region, vertical diffusion is much more important than horizontal.

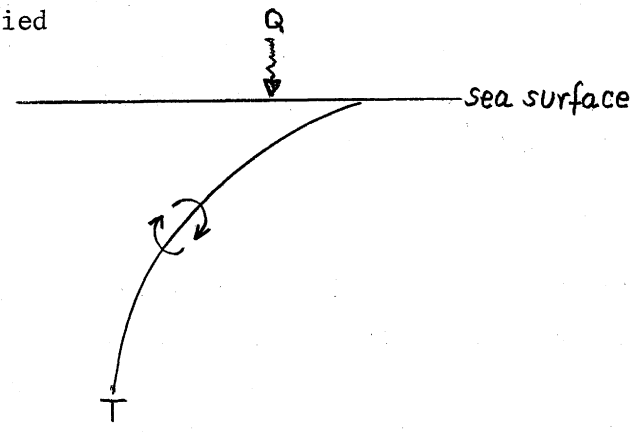

When Eqs. 1-3 are expressed in spherical coordinates, the following equations result. From Eq.1, the momentum equations are:

$$u = -\frac{1}{fa} P_\varphi \tag{5}$$

$$v = \frac{1}{fa\cos\varphi} P_\lambda \tag{6}$$

$$\rho = -\frac{1}{g} P_z \tag{7}$$

The continuity equation (2) becomes:

$$\frac{u_\lambda}{a\cos\varphi} + \frac{v_\varphi}{a} + w_z = 0 \tag{8}$$

The diffusion Eq. 3 becomes:

$$w = \frac{1}{\rho_z}\left[K\rho_{zz} - \frac{u}{a\cos\varphi}\rho_\lambda - \frac{v}{a}\rho_\varphi\right] \tag{9}$$

Substituting P for ρ using Eq. 7 in Eq. 9, then using Eqs. 5 and 6, the continuity equation may be rewritten as an equation for P.

$$K\sin\varphi\cos\varphi\left[P_{zz}P_{zzzz} - P_{zzz}^2\right] = P_\varphi\left[P_{zzz}P_{\lambda z} - P_{zz}P_{\lambda zz}\right] + \\ + P_\lambda\left[P_{zz}P_{\varphi zz} - P_{zzz}P_{\varphi z} + \cot\varphi P_{zz}^2\right] \tag{10}$$

where $K = 2\Omega a^2 K$

Needler (1967) arrived at this equation in nondimensionalized form using the variables

$$P = \overline{P}P'; \quad z = Hz' \qquad K = \frac{2\Omega K a^2}{\overline{P}H^2} \tag{11}$$

The dimensional Eq. 10 will, however, continue to be used here.

Welander (1959), arrived at a simplified form of Eq. 10 by using a variable M, essentially the vertical integral of P with the barotropic mode included. His equation was:

$$K\sin 2\varphi M_{zzzz} + \cot\varphi M_\lambda M_{zzz} + M_\lambda M_{\varphi zz} - M_{\varphi z}M_{\lambda zz} = 0 \tag{12}$$

The solutions to (12) are no simpler than the solutions to (10), so (10) will be used in the following analysis.

Since the model is geostrophic and hydrostatic, what can be done with boundary conditions is limited. On the surface, an Ekman layer may be introduced to give a density distribution at its base and, coupled with a known wind stress, a vertical velocity into the interior. On the bottom zero normal velocity and zero heat flux conditions could be applied. Available solutions are not general enough to satisfy all these conditions.

Similarity theory has provided two solutions to Eq. 10. The restrictions imposed by this technique may be lessened by more general forms of the solutions.

For the similarity solutions, the following substitution was tried:

$$P(\lambda, \varphi, z) = q_f(\lambda, \varphi)\, G(\eta) \tag{13}$$

where $\eta = z\, k(\lambda, \varphi)$

Surface boundary conditions then correspond to conditions at G(0).

Substitution of (13) into (10) gives:

$$\begin{aligned} k \sin\varphi \cos\varphi K^3 \left[G'' G^{IV} - G'''^2\right] &= J(k, q_f) G' G G''' + \\ &+ (\cot\varphi\, k\, q_{f\lambda} - 2J) G G'' G'' - J_\eta G' G' G''' + \\ &+ (\cot\varphi\, q_f k_\lambda + J) G' G'' G'' \end{aligned} \tag{14}$$

where J(k,q) is the Jacobean of k and q with respect to λ and φ.

To solve this equation it is necessary to remove the λ and φ dependence by choosing k and q as follows:

$$k = (\sin\varphi)^m \left[\lambda + E(\varphi)\right]^n \tag{15a}$$

$$q_f = (\sin\varphi)^{2m+2} \left[\lambda + E(\varphi)\right]^{-2n+1} \tag{15b}$$

When these are substituted into Eq. 14, the following equation results:

$$\begin{aligned} K\left(G^{IV} G'' - G'''^2\right) &= (2n-m) G G' G''' + (2m - 2n + 1) G G''^2 - \\ &- (2n-m)\eta G'^2 G''' + (3n-m)\eta G' G''^2 \end{aligned} \tag{16}$$

This is solved, as in Koslov (1966) by first balancing the coefficients of η.

$$\left\{\frac{3n-m}{2n-m} G''^2 - G' G'''\right\} G' = 0 \tag{17}$$

If G' = 0, then G = constant, implying a barotropic field which is not of interest here. For the other solution, if G' ≠ 0 and

$$\frac{3n-m}{2n-m} \neq 0, 1, \infty \tag{18}$$

then

$$G = \alpha (\eta + \eta_0)^{\frac{m}{n}-1} + \theta \tag{19}$$

For compactness now let $\eta + \eta_0 = \zeta$, $\frac{m}{n} - 1 = \omega$.

The remaining terms of Eq.(16) are:

$$K\left(G^{IV}G'' - G'''^{2}\right) = (2n-m)\,G\,G'\,G''' + (2m-2n+1)\,G\,G''\,G'' \tag{20}$$

Putting (19) into (20) gives:

$$(m-2n)\left\{\frac{m-3n}{n}K\zeta^{-2} - (m-3n)(\alpha\zeta^{\omega}+\theta) + (2m-2n+1)(\alpha\zeta^{\omega}+\theta) = 0\right\} \tag{21}$$

A solution can be found for $m = 2n$, corresponding to zero horizontal advection.

If $m \neq 2n$, then:

$$\frac{m-3n}{n}K\zeta^{-2} + (m+n+1)(\alpha\zeta^{\omega}+\theta) = 0 \tag{22}$$

Balancing powers of ζ gives either:

$$\omega = -2\,, \quad \theta = 0 \tag{23a}$$

or

$$m = 3n\,, \quad \omega = 0 \tag{23b}$$

Equation (23b) corresponds to a barotropic field.

Putting (23a) into (19) gives:

$$G = \frac{4K}{(\eta+\eta_0)^2} \tag{24}$$

This form of solution was guessed at by Fofonoff (1962).

If, in Eq.(17), $\frac{3n-m}{2n\mp m} = 1$,

then $G''^{2} - G'\,G''' = 0$ (25)

yielding a solution:

$$G = a + b\,e^{c\eta} \tag{26}$$

Putting this result into (20) gives m = -1.

It is also possible to obtain this result from the conservation of potential vorticity.

It can be shown that this exponential behaviour follows from:

$$\sin\varphi\,\frac{\partial\rho}{\partial z} = c\rho \tag{27}$$

with no Bernoulli function as in Welander (1971). The solution to (27) is:

$$\rho = b e^{cz/\sin\varphi} \tag{28}$$

Note that this solution, of the same form as Eq.(26), comes from a completely conservative system, - with no diffusion at all.

Now that the form of the solutions has been found, it is necessary to add the scale depth from observations. One approach is to use the thermal wind equations which give a thermocline depth that is more or less realistic.

The inverse square solution (Eq.22) was arrived at by Fofonoff (1962) and exponential one (Eq.26) by Welander (1959) and Blandford (1965). In the first case the surface boundary conditions must be fitted to the arbitrary mathematical forms of k and q (Eqs.15). In the exponential form the surface density field may be exactly specified.

These solutions may be generalized by assuming a form for P based on the similarity solution. Needler (1967) and Welander (1959) took

$$P = A(\lambda,\varphi) + M(\lambda,\varphi)\, e^{K(\lambda,\varphi)z} \tag{29}$$

where $A(\lambda,\varphi)$ is the barotropic part of the pressure field. When this is substituted into the pressure equation (10) the result is:

$$[A_\lambda + (M_\lambda + z M K_\lambda) e^{Kz}][K_\varphi + K\cot\varphi] - [A_\varphi + (M_\varphi + z M K_\varphi) e^{Kz}] K_\lambda = 0 \tag{30}$$

which is satisfied as long as the following conditions are true.

$$K_\lambda = 0 \tag{31a}$$

$$A_\lambda [K_\varphi + K\cot\varphi] = 0 \tag{31b}$$

$$M_\lambda [K_\varphi + K\cot\varphi] = 0 \tag{31c}$$

The solution of the conditions above where

$$K = \frac{c}{\sin\varphi} \tag{32}$$

has been investigated. It gives the same general exponential form of solution as used by Welander (1959) and Blandford (1965). It can, however, satisfy arbitrary boundary conditions where $M(\lambda,\varphi)$ represents the surface density field.

This same generalization technique used on the inverse square solution yields

$$P = C(\lambda,\varphi) + \frac{B(\lambda,\varphi)}{[z + q_b(\lambda,\varphi)]^2} \tag{33}$$

When this is substituted into Eq.(10) the following equations result:

$$B = 4K\lambda \sin^2\varphi + E(\varphi) \tag{34}$$

$$\left(\frac{\partial\varphi}{\partial\lambda}\right)_{q_b=\text{constant}} = \frac{4K\sin^2\varphi}{4K\lambda\sin\varphi\cos\varphi + 3E\cot\varphi - E_\varphi} \tag{35}$$

Thus it seems as if the more general form of the solution has done little to ease the restrictiveness of the boundary conditions imposed by the similarity solution.

This solution does however reproduce the observed density profile in a more realistic way than does the exponential form. This is so because the density in the exponential form decays too quickly with depth.

The inverse square solution has not been explored further, but more work has been done on the arbitrary exponential form.

Using the pressure equation (29) with the pressure density relation 7 to solve Eq.(9) for the vertical velocity gives:

$$w = \frac{Kc}{\sin\varphi} + \frac{1}{2\Omega a^2 c}\left\{\frac{J(M,A)}{M\cos\varphi} + \frac{A_\lambda}{\sin\varphi} + \frac{K_z A_\lambda}{\sin\varphi} + \frac{M_\lambda e^{Kz}}{\sin\varphi}\right\} \tag{36}$$

Due to the predominence of vertical mixing over horizontal, this model applies strictly only to the thermocline region but some interesting things may be noticed by looking at Eq.(36) as $z \longrightarrow -\infty$. The exponential term vanishes $\frac{K_z A_\lambda}{\sin\varphi} \longrightarrow -\infty$ unless $A_\lambda \longrightarrow 0$. If this is so then Eq.(26) reduces to:

$$w = \frac{Kc}{\sin\varphi} + \frac{A_\varphi M_\lambda}{2\Omega a^2 c M\cos\varphi} \tag{37}$$

The same solution (without the barotropic term) can be obtained from:

$$w\frac{\partial\rho}{\partial z} = K\frac{\partial^2\rho}{\partial z^2} \tag{38}$$

which is just a balance between vertical advection and diffusion. Therefore the vertical velocity may be represented by:

$$w = w_{\text{ideal fluid}} + w_{-\infty}.$$

This implies that the exponential solution to the diffusive model is a linear superposition of Welander's ideal fluid thermocline model and a balance between vertical diffusion and advection.

Because of the mathematical arbitrariness of these solutions and the need to supply scale heights from the observed density distribution in the ocean, this model does not severely test the role of diffusion in the thermocline. It must also be remembered that these solutions are not closed: they satisfy neither side nor bottom boundary conditions.

Addendum on Fixing the Scale Depth in Diffusive Thermocline Models

Although the general shape of the density profile in a diffusive thermocline model is fixed by the form of the solution, the resemblance between the theoretical profile and ones measured in the ocean depends critically on the scale depth in the solution: typically the depth where

$$\frac{\rho(z)-\rho(-\infty)}{\rho(0)-\rho(-\infty)} = e^{-1} \tag{39}$$

Using the equation

$$w \frac{\partial \rho}{\partial z} = K \frac{\partial^2 \rho}{\partial z}$$

yields a scale depth of

$$H = \frac{K}{w}$$

This is not particularly useful for estimating H since neither K nor w can be reliably measured in the ocean. When the relationship is used, it is with some measured H and estimated K to get an estimate of w for the model.

The scale depth may be estimated by the following technique alluded to earlier.

The geostrophic equation

$$f \underset{\sim}{k} \times \underset{\sim}{v} = -\frac{1}{\rho_m} \nabla P \tag{40}$$

may be cross-differentiated to remove the pressure dependence, and combined with the equation of continuity to yield

$$v = \frac{f}{\beta} \frac{\partial w}{\partial z} \tag{41}$$

This can be integrated from a level of no horizontal motion to the

surface to give a transport in terms of the vertical Ekman velocity w_e

$$V = \frac{f}{\beta} w_e \tag{42}$$

This transport may then be represented by some average velocity times a scale height

$$V = v H \tag{43}$$

The thermal wind equation

$$f \frac{\partial(\rho v)}{\partial z} = \frac{-g}{a \cos\varphi} \frac{\partial \rho}{\partial \lambda} \tag{44}$$

can be scaled to yield

$$\frac{fv}{H} = -g \frac{\Delta\rho}{\rho L} \tag{45}$$

Combining Eqs.(42), (43) and (45), eliminating v and solving for H, the following results:

$$H = \left[\frac{f^2 w_e L}{g\beta \left(\frac{\Delta\rho}{\rho}\right)} \right]^{1/2} \tag{46}$$

Typical oceanic values for these quantities are

$$L = 10^8 \qquad g = 10^3$$

$$w_e = 10^{-4} \qquad \beta = 10^{-13}$$

$$f = 10^{-4} \qquad \frac{\Delta\rho}{\rho} = 10^{-3}$$

These put into Eq.(46) yield H = 300 m, which is reasonable value for the ocean.

There is a discussion of determining scale depth in Veronis (1969).

References

Robinson and Stommel	1959	Tellus 11: 245
Welander	1959	Tellus 11: 309
Fofonoff	1962	The Sea Vol.1, Wiley, New York: 323
Robinson and Welander	1963	J.Mar.Res. 21: 25
Blandford	1965	J.Mar.Res. 23: 18
Kozlov	1966	Izv.Akad.Nauk.USSR Fiz.Atmos.Okean 2: 742
Needler	1967	J.Mar.Res. 25: 329
Veronis	1969	Deep-Sea Res. 16: Suppl. 301
Welander	1971	J.Mar.Res. 29: 60
Needler	1972	Deep-Sea Res. 18: 895

Notes submitted by
Joseph R. Buckley and
Mark Koenigsberg

Lecture #6. Wind-Driven Circulation

The wind blows over the surface of the ocean and exerts a stress on the water beneath. It is observed that the horizontal scale of the ocean gyres is about the same as the scale of the curl of the wind stress. Since the gross features of the gyres (western boundary currents, for example) are present in many different ocean basins we will consider a greatly simplified model where the effect of wind stress on the water is analyzed.

The following assumptions are made: 1) The flow is steady $\left(\frac{\partial}{\partial t} = 0\right)$, and 2) linear (Rossby number R = 0). 3) Both the (explicit) existence of stratification and 4) topography will be ignored. 5) Motion will be taken on the β-plane with 6) Cartesian geometry. It should be noted that in using the β-plane, Coriolis forces arising from the horizontal component of rotation is ignored, and this, in fact, invokes the implicit existence of stratification which is otherwise neglected.

The horizontal momentum equation is

$$f\,\underline{K} \times \underline{V}_H = -\frac{1}{\rho_m}\nabla p + \frac{\partial \underline{\tau}}{\partial z} \tag{1}$$

where p is the modified pressure, f is the Coriolis parameter, ρ_m is the mean density, $\underline{\tau}$ is the stress exerted on the water by the wind, and $\underline{K}$ is the unit vector in the vertical direction. If the first two terms are balanced, the result is geostrophic flow.

$$\underline{V}_H = \frac{\underline{K} \times \nabla p}{f \rho_m} \tag{2}$$

If Eq.(2) is differentiated with respect to z, we obtain (since p, which includes gravity, is hydrostatically independent of z)

$$\frac{\partial \underline{V}_H}{\partial z} = 0 \tag{3}$$

Taking $\underline{K}\cdot$ curl of Eq.(1) (third term omitted) gives

$$\nabla \cdot \underline{V}_H = 0 \tag{4}$$

which combined with the continuity equation

$$\nabla \cdot \underline{V} = 0 \tag{5}$$

makes the vertical velocity independent of height, and identically zero if

it is zero anywhere. This and Eqs.(3) and (4) is the Taylor-Proudman Theorem - valid for steady, inviscid, linear flow in a rotating fluid.

If the first and third terms of Eq.(1) are balanced the structure of the Ekman layer can be obtained (as in previous lecture notes). Now consider the balance of all three terms with

$$f = f_o + \beta y. \tag{6}$$

The vertical equation of motion can be written as

$$\frac{1}{\rho_m}\frac{\partial p}{\partial z} = -g \tag{7}$$

Let the depth of the water be

$$h = H + \eta \qquad \eta/H = O(1/1000) \text{ typically} \tag{8}$$

Then if Eq.(7) is integrated from z = 0 to the surface

$$P = P_{atm} + g\rho_m(h - z). \tag{9}$$

Taking a uniform atmospheric pressure

$$\frac{1}{\rho_m}\nabla_H P = g\nabla_H h, \tag{10}$$

which expresses a change in pressure due to a horizontal change in surface height.

Now integrate the continuity equation from z = 0 to z = h (the vertical velocity vanishes top and bottom) to get

$$U_x + V_y = 0 \tag{11}$$

where

$$\begin{matrix} U \\ V \end{matrix} = \int_0^h \begin{matrix} u \\ v \end{matrix} dz.$$

The horizontal equations of motion likewise become

$$-fV = -\frac{g}{2}\frac{\partial h^2}{\partial x} + \tau_s^x - \tau_b^x \tag{12}$$

$$fU = -\frac{g}{L}\frac{\partial h^2}{\partial y} + \tau_s^y - \tau_b^y \tag{13}$$

where s, b stand for surface, bottom. Let $\phi = U + iV$. Then the Ekman layer solution to these equations is

$$\phi_e = -\phi_g e^{-(1+i)z/\sqrt{2}\delta} \qquad \delta = \sqrt{\nu/f} \tag{14}$$

Differentiating to get the bottom stress

$$\tau_b^x = \sqrt{\frac{\nu f}{2}}\,(U_g - V_g) \tag{15}$$

$$\tau_b^y = \sqrt{\frac{\nu f}{2}}\,(U_g + V_g) \tag{16}$$

where the geostrophic mass flow is independent of height and $HU_g = U$ $HV_g = V$.

Substituting these into Eqs.(12) and (13) yields

$$-fV = -\frac{g}{2}\frac{\partial h^2}{\partial x} + \tau_s^x - KU + KV \tag{17}$$

$$fU = -\frac{g}{2}\frac{\partial h^2}{\partial y} + \tau_s^y - KV - KU \tag{18}$$

with $K = \sqrt{\frac{\nu f}{2}}\frac{1}{H} = \frac{f\delta}{\sqrt{2}H}$. Since $\delta/H = 1/50$ typically, $K << f$ and we ignore the last terms in the above equations. The net result is that bottom friction is being parameterized as $-KU$ and $-KV$.

Cross-differentiation of Eqs.(17) and (18) yields

$$\beta V = K \cdot \nabla \times \tau_s - K(V_x - U_y) \tag{19}$$

Introducing a stream function

$$U = -\psi_y \qquad V = \psi_x \tag{20}$$

we have

$$\frac{K}{\beta}\nabla^2\psi + \psi_x = \frac{K \cdot \nabla \times \tau_s}{\beta} \tag{21}$$

This equation was first considered in this context by Stommel (1948).

Consider a rectangular basin.

$$0 < y < \pi L\,, \quad 0 < y < sL$$

where $\psi = 0$ on the boundaries. Nondimensionalize with a length scale L and a stream-function scale $\frac{\tau}{\beta}$. Since the zonally averaged wind stress over the North Atlantic gives a wind stress curl approximated by a sine wave, consider a wind forcing of the form

$$\frac{K \cdot \nabla \times \tau_s}{\beta} = -\frac{\tau}{L\beta}\sin\frac{y}{L} \tag{22}$$

We have

$$\epsilon\nabla^2\psi + \psi_x = -\sin y \qquad \epsilon = \frac{K}{\beta L} \tag{23}$$

Since $\epsilon = O(10^{-3})$ this is a singular perturbation problem.

If the variable dependence is separated

$$\psi = \phi(x)\sin y \tag{24}$$

the equation

$$\epsilon\left(\frac{d^2}{dx^2}-1\right)\phi+\phi_x=-1 \tag{25}$$

is obtained. The interior solution with $\epsilon=0$ is

$$\phi_i=-x+C \tag{26}$$

which cannot satisfy the boundary condition $\phi=0$ in the boundary. So a boundary layer is needed to satisfy the boundary conditions, and it is expected to appear at x = 0 since the sign of the $\beta\psi_x$ term is positive. In the boundary layer at x = 0, let the balance be

$$\epsilon\left(\frac{d^2}{dx^2}+\frac{d}{dx}\right)\phi=0 \tag{27}$$

where the derivations are of large order. Re-scale the equation $x/\epsilon=\xi$ so that

$$\frac{d^2\phi}{d\xi^2}+\frac{d\phi}{d\xi}=0 \tag{28}$$

which admits a solution of

$$\phi=de^{-\xi}+\text{constant} \tag{29}$$

and exhibits a boundary layer thickness of ϵ near x = 0.

The uniformly valid solution which satisfies all the boundary conditions is

$$\psi=\left(s-x-se^{-x/\epsilon}\right)\sin y. \tag{30}$$

A plot of the streamlines shows the intensification of velocity in the west.

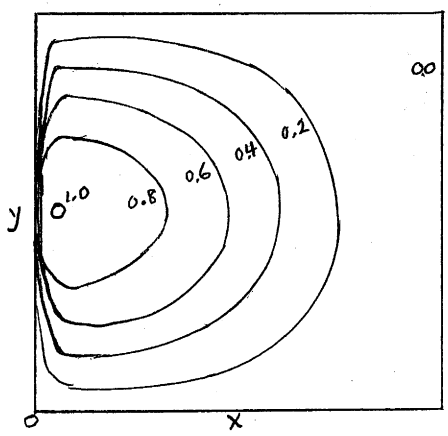

Fig.1

The boundary layer width ϵ can be determined by substitution of values, but since the ocean is really stratified, a modified value of it might have to be used.

The basic balance in the interior is

$$\beta \underline{V} = K \cdot \nabla \times \tau_s \tag{31}$$

which is the Sverdrup transport relation, and is valid in spherical coordinates independently of the β-plane approximation. If Eq.(31) is rewritten as

$$\frac{df}{dt} = \frac{K \cdot \nabla \times \tau_s}{H} \tag{32}$$

it can be seen that the wind stress acting on the ocean increases the vorticity of the ocean. The physics of the Sverdrup balance can be easily understood. If the wind has a negative vorticity (clockwise) as it does in the North Atlantic, then the fluid wants to decrease its value of f and hence flow southward.

The vorticity of the fluid behaves like

$$\nabla^2 \psi \approx -\frac{S}{\epsilon^2} e^{-x/\epsilon} \sin y \tag{33}$$

near x = 0 and becomes very large in this western intensification region. It is here that energy from the wind is dissipated.

Hidaka (1949) and Munk (1950) considered the same model but with a $A \nabla^2 \underline{V}$ frictional term. This produces a balance of

$$\frac{A}{\beta L^3} \phi_{xxxx} \approx \phi_x \tag{34}$$

and gives a boundary layer thickness of

$$\left(\frac{A}{\beta L^3}\right)^{1/3}. \tag{35}$$

The results of both theories are basically the same. 1) There is a southward flow in the interior which is returned in the boundary layer, and 2) the downstream velocity in the western boundary layer is geostrophically balanced (see Eqs.(27) and (19)).

If nonlinear terms are included, the equation becomes

$$\epsilon Z + R \underline{V} \cdot \nabla Z + V = \underline{K} \cdot \nabla \times \tau_s \tag{36}$$

where R = Rossby number and Z = H·(vorticity). For small Rossby numbers, the velocity can be expanded in powers of R

$$\underline{V} = \underline{V}_0 + R \underline{V}_1 + \cdots \tag{37}$$

The boundary layer equations near x = 0 for the stream function ψ become

$$\epsilon \psi_{1xx} + \psi_{1x} = -U_o \frac{\partial}{\partial x}\frac{\partial V_o}{\partial x} - V_o \frac{\partial}{\partial y}\frac{\partial V_o}{\partial x} \tag{38}$$

If this equation is scaled $\frac{x}{\epsilon} = \xi$ and the functions U_o and V_o of the linear problem are introduced, there results

$$\psi_{1\xi\xi\xi} + \psi_{1\xi} = \frac{S^2}{2\epsilon^2} e^{-\xi} \sin 2y \tag{39}$$

with $\psi_1 = 0$ on the wall. The solution is

$$\psi_1 = \frac{-S^2}{2\epsilon^2} \xi e^{-\xi} \sin 2y \tag{40}$$

Then to second order, the total solution in the boundary layer is

$$\psi = S(1-e^{-x/\epsilon}) \sin y - \frac{RS^2}{2\epsilon^2}\frac{x}{\epsilon} e^{-x/\epsilon} \sin 2y \tag{41}$$

$$V = \frac{S}{\epsilon}\left(\sin y + \frac{SR}{2\epsilon^2}\left(\frac{x}{\epsilon} - 1\right) \sin 2y\right) e^{-x/\epsilon} \tag{42}$$

$$Z = -\frac{S}{\epsilon^2}\left(\sin y + \frac{SR}{2\epsilon^2}(x/\epsilon - 2) \sin 2y\right) e^{-x/\epsilon}$$

which is valid only if $R < \epsilon^2$ so that $R\underline{V}\cdot\nabla Z << \epsilon Z$.

The effect is a northward displacement of the intensification, with the dissipation now occurring mostly in the northern part of the western boundary.

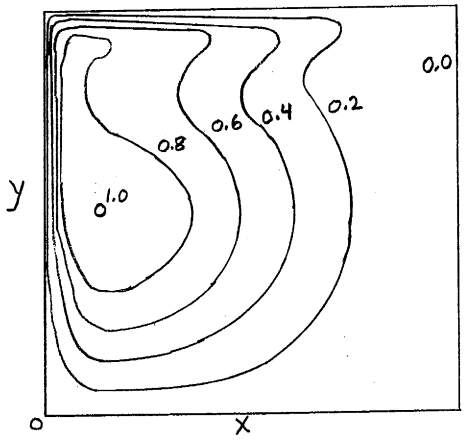

Fig.2

Even with the inclusion of the nonlinear teams, the downstream velocity in the boundary layer is geostrophic. If $R > \epsilon^2$, then the inertial

nonlinearities are more important than the frictional forces and then a full nonlinear theory is needed and produces a scale of the boundary layer of $R^{1/2}$ which (in this case) is greater than ϵ , obtained above.

References

Stommel, H., "The Western Intensification of Wind-Driven Ocean Currents", Trans.American Geophys.Union, 29(2): 202-206, (1948).

Munk, W.H., "On the Wind-Driven Ocean Circulation", J.Meteorology, 7(2): 79-93, (1950).

Notes submitted by
Mark Koenigsberg.

Lecture #7. A Model of World Ocean Circulation

The linearized equations of motion for a steady, wind-driven model of the ocean can be written

$$-fv = -\frac{1}{\rho_a \cos\varphi}\frac{\partial p}{\partial \lambda} + \frac{\partial \tau^\lambda}{\partial z} \tag{1}$$

$$fu = -\frac{1}{\rho_a}\frac{\partial p}{\partial \varphi} + \frac{\partial \tau^\varphi}{\partial z} \tag{2}$$

$$\frac{\partial p}{\partial z} = -g\rho \tag{3}$$

$$\frac{\partial u}{\partial \lambda} + \frac{\partial}{\partial \varphi}(v\cos\varphi) + a\cos\varphi\,\frac{\partial w}{\partial z} = 0 \tag{4}$$

For the model to be discussed, the stratification is idealized as two layers of constant density, the top layer having density ρ_1 and the bottom layer ρ_2 . The ocean bottom is flat; the equations of the bottom, surface and the interface between the two layers are z = 0, z = h_1 and z = h_2 respectively. It is assumed that the zonal wind stress is the most important forcing function and so we take

$$\tau^\varphi = 0, \quad \tau^\lambda = \tau \text{ at } z = h_1 \tag{5}$$

where τ is the zonally averaged wind stress per unit mass. At the interface the stress is assumed zero.

Assuming constant atmospheric pressure, the hydrostatic equation can be integrated to give

$$\frac{1}{\rho_1} \underset{\sim}{\nabla} P_1 = g \underset{\sim}{\nabla} h_1 \tag{6}$$

$$\frac{1}{\rho_2} \underset{\sim}{\nabla} P_2 = g \left[\frac{\Delta\rho}{\rho_2} \underset{\sim}{\nabla} h_2 + \frac{\rho_1}{\rho_2} \underset{\sim}{\nabla} h_1 \right] \tag{7}$$

where the '1' subscript refers to the top layer, the '2' subscript refers to the bottom layer and $\Delta\rho$ is $\rho_2 - \rho_1$.

When upper layer water is present there is no momentum transfer to the lower layer because the interface stress has been assumed to be zero. Hence $\underset{\sim}{\nabla} \rho_2$ must vanish and so by (7)

$$\underset{\sim}{\nabla} h_2 = - \frac{\rho_1}{\Delta\rho} \underset{\sim}{\nabla} h_1 \tag{8}$$

or

$$\underset{\sim}{\nabla} h_1 = \frac{\Delta\rho}{\rho_2} \underset{\sim}{\nabla} h \tag{9}$$

where h, the thickness of the upper layer, is given by

$$h = h_1 - h_2 \tag{10}$$

The transport equations result from (9) and a vertical integration over the top layer. The result is

$$-fV = \frac{-g'}{a\cos\varphi} \frac{\partial}{\partial\lambda} \left(\frac{h^2}{2} \right) + \tau \tag{11}$$

$$fU = \frac{-g'}{a} \frac{\partial}{\partial\varphi} \left(\frac{h^2}{2} \right) \tag{12}$$

$$\frac{\partial U}{\partial\lambda} + \frac{\partial}{\partial\varphi} (V\cos\varphi) = 0 \tag{13}$$

where

$$(U, V) = \int_{h_1}^{h_2} (u, v)\, dz \tag{14}$$

and

$$g' \equiv g \frac{\Delta\rho}{\rho_2} \tag{15}$$

When there is no upper layer water, the Eqs.(11) - (13) can still be used provided we replace g' by g and redefine (U,V) as

$$(U, V) = \int_0^{h_1} (u, v)\, dz \tag{16}$$

Upon cross-differentiating Eqs.(11) and (12) we obtain the Sverdrup relation

$$\beta V = \underset{\sim}{k} \cdot \underset{\sim}{\nabla} \times \underset{\sim}{\tau} \equiv - \frac{1}{a\cos\varphi} \frac{\partial}{\partial\varphi} (\tau\cos\varphi) \tag{17}$$

where

$$\beta = \frac{1}{a}\frac{\partial f}{\partial \varphi} \tag{18}$$

and $\underline{k}$ is the unit vector in the z direction.

Use of (11) and (17) gives

$$\frac{\partial h^2}{\partial \lambda} \equiv \frac{2a}{g'}\left[a \sin\varphi\, \underline{k}\cdot\nabla\times\underline{\tau} + \tau\cos\varphi\right], \tag{19}$$

and then integration between longitudes λ and λ_e yields

$$h^2 = h_e^2 - \frac{2a}{g'}\left[a\sin\varphi\,\underline{k}\cdot\nabla\cdot\underline{\tau} + \tau\cos\varphi\right](\lambda_e - \lambda) \tag{20}$$

where h_e is the value of h at λ_e, a longitude near the eastern boundary.

The Western Boundary Layer

As in, for example, Stommel's model, a western boundary layer is used in an attempt to match the interior Sverdrup transport. For this boundary layer the following assumptions are made:

(i) the value of h offshore of the boundary layer matches the interior value at longitude λ_w;

(ii) the boundary layer is infinitesimally thin;

(iii) the zonal flow at the western wall is zero;

(iv) the flow along the axis of the boundary layer is geostrophic;

(v) there is no specification of the complete dynamical balance for U (i.e., we do not have a closed system of equations).

In the theory to follow, we consider the North Pacific to be an ocean basin closed to the north at the 57.5°N latitude line. A similar analysis can be applied to other ocean basins.

It will be found later that the western boundary layer separates from the coast. To make allowance for this we write the geostrophic balance in the western boundary layer as

$$\frac{2f}{g'} V_s = \frac{\partial h^2}{\partial n}, \tag{21}$$

where V_s is the flow along the axis of the boundary layer, $\frac{\partial}{\partial n}$ is the derivative directed to the right of V_s, and the interior lies to the right of the boundary layer.

Integrating across the western boundary layer results in

$$\frac{2f\,T_w}{g'} = -h_{ww}^2 + h_w^2 \tag{22}$$

where h_{ww} is the value of h at the western wall, h_w is the value of h at longitude λ_w and T_w is given by

$$T_w = \int V_s\, dn, \tag{23}$$

the integral being taken across the boundary layer.

The interior transport is

$$T_i = \int_{\lambda_w}^{\lambda_e} Va\cos\varphi\, d\lambda = \frac{a}{2\Omega}\left(\underline{k}\cdot\underline{\nabla}\times\underline{\tau}\right)\Delta\lambda \tag{24}$$

the second equality being obtained using (17) with $\Delta\lambda = \lambda_e - \lambda_w$.

Substituting the result of (24) into (20) applied at $\lambda = \lambda_w$ results in

$$h_w^2 = h_e^2 - \frac{2}{g'}\left(f\,T_i + a\tau\cos\varphi\,\Delta\lambda\right). \tag{25}$$

Eliminating h_w^2 between (25) and (22) yields

$$h_{ww}^2 = h_e^2 - \frac{2}{g'}\left(f(T_w + T_i) + a\tau\cos\varphi\,\Delta\lambda\right) \tag{26}$$

Since the total mass transport across a latitude circle is zero, $T_w + T_i$ is zero and (26) is thus

$$h_{ww}^2 = h_e^2 - \frac{2a\tau\cos\varphi\,\Delta\lambda}{g'} \tag{27}$$

The above formula for calculating h_{ww} is acceptable in tropical and subtropical latitudes where τ is either negative or relatively small. In temperate zones, however, τ is large enough to make h_{ww}^2 zero at some latitude and negative north of that latitude! This difficulty is overcome in the following way. From the equator to the latitude at which h_{ww}^2 vanishes, $\Delta\lambda$ is the width of the ocean basin; north of this latitude, $\Delta\lambda$ is obtained by solving (27) with $h_{ww} = 0$. <u>This in effect means that the western boundary layer must separate from the coast and penetrate into the interior</u>. At the latitude where h_{ww}^2 vanishes, the western boundary current jumps from the coast to its new longitude determined from (27) with $h_{ww} = 0$.

The Eastern Boundary

It turns out that Eqs.(11), (12) and (13) and a constant value at h_e can account for the qualitative variation in the observed thermocline

but for a quantitative realization heating and cooling effects need to be considered. Since we want to be able to compare our results with observations, information accounting for the heating and cooling effects needs to be included in the model. To do this we use two observed values of h_e, the thermocline depth at the eastern boundary $\lambda = \lambda_e$.

For the North Pacific, h_e is taken as given at 27°N and 50°N. Integrating (12) between these latitudes we have

$$h_e^2(27°) - h_e^2(50°) = \frac{2}{g'} \int_{27°}^{50°} a f U_e \, d\varphi \tag{28}$$

If V is eliminated between (13) and (17) we obtain that $\frac{\partial U}{\partial \lambda}$ and hence U are proportional to $\frac{\partial}{\partial \varphi}(\underline{k} \cdot \underline{\nabla} \times \underline{\tau})$. Hence we write

$$a U_e = \nu \frac{\partial}{\partial \varphi}(\underline{k} \cdot \underline{\nabla} \times \underline{\tau}) \tag{29}$$

Combining Eqs.(28) and (29) enables us to determine ν as

$$\nu = \left[h_e^2(27°) - h_e^2(50°)\right] \Big/ 2/g' \int_{27°}^{50°} f \frac{\partial}{\partial \varphi}(\underline{k} \cdot \underline{\nabla} \times \underline{\tau}) \, d\varphi \tag{30}$$

We can now determine h_e for any latitude between 27°N and 50°N since ν is now known and integration of (12) gives

$$h_e^2(\varphi) = h_e^2(27°) - \frac{2\nu}{g'} \int_{27°}^{\varphi} f \frac{\partial}{\partial \varphi}(\underline{k} \cdot \underline{\nabla} \times \underline{\tau}) \, d\varphi \tag{31}$$

Similar arguments can be used to obtain h_e over other latitudinal ranges south of 27°N.

For the interior of the fluid the zonal flow is geostrophic so that if there were no boundary layer at the eastern wall h would be constant along the wall. Since this is not the case, we have to invoke an eastern boundary layer.

The zonal flow at λ_e is non-zero but at the eastern wall the flow is zero so incoming flow must be diverted to the north or to the south in the boundary layer. The sign of $\underline{k} \cdot \underline{\nabla} \times \underline{\tau}$ determines the sign of the meridional transport in the interior and so we require that the sign of $\underline{k} \cdot \underline{\nabla} \times \underline{\tau}$ determines the direction of the meridional transport in the eastern boundary layer. In the case of the North Pacific, $\underline{k} \cdot \underline{\nabla} \times \underline{\tau}$ is negative between 27°N and 40°N and positive between 40°N and 50°N. Thus, incoming flow between 27°N and 40°N is diverted southward and that between 40°N and 50°N is diverted northward. The incoming flow between 40°N and 50°N is provided by T_w.

The Subpolar Region

A difficulty now arises because T_i, T_w and T_e (the transport in the eastern boundary layer) are all positive and so we need a southward return flow to get a balance of transport across a latitude line. This problem is considered after we have investigated the situation north of 50°N.

North of 50°N $\frac{\partial}{\partial \varphi}(\underline{k}\cdot\nabla\times\underline{\tau})$ is negative and so no upper layer water need be supplied by the western boundary layer. Thus $T_w = 0$ in this region.

By setting $h^2 = 0$ in Eq.(20) we can determine λ_s, the longitude where the thermocline surfaces. We have

$$\lambda_e - \lambda_s = g' h_e^2 / 2a \left(a \sin\varphi\, \underline{k}\cdot\nabla\times\underline{\tau} + \tau\cos\varphi\right) \tag{32}$$

Substituting an expression for V in (17) into (13) and then integrating between λ_s and λ_e gives

$$U_e = -\frac{a}{2\Omega}\frac{\partial}{\partial\varphi}\left(\underline{k}\cdot\nabla\times\underline{\tau}\right)\left(\lambda_e - \lambda_s\right) \tag{33}$$

Equation (12) applied at $\lambda = \lambda_e$ is

$$U_e = -\frac{g'}{fa}\frac{\partial}{\partial\varphi}\left(\frac{h_e^2}{2}\right) \tag{34}$$

and elimination of U_e and $\left(\lambda_e - \lambda_s\right)$ between (32), (33) and (34) enables us to write

$$\frac{1}{h_e^2}\frac{\partial}{\partial\varphi}h_e^2 = \frac{a\sin\varphi\frac{\partial}{\partial\varphi}\left(\underline{k}\cdot\nabla\times\underline{\tau}\right)}{a\sin\varphi\,\underline{k}\cdot\nabla\times\underline{\tau} + \tau\cos\varphi} \tag{35}$$

Hence we obtain h_e^2 northward of 50° as

$$h_e^2 = h_e^2(50°)\exp\left\{\int_{50°}^{\varphi}\frac{a\sin\varphi\frac{\partial}{\partial\varphi}\left(\underline{k}\cdot\nabla\times\underline{\tau}\right)}{a\sin\varphi\,\underline{k}\cdot\nabla\times\underline{\tau} + \tau\cos\varphi}\,d\varphi\right\} \tag{36}$$

U_e and λ_s can now be obtained from (34) and (32) and so the solution north of 50°N has been obtained.

In our model, the North Pacific is bounded by an east-west boundary at 57.5°N. A net transport $T_i + T_e$ meets this boundary; since this fluid cannot leak out of the system, it must flow westward along the northern boundary, turn south and join the western boundary current at the latitude of separation. Had our model included heating and cooling, this fluid could be cooled and become lower layer fluid, thus avoiding having a light fluid boundary layer near the pole with lower layer fluid south of it. (See diagram of the "General Circulation of the Ocean", Lecture #8.)

The southward return flow along the western boundary enables us to overcome our earlier problem of an apparent lack of net zero transport across latitude line between 40^{o}N and 50^{o}N. North of the separation point we now have

$$T_i + T_w + T_{wb} + T_e = 0 \tag{37}$$

where T_{wb} is the return flow along the western boundary.

With the new balance given by (37) instead of the original requirement that $T_i + T_w$ vanish, the calculations for h_{ww} and $\Delta\lambda$ for the western boundary layer need to be repeated. The results are

$$h_{ww}^2 = h_e^2 - 2\left[a\tau\cos\varphi\,\Delta\lambda - f(T_e + T_{wb})\right]/g' \tag{38}$$

and

$$\Delta\lambda = \left[g' h_e^2/2 + f(T_e + T_{wb})\right]/a\tau\cos\varphi \tag{39}$$

where h_{ww} now refers to the value of h at the left side of the boundary current in the open ocean.

A similar analysis to the North Pacific can be applied to other world ocean basins and a model of world ocean circulation built (see Lecture #8).

Notes submitted by
Allan J. Clarke

Lecture #8. I. Clarification of Some Points from Yesterday's Lecture:

1. Eastern Boundary Layers

The assumed balance among the Coriolis term, the pressure gradient and the wind stress yields the following relationships between the curl of the wind stress and the direction of the currents:

If $\hat{k}\cdot \mathrm{curl}\,\underline{\tau}$ is negative then v is to the south.

If $\frac{\partial}{\partial\varphi}(\hat{k}\cdot \mathrm{curl}\,\underline{\tau})$ is positive (negative) then u is eastward (westward). Making the additional assumption that the direction of flow in the eastern boundary layer is the same as that of the interior flow near the boundary, the following qualitative picture is obtained.

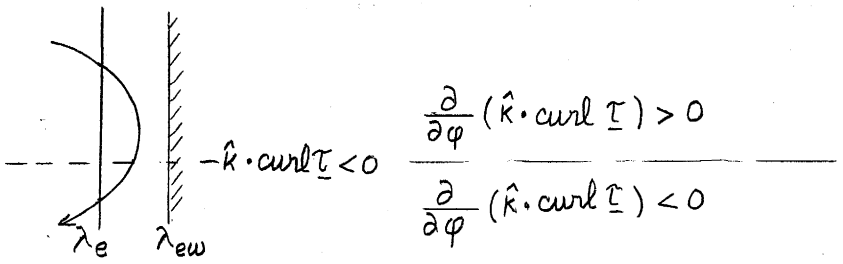

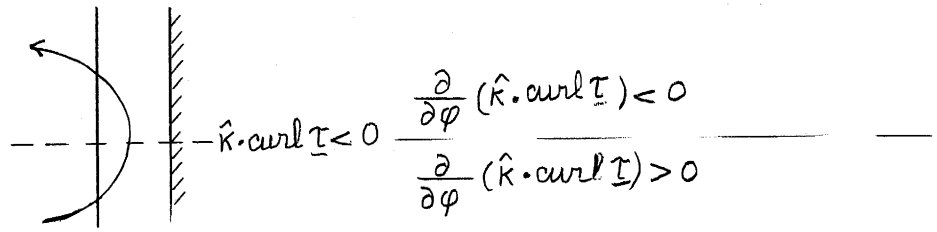

This assumption about the direction of flow in the boundary layer may be expressed in the form

$$U_e = \nu \frac{\partial}{\partial\varphi}(\hat{k}\cdot curl\,\underline{\tau}).$$

The proportionality factor, ν , is assumed constant geostrophically

$$fU_e = \frac{g'}{2}\frac{\partial}{\partial\varphi}(h_e^2).$$

By equating the two expressions for U_e and specifying the values of h_e at two points ν may be determined. Once this has been done U_e and the eastern boundary layer transport T_e may be obtained. We do not know the boundary layer dynamics in detail; e.g., the downstream pressure balance is not known.

Remark: U_e is affected by the meridional component of the local wind stress. This effect could easily be incorporated into the model calculation.

2. The northern boundary and the separation of the western boundary current:

The upper layer of water which impinges on the northern boundary flows around the boundary of the region C (which consists of cold, lower layer water) until it reaches the separation point S. (Whereas in the real ocean this upper layer water would be cooled in the course of such a trip, in the

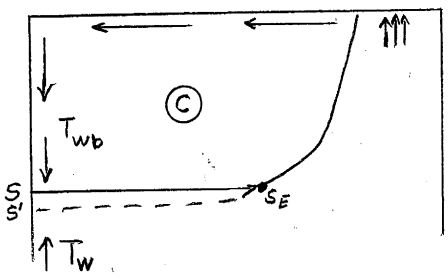

model there is no provision for heat exchanges.) When this southward-flowing water reaches S it merges with the northward-flowing boundary current. Hence the merged boundary current must carry an additional transport T_{wb} toward the north, but the separation point S was determined only in terms of the original transport T_w . If the separation latitude is to remain the same, the transport balance argument requires that the longitude of the boundary layer current must jump abruptly to the east to a point S_e. Note that since $\hat{k} \cdot \text{curl}\, \underset{\sim}{\tau} < 0$ at this latitude the interior flow is to the south so that the separated boundary current will lose water to the south as it flows from S to S_e.

This jump could be avoided by moving the separation point south to a point S' where the combined boundary layer transport T_w and T_{wb} just requires that the thermocline surface at the western wall. This would require a discontinuity in the depth of the thermocline at the point S'. In any case there is some arbitrariness in the choice of a separation latitude - it could be at any point between S and S'.

Perhaps it should again be stated that this model is not a solution to a closed mathematical problem. Rather, it is a construction based on a few simple principles (e.g., geostrophy, transport balances). The given solution is admittedly not unique. The crucial point to bear in mind is that in this model boundary layer separation is determined by the requirements of the general circulation rather than by the details of boundary layer dynamics. Note too that the boundary layer separation is not merely an artifact of the two-layer model. In the continuously stratified ocean the deep density surfaces do get to the surface inshore and to the north of where the western boundary layer leaves the coast.

In the region C in the northeastern Pacific there is no upper layer so the lower layer feels the wind directly. Therefore, the wind drives a circulation in the lower layer. It has been assumed in the present calculation that this lower layer circulation is confined to the region C rather than extending

to other areas. One could do a calculation which permitted the latter (see Kamenkovich and Reznick, 1972, Izv.Atm.Ocean.Phys.8: 238-245), but either way no account is taken of the significant amount of mixing to be expected in the region where the western boundary layer has separated from the coast. There is a lower layer boundary current in this region as well, which enhances the possibility of mixing.

3) Separation at the east:

From the formulas developed in the last lecture one may obtain the relation:

$$h_{ew}^2 = h_{ww}^2 + \frac{2a}{g'} \tau \cos\varphi \Delta\lambda$$

where as before, h_{ew} and h_{ww} are the thermocline depths at the eastern and western walls, respectively. If $\tau < 0$ it could force $h_{ew}^2 \leq 0$; that is, separation at the east. This may well happen in the South Atlantic (the Benguela Current) and possibly in the South Pacific as well.

II. Results of the Model Calculation for the World Oceans.

The results of this calculation are reported in detail in George Veronis' "Model of World Ocean Circulation, I.", J.Mar.Res. 31(3): 228-288, 1973. The remainder of the lecture made liberal use of the figures from that article, the reader will find these to be helpful in considering the following discussion.

For all the calculations $\Delta\rho/\rho$ is taken as .001. The geometry of the world ocean is idealized so that all boundaries are zonal or meridional segments. Features are retained when they are important as ocean boundaries. For example, though New Zealand and Madagascar have about the same latitudinal extent only the former is retained in the idealized geometry. This is because New Zealand is an important barrier to zonal currents in the Southwestern Pacific, while Madagascar has little effect on the gross features of the circulation in the Indian Ocean.

All of the boundary flows will be calculated in the manner discussed yesterday (Lecture #7) and earlier today. However, for a zonally oriented boundary one must also take account of the local wind stress.

Pacific Ocean

The North Pacific has been discussed to some extent in the course of describing the nature of the model. Unlike the North Pacific, which may be taken as closed to the north, the South Pacific is open to the south where it meets the Southern Ocean. The water which leaves the South Pacific at the southeast (i.e., the Cape Horn Current at the tip of South America) cannot simply return to the west as a flow along a zonal boundary (as is the case for the North Pacific). Rather, it must circle the Southern Ocean and re-enter the Pacific along the southern boundary of Tasmania. From there it heads east to New Zealand and circles New Zealand to the south, joining the

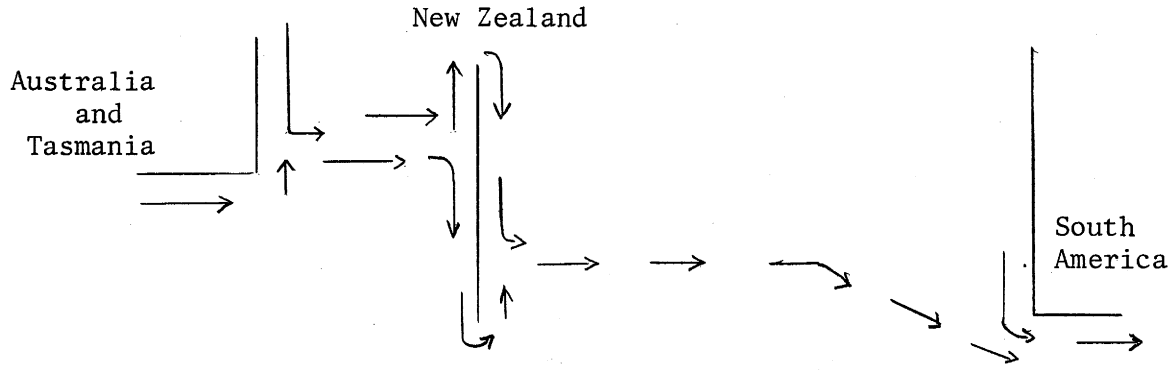

main boundary current on the eastern side. In the real ocean there would be important cooling effects in the Southern Ocean which are not accounted for in the present model.

The thermocline depth at the eastern side, h_e, varies considerably (e.g., from 200 m to 500 m over 30^o of latitude) so the geostrophic U there is substantial. However, the thermocline depth right at the eastern wall, h_{ew} is approximately constant (varying by less than 60 m over the whole latitudinal extent of the basin). Therefore the geostrophic U at the wall is close to zero. Since the boundary layer must serve to bring the transport normal to the wall to zero we may conclude that U in the boundary layer is very nearly in geostrophic balance, even though the model does not impose this condition on the boundary layer dynamics.

In contrast to the situation at the eastern wall, the thermocline depth at the western wall, h_{ww}, varies greatly, so the cross-stream velocity component in the western boundary layer is clearly ageostrophic. Both the depth

and the transport contours close sharply at the western side of the ocean basin and smoothly at the eastern side. That is, the interior flow meshes smoothly with the eastern boundary layer flow. This is related to the observational fact that it is often difficult to define the edge of the eastern boundary current. In contrast, the western boundary layer is sharply defined: the transition from the interior is abrupt.

The eastern boundary layer transports in the Pacific are all small; the maximum is the 7 Sv carried by the Alaska Current. The Alaska, California, Peru and Cape Horn Currents may be readily identified (although the Peru Current extends only from 41°S to 16°S). The Alaska and Cape Horn Currents (and, similarly, the Norwegian Current in the Atlantic) are related to the separation of the western boundary current in an essential way. (See Lecture #7.)

The model calculation yields a 60 Sv transport for the Kuroshio. A later model, which contains the effects of heating and cooling, gives 66 Sv; the observed value is 65 Sv. Separation occurs at 35°N. At this point the model Kuroshio jumps 81° of longitude to the east and its transport decreases from about 30 Sv to 17 Sv. (See the discussion under § 2 above. The point S' where the transport is continuous but h_{ww} is not, would occur at 29°N.) There is a lower layer boundary current under the Kuroshio suggesting instabilities which would cause mixing in this region. The real Kurushio bifurcates into a warm jet and a colder one to the north of this; the latter has been affected by the mixing that took place in the separation region. The model has no provision for mixing: it gives a <u>cold</u> jet to the north of the warm Kuroshio.

The transport in the model's East Australia Current is 70 Sv, which is much greater than the estimates based on observations. These range from 30 Sv to 50 Sv. (Bruce Hamon attributes the discrepancies in the observational estimates to different choices of reference level.) The model boundary current separates at 42°S; in the real ocean separation occurs between 27°S and 35°S. The model which includes heating and cooling yields a transport of 50 Sv; it has the thermocline surface at 30°S, but separation occurs at a higher latitude.

The model is poor near the equator because: the geometry of the coasts is oversimplified; meridional winds are not included in the model, and the ageostrophic (e.g. nonlinear) terms have been left out of the equations.

Indian Ocean

There are some special difficulties with the Indian Ocean circulation. The wind stress data is not good. Moreover, the data used is an annual mean, whereas it is well-known that the seasonal changes in the wind system are significant (viz. the monsoons) and that the ocean's response to these winds shows important time variations. The geometry of the Northern Indian Ocean basin is drastically simplified - the irregular boundaries are neglected. This, together with the use of annual means for the winds, probably accounts for the fact that the Northern Indian Ocean is badly simulated.

The most intense of all the western boundary currents is the Agulhas Current with a maximum transport of 72 Sv. In the present calculation it separates from the coast at the southern tip of Africa. At this point the transport requirements cause it to jump eastward by 59^{o} of longitude. In the course of this journey to the east it loses more than 37 Sv of its original 72 Sv to the interior. This intense return flow has been observed and named the Return Agulhas Current. It is of some interest to ask under what circumstances the Agulhas Current could make it around the Cape of Good Hope and enter the Atlantic. A substantial inflow of the warm water from the Agulhas Current into the colder South Atlantic could be expected to have a significant effect on the atmosphere. This inflow could occur if there were weaker winds over the Indian Ocean. With stronger winds the Agulhas Current would separate from the coast closer to the equator, and return all of its water to the interior of the Indian Ocean.

The Indian Ocean also contains the most intense of the eastern boundary currents - the Flinders Current with a transport of 24 Sv. The Flinders Current is actually along a zonal boundary; in the model it is due to the local wind stress curl causing a northward flow of interior water toward the South Australian coast.

Atlantic Ocean

The model Gulf Stream carries 30 Sv; the Brazil Current has a slightly larger transport. The latter is greater than the observed value. It may be that the Benguela Current actually separates from the coast which would reduce the transport requirements for the Brazil Current. The Atlantic Ocean calculation also yields the Norwegian and Labrador Currents (the latter in the cyclonic gyre of lower layer water in the North Atlantic) as well as a single current which may be identified with the Portugal and Canary Currents. (There is some observational question as to whether these are distinct currents.)

Southern Ocean

The method of calculation requires a meridional boundary so that a Sverdrup balance will hold in the interior. To this end a barrier is introduced at 50^{o}W (the South Sandwich and South Shetland Islands). The calculation gives a transport of 220 Sv in the Falkland Current and the geometry of the basin suggests that this be interpreted as the magnitude of the transport through the Drake Passage.

Notes submitted by
Mark A. Cane

RECIPES FOR MIXED LAYERS IN THE OCEAN (Lecture #1)

Pearn P. Niiler

Introduction

The following pair of lectures will be concerned with a description of the surface mixed layer in the ocean. Parameterization of the mixed layer is commonly approached in one of two ways. In the first method the mean flow is parameterized to fit observations and the eddy terms are then deduced. In the second method, the form of the eddy diffusion terms is found through a sequence of turbulent similarity arguments and then the mean flow and the turbulence intensity are solved for simultaneously. The first approach will be followed here. Instead of deriving a theory from "first" principles, the method will be one which relies on observations from which the descriptive "recipes" can be developed.

Qualitative Description of the Mixed Layer

For an example, a typical vertical temperature profile of the Florida Current is approximated below (Niiler and Richardson, 1973).

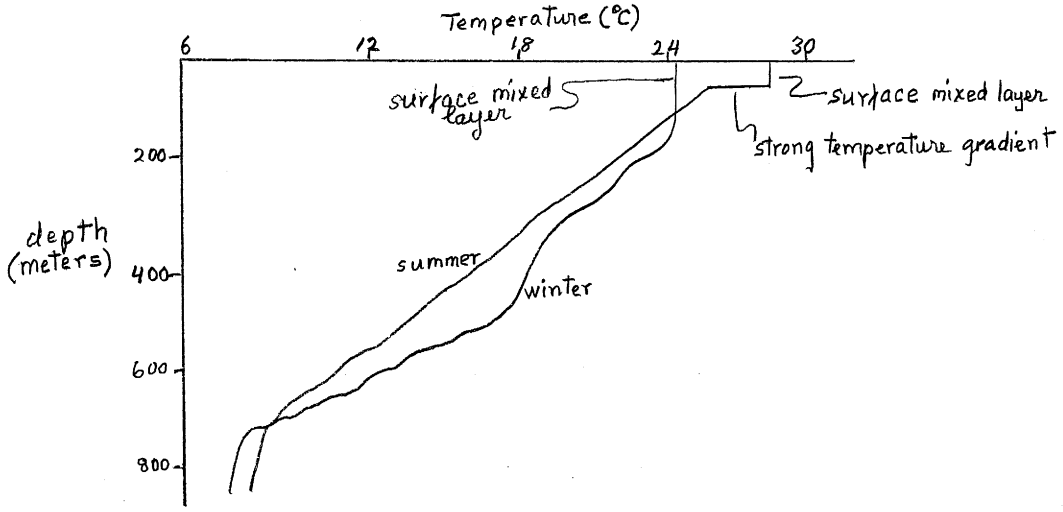

Two important points should be noted:

1) Near the surface a mixed layer of uniform density (temperature) exists whose depth is greater in winter than in summer.

2) The thermocline just below the mixed layer is very sharp, especially in summer.

We need not be concerned with the variation in the main thermocline from summer to winter since it has no bearing on the argument which follows. (The variation is caused by advection of different water masses during the two seasons.) Although large horizontal variations in the mixed layer are observed, we will consider only the vertical structure.

Observations of currents near the surface reveal the following pertinent facts:

3) The mixed layer assumes a fairly uniform, vertically independent velocity, while the currents below are often quite different.

4) During a strong surface wind event (passage of a weather front, for instance), the currents in the mixed layer exhibit a strong response within hours with much of the kinetic energy concentrated in motion of the inertial period. The currents below the mixed layer respond only weakly.

The depth of the mixed layer is also observed to change during a surface wind event. The following diagram illustrates how quickly a deepening

may occur during the passage of a front. (Note also the effect of diurnal heating.) (Stommel *et al.*, 1969.)

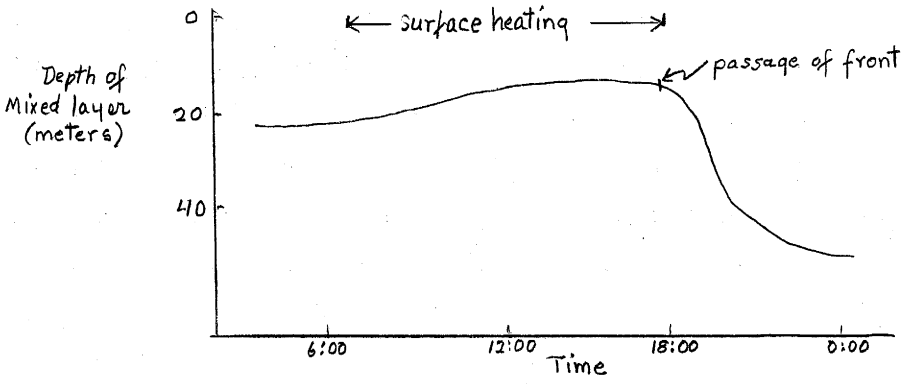

On a much longer time scale, observations show more gradual changes in the mixed layer depth. The following set of diagrams illustrate a depth change during the passage of a weather system (cyclone) on a time scale of days. (Denman and Miyake, 1973.)

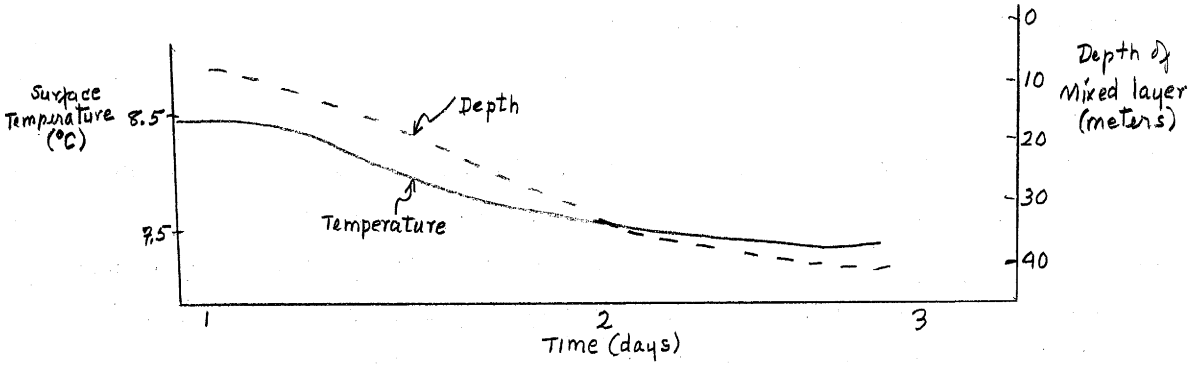

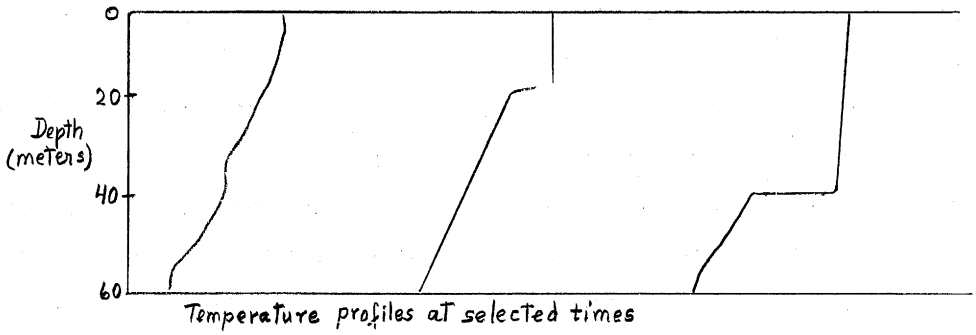

From the last two sets of diagrams we conclude:

5) Deepening of the mixed layer can occur over time scales from an hour to a few days.

6) There are no steady mixed layers if we consider periods longer than a fraction of a day.

A laboratory experiment (Kato and Phillips, 1969) provides one further useful fact. A nonrotating annular basin of stably stratified fluid is impulsively forced from above by a screen which supplies a constant stress in the azimuthal direction creating turbulence near the surface. The depth of the turbulent mixed layer increases in proportion to the cube root of time as the experiment progresses and a rather sharp transition between the mixed layer and the fluid below is always observed. The velocity structure is illustrated below by means of observed displacement of tracers in the fluid.

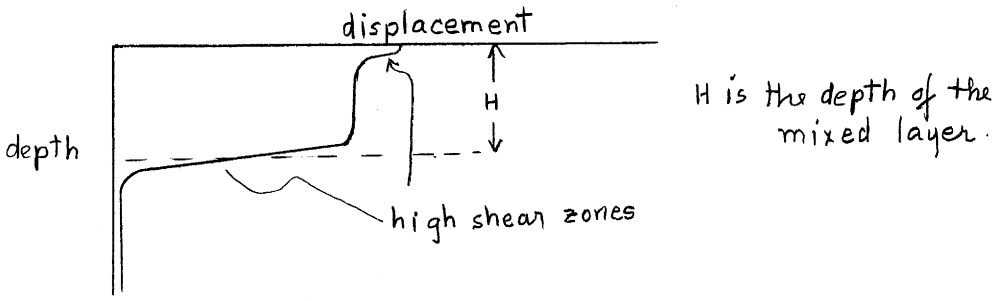

7) The existence of the strong shear zone at the base and top of the mixed layer should be noted.

Development of a Recipe for Vertical Mixing: Basic Equations

The diagrams below summarize the generally observed temperature and velocity profiles in the mixed layer. They also serve to define some of

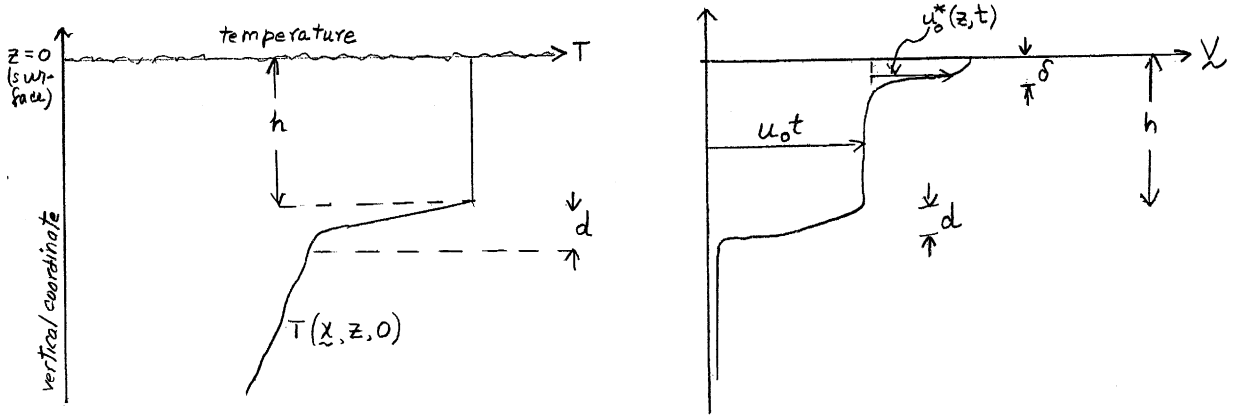

the variables needed in the development of the parameterizations.

To simplify the development we separate each independent variable, ξ , into two parts:

$$\xi(\underline{x}, z, \tau) = \bar{\xi}(z,t) + \xi'(\underline{x}, z, t'), \quad \text{where}$$

$$\bar{\xi}(z,t) = \frac{1}{L^2 \Delta t} \int_0^L \int_0^L \int_t^{t+\Delta t} \xi(\underline{x}, z, \tau)\, d\tau\, d\underline{x}$$

L is a length scale and Δt is large enough to remove the quickly varying part of ξ caused by turbulence. The time dependence (τ) had been separated into two parts, a long time scale, t , and a short time scale, t' .

The above definitions imply

$$\overline{\frac{\partial \xi}{\partial t}} = \frac{\partial \bar{\xi}}{\partial t} \quad \text{and} \quad \overline{\frac{\partial \xi'}{\partial t}} = 0 \quad \text{but} \quad \frac{\partial \xi'}{\partial t'} \neq 0 .$$

The variables for the recipe can now be more explicitly defined. Referring to the above diagram, we can describe the temperature distribution as follows:

$$\bar{T}(z,t) = \bar{T}(0,t) \qquad 0 > z > -h$$

$$\bar{T}(z,t) = \bar{T}(-h-d,t) + \left[\bar{T}(0,t) - \bar{T}(-h-d,t)\right] \frac{z+h+d}{d} \qquad -h > z > -h-d$$

$$\bar{T}(z,t) = \bar{T}(z,0) \qquad -h-d > z$$

The assumed velocity profile for our recipe is:

$$\underset{\sim}{\bar{V}}(z,t) = \underset{\sim}{u_0}(t) + \underset{\sim}{u^*}(z,t) \qquad 0 > z > -\delta$$

$$\underset{\sim}{\bar{V}}(z,t) = \underset{\sim}{u_0}(t) \qquad -\delta > z > -h$$

$$\underset{\sim}{\bar{V}}(z,t) = 0 \qquad -h-\delta > z$$

where $\underset{\sim}{V}$ is a two-dimensional horizontal velocity.

The equations which describe the system are written below. (Boussinesq Approximation.)

1) $$\frac{\partial \underset{\sim}{V}}{\partial t} + \underset{\sim}{V} \cdot \nabla \underset{\sim}{V} + w \frac{\partial \underset{\sim}{V}}{\partial z} + f \times \underset{\sim}{V} = -\frac{1}{\rho_0} \nabla p - \frac{E}{\rho}$$

2) $$\nabla \cdot \underset{\sim}{V} + \frac{\partial w}{\partial z} = 0$$

3) $$\frac{\partial p}{\partial z} = -g\rho$$

$$4)\quad \rho \cdot C_p\left(\frac{\partial T}{\partial t} + \underset{\sim}{v}\cdot\nabla T + w\frac{\partial T}{\partial z}\right) + wg\rho_0 = k\nabla^2 T + \dot{q} + \varphi$$

where ρ_0 is a constant average density

$\underset{\sim}{F}$ is frictional stress

$\dot{q}$ is diabatic heating

φ is a viscous dissipation term

If we average the equations in space and time (apply ($\overline{\ }$) operator), the set reduces to

$$1a)\quad \frac{\partial \overline{\underset{\sim}{v}}}{\partial t} + \nabla\cdot\left(\overline{\underset{\sim}{v}'\underset{\sim}{v}'}\right) + \frac{\partial(\overline{w'\underset{\sim}{v}'})}{\partial z} + f\times\overline{\underset{\sim}{v}} = -\frac{\overline{F}}{\rho_0}$$

$$2a)\quad \frac{\partial \bar{p}}{\partial z} = -g\bar{\rho}$$

$$3a)\quad \nabla\cdot\overline{\underset{\sim}{v}} = 0 \qquad \frac{\partial \bar{w}}{\partial z} \text{ which implies } \bar{w} = 0 \text{ if } \bar{w} = 0 \text{ at great depths.}$$

Neglecting viscous dissipation, the heat equation becomes

$$4a)\quad \frac{\partial \bar{T}}{\partial t} + \nabla\cdot\left(\overline{\underset{\sim}{v}'T'}\right) + \frac{\partial \overline{w'T'}}{\partial z} = \frac{\overline{\dot{q}}}{\rho_0 C_p}$$

Finally, we will assume that the time averaged correlation terms are horizontally uniform so that we neglect $\nabla\cdot\overline{\underset{\sim}{v}'\underset{\sim}{v}'}$ and $\nabla\cdot\overline{\underset{\sim}{v}'T'}$.

The system for the perturbation fields may also be written down with no further approximations:

$$1b)\quad \frac{\partial \underset{\sim}{v}'}{\partial t} + \overline{\underset{\sim}{v}}\cdot\nabla\underset{\sim}{v}' + w'\frac{\partial \underset{\sim}{v}}{\partial z} + \nabla\cdot\underset{\sim}{v}'\underset{\sim}{v}' + \frac{\partial}{\partial z}w'\underset{\sim}{v}' - \frac{\partial(\overline{w'\underset{\sim}{v}'})}{\partial z} = -\frac{1}{\rho_0}\nabla p' - \frac{\underset{\sim}{F}'}{\rho_0}$$

$$2b)\quad \nabla\cdot\underset{\sim}{v}' + \frac{\partial w'}{\partial z} = 0$$

$$3b)\quad \frac{1}{\rho_0}\frac{\partial p'}{\partial z} = \alpha g T' \quad \text{where} \quad \alpha = \frac{1}{h}\int_0^h \overline{\frac{1}{\rho}\frac{\partial \rho}{\partial z}}\,dz\,.$$

Expressions for $\overline{w'T'}$ and $\frac{\partial T_s}{\partial t}$

Using the mean field equations and the assumed profile for $\bar{T}(z,t)$, we may develop an expression for $\overline{w'T'}$ in terms of the mean field and the rate of deepening of the mixed layer to replace Eq.(4a) by one involving only mean field variables. The procedure will be to calculate $\overline{w'T'}$ at the base of the mixed layer and at the ocean surface. The expressions deduced will be used as boundary conditions for calculating $\overline{w'T'}$ throughout the mixed layer. The rate of temperature change in the mixed layer will also be deduced.

In the entrainment layer $(-h > z > -h-d)$, $\dot{q}_o = 0$, and we can integrate the heat equation through this layer. We assume no mixing below $z = -h-d$ so that below the entrainment region $\overline{w'T'} = 0$. Then,

$$\int_{-h(t)-d}^{-h(t)} \frac{\partial \bar{T}(z,t)}{\partial t}\, dz + \int_{-h-d}^{-h} \overline{T'w'}\, dz = 0.$$

Substituting the assumed profile for $\bar{T}$ and carrying out the integration gives for the entrainment region:

$$\overline{w'T'} = \left[\bar{T}(-h-d,t) - \bar{T}(o,t) + d\,\gamma(-h-d,t)\right] \frac{\partial h}{\partial t} - d\,\frac{\partial}{\partial t}\bar{T}(o,t)$$

where $\gamma(-h-d,t) = \frac{\partial \bar{T}}{\partial z}$ evaluated just below $z = -h-d$. Assuming the thickness of the entrainment region is very small (as observations indicate), we deduce a parameterization for $\overline{w'T'}$ in the entrainment layer:

$$5)\quad \overline{w'T'}\,(z = -h) = \left[\bar{T}(-h,t) - \bar{T}(o,t)\right] \frac{\partial h}{\partial t}$$

where $\bar{T}(-h,t)$ is evaluated just below the entrainment region.

In a thin layer near the ocean surface we can not neglect the diabatic heating $\dot{\bar{q}}$. Integrating over the surface layer (where $\dot{\bar{q}}$ is completely absorbed but not stored)

$$\int_{o}^{-\delta} \frac{\partial \bar{T}}{\partial t}\, dz + \int_{o}^{-\delta} \frac{\partial (w'T')_o}{\partial z}\, dz = \int_{o}^{-\delta} \frac{\dot{\bar{q}}}{\rho_o c_p}\, dz \approx \frac{\dot{\bar{q}}}{\rho_o c_p} \int_{o}^{-\delta} dz -$$

$$-\delta \frac{\partial \bar{T}(o,t)}{\partial t} + \overline{w'T'}(-\delta) = \frac{-\delta \dot{\bar{q}}}{\rho_o c_p}$$

Letting $\delta \dot{\bar{q}} = \dot{\bar{Q}}$ where $\dot{\bar{Q}}$ is an energy flux (positive down) in units of energy per unit time per unit area, and letting $\delta \to 0$ we get:

$$6)\quad \overline{w'T'}\,(z = 0) = -\frac{\dot{\bar{Q}}}{\rho \cdot c_p}$$

Equations (5) and (6) give us boundary conditions on $\overline{w'T'}$ for the mixed layer. If we assume $\dot{\bar{q}}$ is zero in the mixed layer itself we can solve Eq. (4a) as follows: (Remember $\bar{T}(z,t) = \bar{T}(o,t) = \bar{T}$ in the mixed layer.)

$$\frac{\partial \bar{T}}{\partial t} + \frac{\partial \overline{w'T'}}{\partial z} = 0 \qquad o > z > -h$$

$$\overline{w'T'} = -\frac{\partial \bar{T}}{\partial t} z + C$$

Using Eq. (6) gives:

$$C = -\frac{\dot{\bar{Q}}}{\rho_o c_p}$$

Using Eq.(5) we find the rate of temperature change in terms of surface heating and rate of deepening.

$$8)\quad h\frac{\partial \bar{T}}{\partial t} = \left[\bar{T}(-h,t)-\bar{T}\right]\frac{1}{h}\frac{\partial h}{\partial t} + \frac{\bar{\dot{Q}}}{\rho_0 C_p}$$

where $\bar{T}(-h,t)$ is evaluated just below the mixed layer. The parameterization for $\overline{w'T'}$ may now be written

$$9)\quad -\rho_0 C_p \overline{w'T'} = \bar{\dot{Q}} + \frac{z}{h}\left\{\bar{\dot{Q}} - C_p\rho_0\left[\bar{T}-\bar{T}(-h,t)\right]\frac{\partial h}{\partial t}\right\}$$

We can put (8) and (9) into slightly different terms if we assume that at time $t=0$, a linear stratification, Γ, exists with surface temperature, $\bar{T}(0,0)$. If T_s is the deviation from the initial surface temperature, the following relationships hold:

$$\bar{T}(0,t) = \bar{T}(0,0) + T_s$$

and since in the mixed layer the temperature is constant

$$\bar{T}(z,t) = \bar{T}(0,0) + T_s \quad \text{in the mixed layer.}$$

Below the mixed layer, the initial temperature remains unchanged so

$$\bar{T}(z,t) = \bar{T}(0,0) + \Gamma z \quad \text{below the mixed layer where}$$

$$\Gamma = \left.\frac{\partial \bar{T}}{\partial z}\right|_{t=0} \quad \text{is constant.}$$

If we substitute the above expressions for $\bar{T}(-h,t) - \bar{T}$ in Eqs.(8) and (9) we obtain:

$$8a)\quad h\frac{\partial T_s}{\partial t} = -\left(T_s + \Gamma h\right)\frac{\partial h}{\partial t} + \frac{\bar{\dot{Q}}}{\rho_0 C_p}$$

$$9a)\quad -\rho_0 C_p \overline{w'T'} = \bar{\dot{Q}} + \frac{z}{h}\left[\bar{\dot{Q}} - C_p\rho_0\left(T_s + \Gamma h\right)\frac{\partial h}{\partial t}\right]$$

When referring to these equations one should remember that the whole mixed layer is at the temperature $T_s + \bar{T}(0,0)$.

Expressions for $\overline{\underset{\sim}{v}'w'}$ and $\frac{\partial u_o}{\partial t}$

The velocity profile may be treated in a similar manner to provide an expression for $\overline{\underset{\sim}{v}'w'}$ and $\frac{\partial u_o(t)}{\partial t}$. We assume that $\bar{\underset{\sim}{F}} = 0$ except near the surface.

Equation (1b) may be integrated vertically through the entrainment layer $(-h>z>-h-d)$ to yield:

$$\frac{d}{2}\left(\frac{\partial}{\partial t}+\underset{\sim}{f}\times\right)\underset{\sim}{u}_0(t)+\frac{\partial h}{\partial t}\underset{\sim}{u}_0=-\overline{\underset{\sim}{v}'w'}$$

In the limit as $d\longrightarrow 0$ we find

10) $$\overline{w'\underset{\sim}{v}'}\,(z=-h)=-\underset{\sim}{u}_0(t)\,\frac{\partial h}{\partial t}$$

In the surface shear layer we assume $\underline{F}$ is approximately constant. Then Eq.(1b) may be integrated vertically from $z=0$ to $z=-\delta$ to give

$$\overline{\underset{\sim}{v}'w'}\,(z=-\delta)=\left(\frac{\partial}{\partial t}+\underset{\sim}{f}\times\right)\left(\delta\underset{\sim}{u}_0(t)+\int_0^{-\delta}\underset{\sim}{u}_0^*(z,t)\,dz\right)+\delta\,\frac{\underset{\sim}{F}_0}{\rho_0}$$

Letting $\tau_0=-\delta F_0$ be the shearing stress acting on the surface, and taking a limit as $\delta\longrightarrow 0$ we get:

11) $$\overline{\underset{\sim}{v}'w'}\,(z=0)=-\tau_0/\rho_0$$

With Eqs.(10) and (11) providing boundary conditions for the mixed layer, Eq.(16) may be solved in a similar manner as the temperature equation. The result is:

12) $$\frac{\partial h\,\underset{\sim}{u}_0}{\partial t}=\underset{\sim}{\tau}_0/\rho_0-\underset{\sim}{f}\times h\,\underset{\sim}{u}_0$$

and

13) $$-\rho_0\left(\overline{\underset{\sim}{v}'w'}\right)=\frac{z}{h}\left(\underset{\sim}{\tau}_0-\rho_0\,\underset{\sim}{u}_0\,\frac{\partial h}{\partial t}\right)+\underset{\sim}{\tau}_0$$

Perturbation Energy Equation

Our system of equations is not yet closed because we do not know the rate at which the mixed layer deepens. We appeal to the perturbation energy equation to proceed further.

The perturbation energy equation is formed as follows: First combine the perturbation horizontal momentum equation with the perturbation equation of hydrostatic balance to form a three-dimensional momentum equation. Let the viscous forces be represented by the form $\frac{F'}{\rho_0}=-\nu\nabla^2\underset{\sim}{v}'$. Then Eqs.(1b) and (3b) become:

$$\frac{\partial\underset{\sim}{v}'}{\partial t}+\overline{\underset{\sim}{v}}\cdot\nabla\underset{\sim}{v}'+w'\frac{\partial\overline{\underset{\sim}{v}}}{\partial z}+\nabla\cdot\underline{v}'\underline{v}'+\frac{\partial}{\partial z}\left(w'\underline{v}'-\overline{w'\underline{v}'}\right)+\underset{\sim}{f}\times\underset{\sim}{v}'=$$

$$=-\frac{1}{\rho_0}\nabla p'-\frac{\hat{k}}{\rho_0}\frac{\partial p'}{\partial z}+\hat{k}\alpha g T'+\nu\nabla^2\underset{\sim}{v}'$$

After dotting the equation with $\underset{\sim}{v}' + \hat{\underset{\sim}{k}} w'$, we use the continuity equation to manipulate the equation into the following form

$$\frac{1}{2}\frac{\partial}{\partial t}\underset{\sim}{v}'\cdot\underset{\sim}{v}' + (\overline{\underset{\sim}{v}}\cdot\nabla)\frac{\underset{\sim}{v}'\cdot\underset{\sim}{v}'}{2} + \frac{1}{2}\nabla\cdot(\underset{\sim}{v}'\underset{\sim}{v}'\cdot\underset{\sim}{v}') + \frac{1}{2}\frac{\partial}{\partial z}(w'\underset{\sim}{v}'\cdot\underset{\sim}{v}') +$$

$$+ w'\underset{\sim}{v}'\frac{\partial\overline{\underset{\sim}{v}}}{\partial z} - \underset{\sim}{v}'\frac{\partial}{\partial z}\overline{w'\underset{\sim}{v}'} + \frac{1}{\rho_0}\nabla p'\underset{\sim}{v}' + \frac{1}{\rho_0}\frac{\partial p'w'}{\partial z} =$$

$$= \alpha g T'w' + \frac{\nu}{2}\nabla^2\underset{\sim}{v}'\cdot\underset{\sim}{v}' - \nu(\nabla\underset{\sim}{v}')\cdot(\nabla\underset{\sim}{v}').$$

If we apply the averaging operator, ($\overline{\ }$), the horizontal gradients are eliminated among others and replacing $\overline{\underset{\sim}{v}'\cdot\underset{\sim}{v}'}$ by $\overline{c'^2}$ we get the perturbation kinetic energy equation:

$$\frac{\partial}{\partial t}\frac{\overline{c'^2}}{2} + \frac{\partial}{\partial z}\left[\overline{w'\left(\frac{p'}{\rho_0} + \frac{c'^2}{2}\right)}\right] + \overline{w'\underset{\sim}{v}'}\frac{\partial\overline{\underset{\sim}{v}}}{\partial z} = \alpha g\overline{T'w'} - \nu\overline{(\nabla\underset{\sim}{v}'\cdot\nabla\underset{\sim}{v}')}$$

References

Denman, K.L. and M. Miyake (1973) Upper layer mocification at ocean station PAPA: Observations and simulation. J.Phys.Oceanogr.,3: 185-196.

Kraus, E.B. and J.S.Turner (1967) A one-dimensional model of the seasonal thermocline, Part II. Tellus 19: 98-105.

Miropolskiy, Yv.Z. (1970) Nonstationary model of the wind-convection mixing layer in the ocean. IZV.,Atm. and Ocean. Phys. 6(12): 1284-1294.

Niiler, P.P. Deepening of the wind mixed layer. To appear in J.F.M.

Pollard, R.T., P.B.Rhines and Rory Thompson (1973) The deepening of the wind-mixed layer. Geophys.Fluid Dyn., 4: 381-404.

Stommel, H., K.Saunders, W.Simmons and J.Cooper (1969) Observations of the diurnal thermocline. Deep-Sea Res. 16. Suppl., 269-284.

Niiler, P.P. and W.S.Richardson (1913) Seasonal variations of the Florida Current, J.M.R. 31(3): 144-167.

Notes submitted by

Karl E. Taylor

RECIPES FOR MIXED LAYERS IN THE OCEAN (Lecture #2).

Pearn P. Niiler

In the last lecture we derived two of the three equations that are needed in order to find $h(t)$:

$$\frac{\partial h\underset{\sim}{v}}{\partial t} = \frac{\underset{\sim}{\tau}_o}{\rho_o} - \underset{\sim}{f} \times h\underset{\sim}{v} \tag{1}*$$

$$h\frac{\partial T}{\partial t} + (T + \Gamma h)\frac{\partial h}{\partial t} = \frac{\dot{Q}_o}{c_p \rho_o}. \tag{2}$$

We also derived the perturbation kinetic energy equation:

$$\frac{\partial}{\partial t}\left(\frac{\overline{c'^2}}{2}\right) + \frac{\partial}{\partial z}\left[\overline{w'\left(\frac{p'}{\rho_o} + \frac{c'^2}{2}\right)}\right] + \overline{w'\underset{\sim}{v}'} \cdot \frac{\partial \underset{\sim}{U}}{\partial z} = \frac{\alpha g}{\rho_o}\overline{w'T'} - \overline{\nu \nabla \underset{\sim}{v}' \cdot \nabla \underset{\sim}{v}'} \tag{3}$$

In this lecture we will obtain the third equation from (3) and will solve the set of equations for $h(t)$.

1) The Perturbation Kinetic Energy Equation in the Mixed Layer

The terms in Eq.(3) represent the change in perturbation kinetic energy, the gradient of the vertical flux of perturbation energy, the production of perturbation kinetic energy, the vertical potential energy flux, and viscous dissipation, respectively. Conventional wisdom gives us estimates of the magnitudes of all terms but the second, and they are listed in Table 1.

$\frac{\partial}{\partial t}\left(\frac{\overline{c'^2}}{2}\right)$ is negligible in all regions of the mixed layer. In the intermediate layer $\frac{\partial U}{\partial z} = 0$, and (3) reduces to

$$\frac{\partial}{\partial z}\left[\overline{w'\left(\frac{p'}{\rho_o} + \frac{c'^2}{2}\right)}\right] + \varepsilon = \frac{\alpha g}{\rho_o}\overline{w'T'}, \quad -h < z < -\delta \tag{4}$$

where

$$\varepsilon \equiv \nu \overline{\nabla \underset{\sim}{v}' \cdot \nabla \underset{\sim}{v}'}$$

The mean flow has strong vertical shear in the surface and entrainment layers. There the energy balance is dominated by the second, third, and fifth terms of (3) and it reduces to

---

* Note the slight changes in notation in (1) - (3) as compared to their counterparts, (8a) and (12), in the previous lecture. The notation here agrees with Niiler (1974).

TABLE I

BALANCE WITHIN THE PERTURBATION K.E. EQUATION

Perturbation Energy Flux	Estimator	Ordered Magnitude in cm^2/sec^2	Reference
$\frac{\partial}{\partial t}\frac{1}{2}\overline{C'^2}$	$\frac{3\pi}{T}U^{*2}$	3×10^{-4}	Phillips (1966)
$\overline{\vec{V}'W'}\cdot\frac{\partial\vec{U}}{\partial z}$	$\frac{\tau_o(\Delta U)}{h}$	$3\times\Delta U(cm/sec)^{-1}\times10^{-4}$	Eq. (13)(in previous lecture)
$\alpha g\frac{\overline{W'T'}}{\rho_o}$	$\frac{\alpha g}{\rho_o^2 C_p}\dot{Q}_{max}$	4×10^{-3}	Eq.(9a), in previous lecture; Denman & Miyake (1973)
$\nu\overline{\nabla V'\cdot\nabla V'}$	Shape of turbulent K.E. spectra	$6\text{-}7\times10^{-3}$	Grant, *et al.* (1968)

Parameters:

T = 1 day = 10^5 sec

U^{*2} = (τ_o/ρ_o) = cm^2/sec^2

h = 100 m

ΔU = vertical contrast of horizontal velocity within mixed layer

$\frac{\alpha g}{\rho_o}$ = 2×10^{-1} $cm/sec^2\ ^oC$

$\rho_o C_p$ = 1 $cal/cm^3\ ^oC$

$\dot{Q}_{max}$ = 2×10^{-2} $cal/cm^2 sec$

$$\frac{\partial}{\partial z}\left[\overline{W'\left(\frac{P'}{\rho_o}+\frac{C'^2}{2}\right)}\right]+\overline{W'V'}\frac{\partial U}{\partial z}+\varepsilon=0,\qquad \begin{matrix}-\delta<z<0\\ -h-d<z<-h\end{matrix} \tag{5}$$

Integrating (4) and (5) through the three layers yields:

$$\left[\overline{W'\left(\frac{P'}{\rho_o}+\frac{C'^2}{2}\right)}\right]\Bigg|_{-h}^{-\delta}+\int_{-h}^{-\delta}\varepsilon\,dz=\int_{-h}^{-\delta}\frac{\alpha g}{\rho_o}\overline{W'T'}\,dz \tag{6}$$

$$\left[\overline{w'\left(\frac{p'}{\rho_0}+\frac{c'^2}{2}\right)}\right]\Bigg|_{-\delta}^{0} = -\int_{-\delta}^{0}\overline{w'\underset{\sim}{v}'}\cdot\frac{\partial \underset{\sim}{U}^*}{\partial z}\,dz-\int_{-\delta}^{0}\varepsilon\,dz \tag{7}$$

$$\left[\overline{w'\left(\frac{p'}{\rho_0}+\frac{c'^2}{2}\right)}\right]\Bigg|_{-h-d}^{-h} = -\int_{-h-d}^{-h}\overline{w'\underset{\sim}{v}'}\cdot\frac{\partial \underset{\sim}{U}}{\partial z}\,dz-\int_{-h-d}^{-h}\varepsilon\,dz. \tag{8}$$

The stress in the surface layer is assumed to be constant and equal to the value at the surface, so

$$\int_{-\delta}^{0}\overline{w'\underset{\sim}{v}'}\cdot\frac{\partial \underset{\sim}{U}^*}{\partial z}\,dz = -\frac{\underset{\sim}{\tau}_0}{\rho_0}\cdot\underset{\sim}{U}_0^* \tag{9}$$

(terms of $O(d/h)$ neglected). Both the velocity and the stress are linear functions of z in the entrainment layer

$$\underset{\sim}{U}(z) = \underset{\sim}{V}\,\frac{z+h+d}{d} \tag{10}$$

$$\overline{w'\underset{\sim}{v}'} = \underset{\sim}{V}\,\frac{\partial h}{\partial t}\,\frac{z+h+d}{d}. \tag{11}$$

Using (10) and (11) we find

$$\int_{-h-d}^{-h}\overline{w'\underset{\sim}{v}'}\,\frac{\partial \underset{\sim}{U}}{\partial z}\,dz = -\frac{1}{2}\underset{\sim}{V}\cdot\underset{\sim}{V}\,\frac{\partial h}{\partial t} \tag{12}$$

(terms of $O(d/h)$ neglected).

Adding (6), (7), and (8) and using (9) and (12) together with

$$\left[\overline{w'\left(\frac{p'}{\rho_0}+\frac{c'^2}{2}\right)}\right]\Bigg|_{-h-d} = 0 \tag{13}$$

and the simplification

$$\varepsilon_0 = \int_{-h-d}^{0}\varepsilon\,dz, \tag{14}$$

we have

$$\overline{w'\left(\frac{p'}{\rho_0}+\frac{c'^2}{2}\right)}\Bigg|^{0} + \varepsilon_0 - \frac{\underset{\sim}{\tau}_0}{\rho_0}\cdot\underset{\sim}{U}_0^* - \frac{1}{2}\underset{\sim}{V}\cdot\underset{\sim}{V}\,\frac{\partial h}{\partial t} = \frac{\alpha g}{\rho_0}\int_{-h}^{0}\overline{w'T'}\,dz \tag{15}$$

(terms of $O(d/h)$ neglected).

The terms in (15) are the flux of turbulent energy due to the surface processes, the dissipation, the turbulent kinetic energy produced by the velocity shear in the surface layer and in the entrainment layer, and the change of the potential energy of the mean flow.

The expression for $\overline{W'T'}$ from the last lecture (Eq.9a) is

$$-\rho_0 c_p \overline{W'T'} = \dot{Q}_0 + \frac{z}{h}\left[\dot{Q}_0 - c_p \rho_0 (T+\Gamma h)\frac{\partial h}{\partial t}\right]. \tag{16}$$

Integrating (16) from $-h$ to 0 we have

$$-\frac{\alpha g}{\rho_0}\int_{-h}^{0}\overline{W'T'}\,dz = \frac{\alpha g}{\rho_0}\left[\frac{h\dot{Q}_0}{2\rho_0 c_p} + \frac{h}{2}(T+\Gamma h)\frac{\partial h}{\partial t}\right]. \tag{17}$$

Substituting (17) into (15) we have

$$\overline{W'\left(\frac{p'}{\rho_0}+\frac{c'^2}{2}\right)}\Bigg|^{0} + \varepsilon_0 - \frac{\tau_0}{\rho_0}\cdot\underset{\sim}{U}_0^* - \frac{1}{2}\underset{\sim}{V}\cdot\underset{\sim}{V}\frac{\partial h}{\partial t} = \frac{\alpha g}{\rho_0}\left[\frac{h\dot{Q}_0}{2\rho_0 c_p} + \frac{h}{2}(T+\Gamma h)\frac{\partial h}{\partial t}\right] \tag{18}$$

2. Solutions to Mixed Layer Formation

We will parameterize the energy flux from the surface by

$$\overline{W'\left(\frac{p'}{\rho_0}+\frac{c'^2}{2}\right)}\Bigg|^{0} + \varepsilon_0 - \frac{\tau_0}{\rho_0}\cdot\underset{\sim}{U}_0^* = -m_0\left|\underset{\sim}{U}_0^*\right|^3 = -m_0\left|\frac{\tau_0}{\rho_0}\right|^{3/2}, \tag{19}$$

where m_0 is an $O(1)$ quantity. Our independent variables will be

$\underset{\sim}{U}_E = h\underset{\sim}{V}$	Ekman transport
$\theta = \rho_0 c_p (T + \frac{\Gamma h}{2})h$	heat content
h	depth of mixed layer

Expressing (1), (2), and (18) in terms of the above variables with the parameterization (19) we have

$$\frac{\partial \underset{\sim}{U}_E}{\partial t} + \underset{\sim}{f}\times\underset{\sim}{U}_E = \frac{\tau_0}{\rho_0} \tag{20}$$

$$\frac{\partial \theta}{\partial t} = \dot{Q}_0 \tag{21}$$

$$\frac{\partial h}{\partial t}\left[\frac{\alpha g}{c_p \rho_0^2}\theta h^2 + \frac{N^2 h^4}{2} - \underset{\sim}{U}_E\cdot\underset{\sim}{U}_E\right] = 2m_0 h^2\left|\frac{\tau_0}{\rho_0}\right|^{3/2} - \frac{\alpha g}{c_p\rho_0}\dot{Q}_0 h^3, \tag{22}$$

where $N = \left(\frac{\alpha g}{\rho_0}\Gamma\right)^{1/2}$ is the Väisälä frequency of the ocean below the mixed layer.

Consider the case of initial deepening without heating. The stress is in the x-direction and all independent variables are initially zero.

$$\underset{\sim}{U}_E = \theta = h = 0, \quad t = 0$$
$$\dot{Q}_0 = 0$$
$$\tau_0 = \tau_0 \hat{\imath}$$

The solutions of (20) and (21) are

$$\underset{\sim}{U}_E = \frac{\tau_o}{f\rho_o}\left[\sin(ft), \cos(ft) - 1\right] \tag{23}$$

$$\theta(t) = 0. \tag{24}$$

Inserting the above solutions into (22) yields

$$\frac{\partial h}{\partial t}\left[\frac{N^2h^4}{2} - \left(\frac{\tau_o}{f\rho}\right)^2 2(1-\cos(ft))\right] = 2m_o\left(\frac{\tau_o}{\rho_o}\right)^{3/2}h^2. \tag{25}$$

The solution at the initial time $t < N^{-1} < f^{-1}$ is found by expanding $\cos(ft)$ in a series about $t = 0$ and assuming a solution of the form

$$h \sim a t^{K_o} + b t^{K_1}. \tag{26}$$

Plugging (26) into (25) and balancing the first and last terms in (25) gives

$$h \sim (12m_o)^{1/3}\left(\frac{\tau_o}{\rho N^2}\right)^{1/2}(tN)^{1/3} + \frac{1}{30m_o}\left(\frac{\tau_o}{\rho N^2}\right)^{1/2}(tN) + \ldots \tag{27}$$

The above solution agrees well with the experimental results of Kato and Phillips (1969). If we numerically integrate the equations for long time, we get the results qualitatively pictures in Fig.1. The experiments of

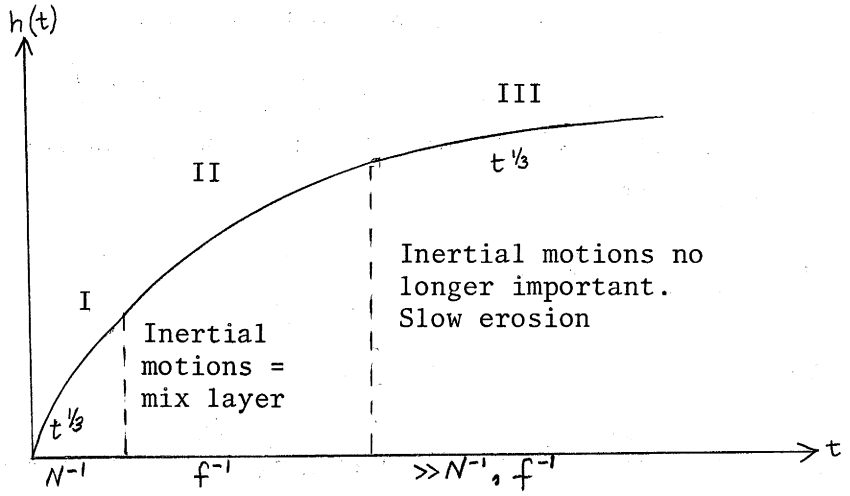

Fig.1

Kato and Phillips cover region I. Regions II and III are suggestive of the analysis by Pollard, Rhines, and Thompson (1973) and Kraus and Turner (1967), respectively.

In order to study the deepening for long time with constant hearing, we rescale as follows:

$t \quad f^{-1}$

$h \quad \tau_0^{1/2}(\rho_0 N f)^{-1/2}$

$\theta \quad \dot{Q}_0/f$ where $\dot{Q}_0$ is the heating rate.

(20)-(22) become

$$\frac{\partial \underset{\sim}{U}_E}{\partial t} + \hat{K} \times \underset{\sim}{U}_E = \underset{\sim}{\tau} \tag{28}$$

$$\frac{\partial \theta}{\partial t} = \dot{Q} \tag{29}$$

$$\frac{\partial h}{\partial t}\left[B\theta h^2 + \frac{h^4}{2} - \underset{\sim}{U}_E \cdot \underset{\sim}{U}_E\right] = A|\underset{\sim}{\tau}|^{3/2} h^2 - B\dot{Q} h^3 \tag{30}$$

where

$$A = 2m_0\left(\frac{f}{N}\right)^{1/2} < 1$$

$$B = (\dot{Q}_0 N/c_p \tau_0 \Gamma) < 1.$$

The equasions have been integrated numerically and the results of one run are shown in Fig.2 (see Niiler, 1974, for a more complete description). If the initial value of $h < 2$, h increases rapidly to $h \simeq 2$ $(h \simeq 2\tau_0^{1/2}(\rho_0 N f)^{-1/2})$ in half a pendulum day. For long time $h \to A/B$ if $\dot{Q} \neq 0$ and $(6At)^{1/2}$ if $\dot{Q} = 0$ the function $E \equiv \frac{1}{2}\underset{\sim}{V} \cdot \underset{\sim}{V} \frac{\partial h}{\partial t}$ is the rate at which turbulent energy is released by the wind-driven inertial motions at the base of the mixed layer. The peak at $t \simeq 1$ shows the importance of the inertial motions in the initial deepening of the mixed layer. $F \equiv h^* - h$ is the difference between the layer depth without and with mean motion energetics. Over a longer time F eventually increases to zero.

References

Denman, K.L., and M. Miyake 1973 Upper layer modification at ocean station PAPA: Observations and simulation. J.Phys.Oceanogr.,3: 185-196.

Grant, H.L., A. Moilliet, and V.M.Vogel 1965 Some observations of the occurrence of turbulence in and above the thermocline. J.Fluid Mech.,34: 443-448.

Kato, H., and OlM.Phillips 1969 On the penetration of a turbulent layer into stratified fluid. J.Fluid Mech.,37: 643-655.

Kraus, E.B., and J.S.Turner 1967 A one-dimensional model of the seasonal thermocline, Part II. Tellus, 19: 98-105.

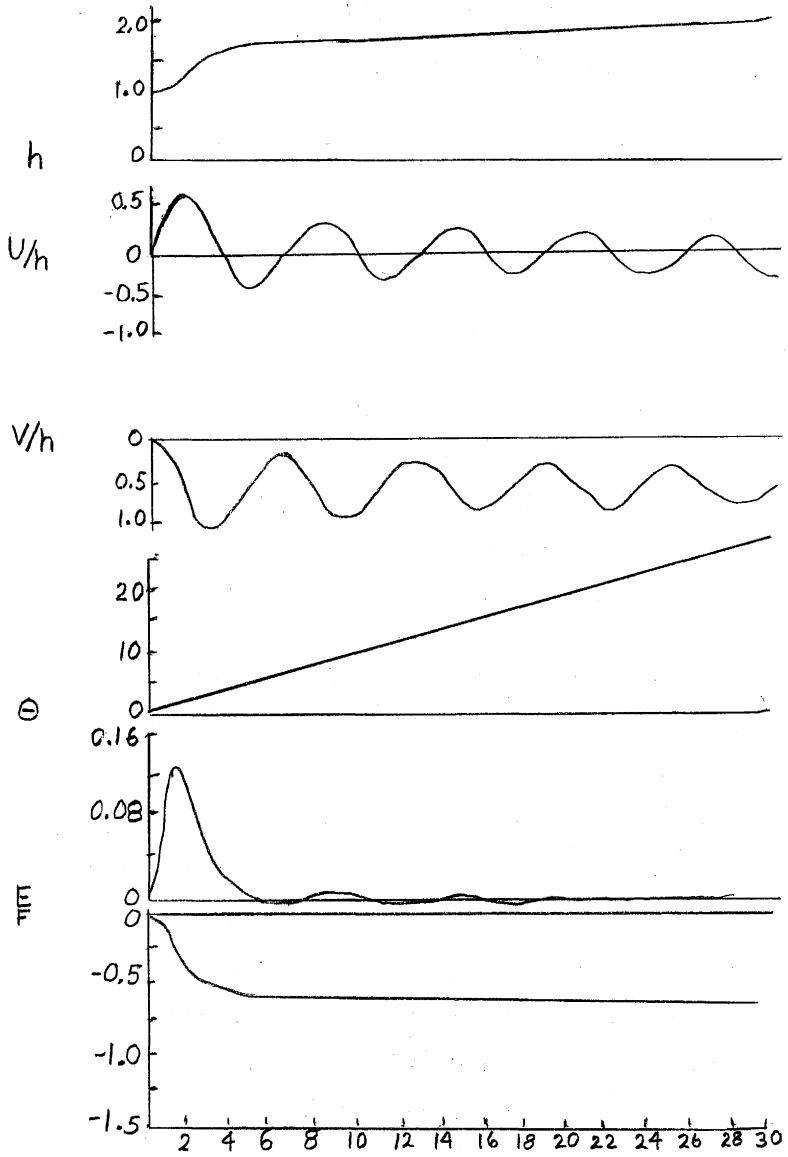

Fig.2

Niiler, P.P. 1974 Deepening of the wind-mixed layer. Unpublished ms.

Phillips, O.M. 1966 The Dynamics of the Upper Ocean. Cambridge University Press, 264 pp.

Pollard, R.T., P.B.Rhines, and Rory Thompson 1973 The deepening of the wind-mixed layer. J.Geophys.Fluid Mech.,3: 381-404.

Notes submitted by

Robert E. Hall.

FREE EQUATORIAL WAVES

Dennis W. Moore

Basic State

Ocean at rest

Density $\rho = \rho_s(z)$

Pressure hydrostatic

$\frac{d\rho_s}{dz} \leq 0$ for stability

Linear Perturbations

u is velocity in the eastward (x) direction

v is velocity in the northward (y) direction

w is vertical (z) velocity

p' is pressure perturbation

ρ' is density perturbation

Assume: The pressure remains hydrostatic. The Boussinesq approximation is valid.

Frictional effects are negligible.

Equatorial β plane: $f = \beta y$

Time Scale $T = \frac{1}{2\Omega}$

Horizontal Length Scale L = R = earth's radius.

Vertical Length Scale H = depth of ocean.

Velocity Scale U for horizontal velocities.

Velocity Scale $\frac{H}{R}U$ for vertical velocity.

Perturbation Pressure scaled by $2\Omega U \rho_0 R$

Perturbation Density scaled by $\frac{2\Omega U \rho_0 R}{gH}$

Let $-\Delta\rho = \rho_s(z_D = H) - \rho_s(z_D = 0)$,

so that $\frac{d\rho_s}{dz} = -\frac{\Delta\rho}{H} s(z)$,

and $s(z)$ is dimensionless, and non-negative.

Nondimensional equations:

$$u_t - yv + p_x = 0, \tag{1}$$

$$v_t + yu + p_y = 0, \tag{2}$$

$$u_x + v_y + w_z = 0, \tag{3}$$

$$p_z = -\rho, \tag{4}$$

$$\text{and } \rho_t - \textcircled{H} w s(z) = 0 \tag{5}$$

$\textcircled{H} = \frac{\Delta\rho}{\rho_0} \frac{g H}{(2\Omega R)^2}$ depends on the density structure of the basic state, and not on the velocity scale of the perturbation.

Equations (4) and (5) give

$$w = \frac{-p_{zt}}{\textcircled{H} s(z)}$$

and substituting this in the continuity equation gives:

$$u_x + v_y = \frac{\partial}{\partial z}\left(\frac{p_{zt}}{\textcircled{H} s(z)}\right) = \mathcal{L} p_t$$

$$\text{where } \mathcal{L} = \frac{\partial}{\partial z}\left(\frac{1}{\textcircled{H} s(z)} \frac{\partial}{\partial z}\right).$$

A single equation for v may be obtained by the following manipulation:

$$\left(-\gamma \mathcal{L} \frac{\partial}{\partial t} - \frac{\partial^2}{\partial x \partial y}\right)\left[u_t - \gamma v + p_x\right] + \left(\frac{\partial^2}{\partial x^2} - \mathcal{L}\frac{\partial^2}{\partial t^2}\right)\left[v_t + \gamma u + p_y\right] +$$

$$+ \left(\frac{\partial^2}{\partial y \partial t} - \gamma \frac{\partial}{\partial x}\right)\left[u_x + v_y - \mathcal{L} p_t\right] = v_{xxt} + v_{yyt} + v_x + \mathcal{L}\left(\gamma^2 v_t + v_{ttt}\right) = 0$$

Vertical Separation

Consider the equations

$$u_t - \gamma v + p_x = 0 \tag{6}$$

$$v_t + \gamma u + p_y = 0 \tag{7}$$

$$u_x + v_y = \mathcal{L} p_t \tag{8}$$

$$\text{where } \mathcal{L} = \frac{\partial}{\partial z}\left(\frac{1}{\textcircled{H} s(z)} \frac{\partial}{\partial z}\right).$$

We can seek separable solutions of the form

$$u = F(z)\, u(x, y, t)$$

$$v = F(z)\, v(x, y, t)$$

$$p = F(z)\, p(x, y, t).$$

Then Eqs. (6), (7), and (8) are separable in z if $\mathcal{L} F(z) = -\lambda F(z)$, where λ is an eigenvalue. We wish to solve $\frac{\partial}{\partial z}\left(\frac{1}{\textcircled{H} s(z)} \frac{\partial F}{\partial z}\right) = -\lambda F$.

Let $G(z) = \frac{1}{\Theta s(z)} \frac{\partial F}{\partial z}$

Then $G_z = -\lambda F$

and $F_z = \Theta s(z) G \Rightarrow G_{zz} = -\lambda \Theta s(z) G.$ (9)

Note that the vertical velocity w is given by $w = -G(z) p_t(x,y,t)$, so $w = 0$ at $z = 0$ and $z = 1$ means $G = 0$ at $z = 0$ and 1.

Equation (9) with these boundary conditions is of Sturm-Liouville type, so there exists a countable set of eigenfunctions $F_n(z)$, $G_n(z)$ with non-negative eignevalues λ_n. Note $F_0(z) = 1$, $G_0(z) = 0$, $\lambda = 0$ is a solution: The barotropic mode.

For the barotropic mode the dimensional equation is

$$\nabla^2 V_t + \beta V_x = 0$$

and there is no distinction between mid-latitude and equatorial motions. If we use a free surface b.c. rather than a rigid lid, the barotropic mode has vertical structure.

A simple case is $s(z) = 1$ corresponding to uniform stratification.

Then $\lambda_0 = \frac{1}{\Theta} \left[\frac{\Delta\rho}{\rho_0} - O\left(\frac{\Delta\rho}{\rho_0}\right)^2 \right]$,

$F_0(z) = 1 - \left(\frac{\Delta\rho}{\rho_0}\right) \frac{z^2}{2} + O\left(\frac{\Delta\rho}{\rho_0}\right)^2$

Note $$\lambda_0 \simeq \frac{1}{\Theta} \frac{\Delta\rho}{\rho_0} = \frac{(2\Omega R)^2}{gH} \simeq O(10).$$

For the baroclinic modes with $s(z) = 1$,

$$F_n(z) \simeq \cos n\pi z$$

and $\lambda_n = \frac{1}{\Theta} \left[n^2\pi^2 + O\left(\frac{\Delta\rho}{\rho_0}\right) \right]$.

$\frac{1}{\Theta} = \frac{(2\Omega R)^2}{\left(\frac{\Delta\rho}{\rho_0}\right) gH} = O(10^4)$.

So the λ_n are large for the baroclinic modes.

Let λ be a non-zero eigenvalue for the vertical separation problem. The horizontal time dependent motion is governed by

$$u_t - yv + p_x = 0$$

$$v_t + yu + p_y = 0$$

$$\lambda p_t + u_x + v_y = 0$$

The equation for V alone is

$$\nabla^2 V_t + V_x - \lambda \left(V_{ttt} + y^2 V_t \right) = 0$$

Consider the possible solutions for which $V \equiv 0$. Then

$$u_t + p_x = 0$$

$$\text{and} \quad \lambda p_t + u_x = 0$$

$$\Rightarrow \lambda u_{tt} - u_{xx} = 0$$

$$u = u(x \pm \lambda^{-1/2} t)\, u(y), \quad p = \mp \lambda^{-1/2} u,$$

with u an arbitrary function.

Then

$$y u + p_y = 0$$

$$\Rightarrow \lambda y u_t - u_{xy} = 0$$

$$\Rightarrow \pm \lambda^{1/2} y u = u_y$$

$$u = u_0 e^{\pm \frac{\lambda^{1/2} y^2}{2}} .$$

For boundedness at $|y| = \infty$ take - sign.

$$\therefore u = u(x - \lambda^{-1/2} t)\, e^{-\frac{\lambda^{1/2} y^2}{2}} = \lambda^{1/2} p .$$

This is the equatorially trapped Kelvin wave, propagating to the east with phase speed $\lambda^{-1/2}$:

Let

$$x = \lambda^{-1/4} x,$$

$$y = \lambda^{-1/4} y,$$

$$t = \lambda^{1/4} t,$$

and

$$p = \lambda^{-1/2} p .$$

This reduces formally to $\lambda = 1$ in above equations. So the canonical system is

$$u_t - y v + p_x = 0,$$

$$v_t - y u + p_y = 0,$$

and

$$p_t + u_x + v_y = 0,$$

but now time and length scales are different for each baroclinic mode.

Separable Solutions

$$V_{xxt} + V_{yyt} + V_x - V_{ttt} - y^2 V_t = 0$$

admits solutions of the form

$$V = e^{i(kx-\omega t)} \psi_m(y),$$

where

$$\psi_m(y) = \frac{e^{-y^2/2} H_m(y)}{\sqrt{2^m m!}\sqrt{\pi}},$$

where H_m is the m^{th} Hermite Polynomial. We call $\psi_m(y)$ a Hermite Function. It satisfies the equation

$$\frac{d^2\psi_m}{dy^2} + (2m+1-y^2)\psi_m = 0$$

so the function ψ_m is oscillatory for $|y| \le \sqrt{2m+1}$, and monotonic (exponentially decaying) for $|y| > \sqrt{2m+1}$. The functions ψ_m have been normalized so that

$$\int_{-\infty}^{\infty} \psi_m(y)\,\psi_n(y)\,dy = \delta_{mn}.$$

Dispersion Relation:

Substituting the solution for V into the differential equation gives the dispersion relation

$$K^2 + \frac{K}{\omega} - \omega^2 + 2m+1 = 0,$$

which may be solved for K as a function of ω to give

$$K = -\frac{1}{2\omega} \pm \sqrt{\omega^2 + \frac{1}{4\omega^2} - (2m+1)}$$

If $m = 0$, the quantity under the radical is a perfect square, and the roots are

$$K = \omega - \frac{1}{\omega} \quad \text{and} \quad K = -\omega.$$

The solution with

$$V = e^{i((\omega-\frac{1}{\omega})x-\omega t)} \psi_0(y)$$

is called a Yanai Wave.

The corresponding u and p fields are

$$u = p = \frac{i\omega}{\sqrt{2}} e^{i((\omega-\frac{1}{\omega})x-\omega t)} \psi_1(y),$$

and involve only a single Hermite Function.

The other $m = 0$ root, $K = -\omega$, is not acceptable on an equatorial β-plane because the corresponding u field grows exponentially in y for

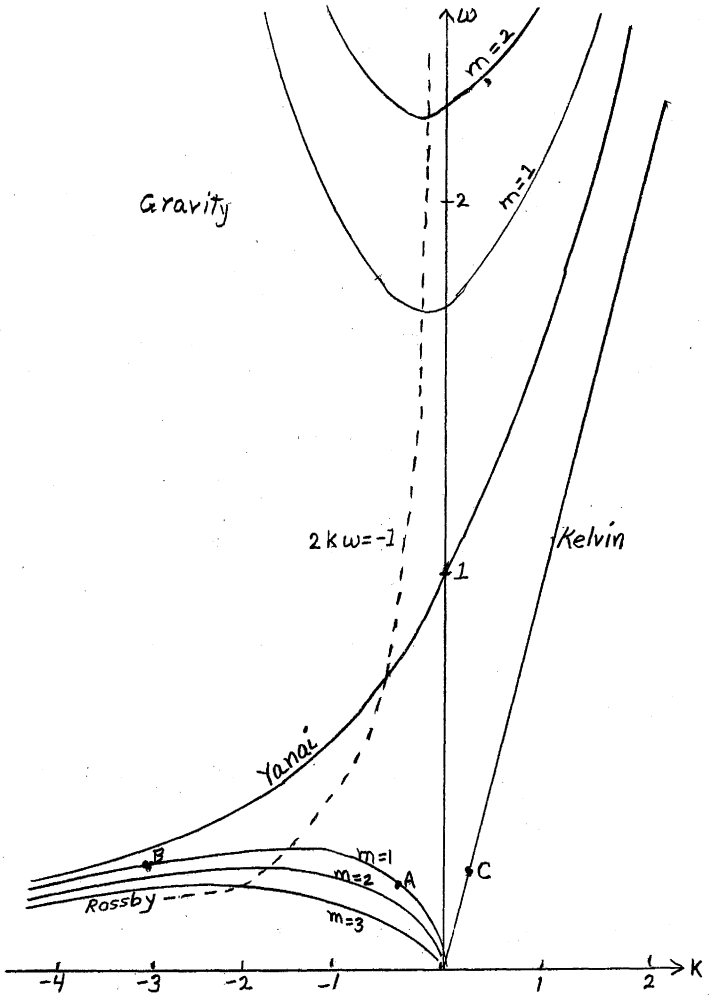

Dispersion relation for waves
on an equatorial beta plane.

large y . For $m \geq 1$,the wave number K is real for real ω as long as the quantity in the radical is positive, which means $|\omega| \geq \sqrt{\frac{m+1}{2}} + \sqrt{\frac{m}{2}}$, or else $|\omega| \leq \sqrt{\frac{m+1}{2}} - \sqrt{\frac{m}{2}}$. This divides the fast gravity waves from the slow planetary waves (see dispersion diagram).

For $\sqrt{\frac{m+1}{2}} + \sqrt{\frac{m}{2}} > |\omega| > \sqrt{\frac{m+1}{2}} - \sqrt{\frac{m}{2}}$, the wave numbers K are complex, with real part $K_{real} = -\frac{1}{2\omega}$ corresponding to westward phase propagation, and imaginary part $K_{Im} = \pm\sqrt{2m+1-\omega^2 - \frac{1}{4\omega^2}}$ corresponding to exponential decay toward the east or the west, depending on choice of sign.

For $m \geq 1$, the u and p fields corresponding to

$$V = e^{i(kx-\omega t)}\psi_m(y) \qquad (10)$$

are $$u = \frac{i}{2} e^{i(kx-\omega t)} \left[\frac{\sqrt{2(m+1)}\,\psi_{m+1}(y)}{\omega - k} + \frac{\sqrt{2m}\,\psi_{m-1}(y)}{\omega + k} \right] \tag{11}$$

and $$p = \frac{i}{2} e^{i(kx-\omega t)} \left[\frac{\sqrt{2(m+1)}\,\psi_{m+1}(y)}{\omega - k} - \frac{\sqrt{2m}\,\psi_{m-1}(y)}{\omega + k} \right] \tag{12}$$

and involve Hermite functions of one order higher and one order lower than the v field.

Energy Density and Energy Flux

In what follows u, v and p mean the real parts of u, v and p.

Multiply

u	by	$u_t - yv + p_x = 0$
v		$v_t + yu + p_y = 0$
p		$p_t + u_v + v_y = 0$

and add

$$\frac{\partial}{\partial t}\left(\frac{u^2+v^2+p^2}{2}\right) = -(up)_x - (vp)_y .$$

Define

$$E = \int_{-\infty}^{\infty} \overline{\frac{u^2+v^2+p^2}{2}}\, dy \quad \text{and} \quad F = \int_{-\infty}^{\infty} \overline{up}\, dy,$$

where the overbar denotes a time average. Then if $v = A e^{i(kx-\omega t)} \psi_m(y)$, etc., with complex amplitude A, we find

$$E = \frac{|A|^2}{4}\left[1 + \frac{m+1}{(\omega-k)^2} + \frac{m}{(\omega+k)^2}\right],$$

and

$$F = \frac{|A|^2}{4}\left[\frac{m+1}{(\omega-k)^2} - \frac{m}{(\omega+k)^2}\right].$$

Exercise for enterprising students:

a) Prove that $C_g E = F$,

where $C_g = \frac{\partial \omega}{\partial k} = \frac{2k + \frac{1}{\omega}}{2\omega + \frac{k}{\omega^2}}$

b) If $v = \sum_{\substack{m \\ s=\pm}} A_{ms} e^{i(kx-\omega t)} \psi_m(y)$, etc.

that $$F = \overline{up} = \sum_{\substack{m \\ s=\pm}} \frac{|A_{ms}|^2}{4} F_{ms}.$$

Half Basin Modes

1. Western Boundary

We require $u = 0$ at the boundary for all time. Consider a single incoming wave $(C_g < 0)$, characterized by ω, m and k (see Eqs.10-12). This wave will either be a planetary or a gravity wave. For these waves there is always another wave of the same frequency, the same value of m and an eastward group velocity. (E.g., see points A $(C_g < 0)$ and $B(C_g > 0)$ on the dispersion diagram. This example has $m = 1$.) The u field corresponding to point A has a y structure of the form

$$u_A \propto \frac{\sqrt{2m+1}}{\omega - k_A} \psi_{m+1}(y) + \frac{\sqrt{2m}}{\omega + k_A} \psi_{m-1}(y)$$

while for point B

$$u_B \propto \frac{\sqrt{2m+1}}{\omega - k_B} \psi_{m+1}(y) + \frac{\sqrt{2m}}{\omega + k_B} \psi_{m-1}(y)$$

By adding a suitable multiple of u_B we can cancel the $\psi_{m+1}(y)$ part of u_A. This will leave a part proportional to $\psi_{m-1}(y)$, which may be cancelled by the wave with frequency ω, $C_g > 0$ and north-south structure characterized by $m-2$.* Continuing in this way we eventually are left with a u field proportional to ψ_0 (if m is odd). This field can be cancelled by a Kelvin wave which has a y structure proportional to ψ_0 and always has group velocity to the east. (If m is even we will eventually be left with u proportional to ψ_1. This may be cancelled by the Yanai wave.)

2. Eastern Boundary

At the eastern boundary, if one were to carry out the same procedure as above, one would eventually be left with a part proportional to ψ_0 or ψ_1. However, in this case there is no mode with a field proportional to ψ_0 or ψ_1 and with group velocity to the west. Therefore one is forced to satisfy the boundary condition $u = 0$ by using an infinite series of higher m modes. (See D.Moore's PhD thesis, Harvard Univ.,1968.) This series converges and for large y represents a Kelvin wave propagating away from the equator along the eastern boundary.

*(In our example, this is point C on the dispersion diagram: the Kelvin wave.)

Notes submitted by
Allan J. Clarke
and Mark A. Cane

FORCED EQUATORIAL WAVE MOTIONS

Dennis W. Moore

The forced problem in the equatorial region is examined by Lighthill (1969). Although there is an error in his analysis (he ignores the equatorial Kelvin wave), his approach to the problem is good. We will examine and extend his results. This lecture will be divided into three sections. First, we will examine the vertical structure of the modes. Second, we will derive the response of an equatorial ocean to forcing. Third, we will look at the effects of meridional boundaries.

I. Vertical Structure

Lighthill treats the surface stress as a body force $\mathcal{F}(z)$ acting on the top mixed layer of dimensionless thickness .05.

$$\mathcal{F}(z) = \begin{cases} 1 & .95 \leq z \leq 1 \\ 0 & 0 \leq z < .95 \end{cases}$$

Let $F_n(z)$ be the eigenfunction giving the vertical structure of the horizontal velocity in the n^{th} mode. $n = 0$ is the barotropic mode while $n = 1,2,3, \ldots$ are the baroclinic modes. F_n is determined by the density profile as shown in the previous lecture. $\mathcal{F}$, $-\bar{\rho}$, F_0, F_1 and F_2 are plotted in Fig.1.

Now expand F in a series of the eigenfunctions F_n

$$\mathcal{F}(z) = \sum_{n=0}^{\infty} a_n F_n(z),$$

where F_n is normalized so that

$$\int_0^1 F_n(z)\, F_m(z)\, dz = \delta_{nm}$$

In the usual manner we find

$$a_n = \int_0^1 \mathcal{F}(z) F_n(z)\, dz = \int_{.95}^1 F_n(z)\, dz,$$

and in particular

$$a_0 = .05.$$

Completeness implies

$$\sum_{n=0}^{\infty} a_n^2 = \int_0^1 \mathcal{F}^2(z)\, dz = .05$$

or

$$\sum_{n=0}^{\infty} \left(\frac{a_n}{a_0}\right)^2 = 20.$$

The R.M.S. forcing amplitude of the barotropic mode accounts for 1/20 of the total.

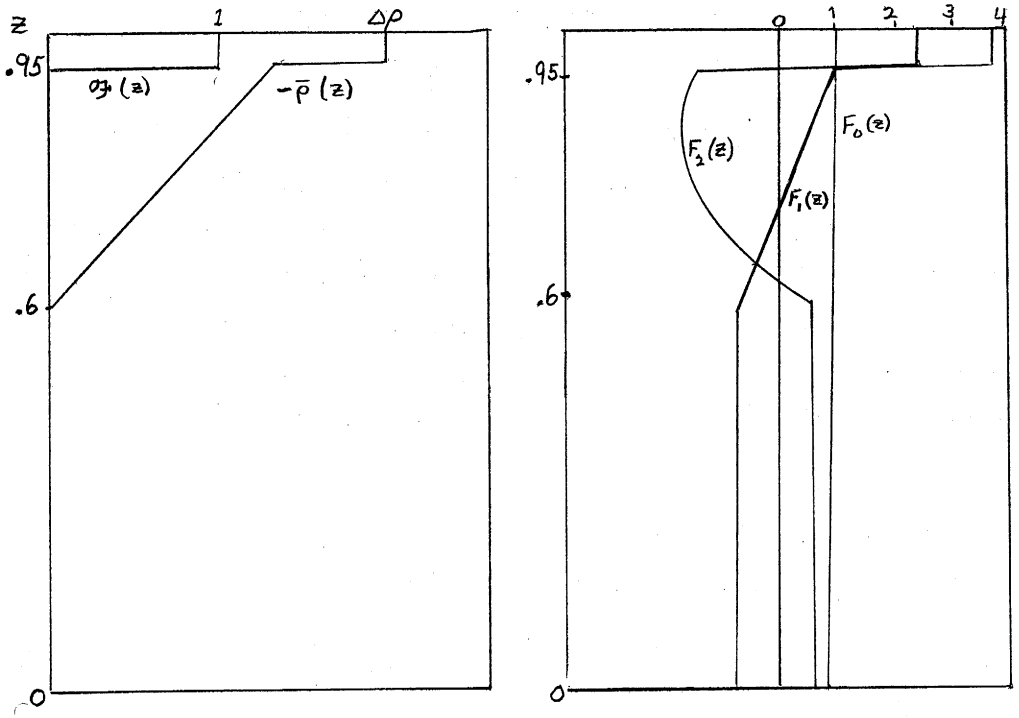

Fig.1

Numerical computation shows that

$$\left(\frac{a_1}{a_0}\right)^2 = 13.93, \quad \left(\frac{a_2}{a_0}\right)^2 = 4.97, \quad \left(\frac{a_3}{a_0}\right)^2 = .09,$$

and

$$\sum_{n=0}^{3}\left(\frac{a_n}{a_0}\right)^2 = 19.986 .$$

This kind of forcing projects onto the 1st and 2nd baroclinic modes and the barotropic mode, in that order, with little energy in the higher vertical modes.

II. Forced Response

Let us consider forcing an equatorial ocean initially at rest by an x-independent zonal wind. The response in each baroclinic mode will be given by the solution of

$$u_t - yv + P_x = A(y)\,S(t), \quad \text{step function in time}$$

$$v_t - yu + P_y = 0,$$

and

$$u_x + v_y + P_t = 0 .$$

If the solution is x-independent we find for $t > 0$

$$u_t + yv + Px = A(y)$$

$$v_t + yu + Py = 0$$

$$P_t + v_y = 0$$

Solving for v we get $v_{tt} + y\left[yv + A(y)\right] - v_{yy} = 0$

Let $A(y) = \sum_{n=0}^{\infty} C_n \psi_n(y)$.

Then $yA(y) = \sum_{n=0}^{\infty} C_n \left[\sqrt{\frac{n+1}{2}}\,\psi_{n+1}(y) + \sqrt{\frac{n}{2}}\,\psi_{n-1}(y)\right]$.

Let $v = \sum_{n=0}^{\infty} v_n(t)\,\psi_n(y)$, where

$$v_{n_{tt}} + (2n+1)v_n + \sqrt{\frac{n}{2}}\,C_{n-1} + \sqrt{\frac{n+1}{2}}\,C_{n+1} = 0$$

Then $$v_n = \frac{\sqrt{\frac{n}{2}}\,C_{n-1} + \sqrt{\frac{n+1}{2}}\,C_{n+1}}{2n+1}\left[\cos\sqrt{2n+1}\,t - 1\right],$$

and $$u = tA(y) + y\sum_{n=0}^{\infty} d_n \psi_n \left[\frac{\sin\sqrt{2n+1}\,t}{2} - t\right],$$

where $$d_n = \frac{\sqrt{\frac{n}{2}}\,C_{n-1} + \sqrt{\frac{n+1}{2}}\,C_{n+1}}{2n+1}$$

So, in general

$$u = t u_1(y) + u_2(y,t)$$

$$v = v_1(y) + v_2(y,t)$$

and $$P = tP_1(y) + P_2(y,t)$$

where $$u_1 - yv_1 = A(y)$$

$$yu_1 + P_1 y = 0$$

and $$P_1 + v_1 y = 0$$

Solving for v_1 we find $y\left[yv_1 + A(y)\right] - v_{1yy} = 0$

The "2" field satisfies $u_{2t} - yv_2 = 0$

$$v_{2t} + yu_2 + P_{2y} = 0$$

and $$P_{2t} + v_{2y} = 0$$

Solving for V_2 we find

$$V_{2tt} + y^2 V_2 - V_{2yy} = 0$$

We will call these the inertial oscillations. We will take as an example the case considered by Yoshida (1959).

Let $A(y) \equiv 1$.

V_1 now satisfies $V_{1yy} - y^2 V_1 = y$.

Expanding A we have $1 = \sum_{n=0}^{\infty} I_n \psi_{2n}(y)$,

where $I_n = \frac{2^{1/2} \pi^{1/4}}{2^n n!} \sqrt{(2n)!}$

Solving for V_1 and computing u_1, from the equation of motion above we get

$$u_1(y) = -2 \sum_{m=0}^{\infty} \frac{I_m \psi_{2m}(y)}{(4m+3)(4m-1)},$$

so u_1 looks mostly like $\psi_0(y)$. u_1, V_1, and p_1 are shown in Fig.2. Notice that the equatorial response is highly localized.

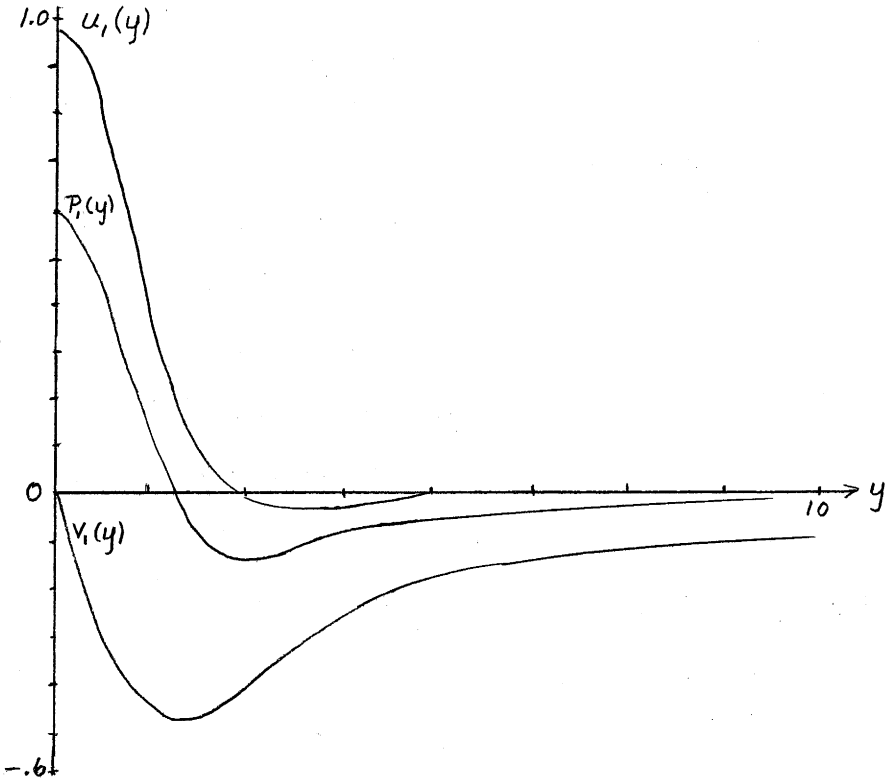

Fig.2

III. Effect of a Meridional Boundary

Consider first the portion of the forced solution that looks like

$$u = t\,\psi_0(y).$$

In order to cancel this at the western boundary x = 0, we must add the free Kelvin wave $u = (x-t)\,\psi_0(y)\,S(t-x)$ where S is a step function. Examining the balance of terms in the x-momentum equation we find that the forcing is balanced by u_t prior to the arrival of the Kelvin wave and by p_x thereafter.

Since the Kelvin wave can only propagate to the east, the reflection from an eastern boundary is another story. The low frequency, westward propagating waves are located just to the left of the origin on the dispersion graph that accompanies the previous lecture. As $\omega \to 0$ we find

$$c_p = \frac{\omega}{K} \doteq -\frac{1}{2n+1}.$$

In order to cancel the aforementioned solution at the eastern boundary, we would need terms that look like

$$v = f_1\left(x + \frac{t}{3}\right)\psi_1(y) + f_3\left(x + \frac{t}{7}\right)\psi_3(y) + \cdots$$

The lower order waves that are trapped closer to the equator propagate westward faster than the higher order waves.

Now let us consider the reflection from a western boundary of the portion of the forced solution that looks like

$$u = t\,\psi_n(y), \quad n \geq 1.$$

We will do this by looking at the forced problem with $A(y) = \psi_{n-1}(y)$. The equations of motion are

$$u_t - yv + p_x = \psi_{n-1}(y)\,S(t)$$
$$v_t + yu + p_y = 0$$
$$p_t + u_x + v_y = 0$$

The x-independent solution is

$$v = -\frac{\sqrt{\frac{n}{2}}}{2n+1}\psi_n(y)\left[1 - \cos\sqrt{2n+1}\,t\right] - \frac{\sqrt{\frac{n-1}{2}}}{2n-3}\psi_{n-2}(y)\left[1 - \cos\sqrt{2n-3}\,t\right]$$

$$u = t\psi_{n-1}(y) - \frac{\sqrt{\frac{n}{2}}}{2n+1}\left[t - \frac{\sin\sqrt{2n+1}\,t}{\sqrt{2n+1}}\right]\left[\sqrt{\frac{n+1}{2}}\psi_{n+1} + \sqrt{\frac{n}{2}}\psi_{n-1}\right] -$$
$$- \frac{\sqrt{\frac{n-1}{2}}}{2n-3}\left[t - \frac{\sin\sqrt{2n-3}\,t}{\sqrt{2n-3}}\right]\left[\sqrt{\frac{n-1}{2}}\psi_{n-1} + \sqrt{\frac{n-2}{2}}\psi_{n-3}\right]$$

We want to add free waves to this so that we can satisfy the b.c. at $x = 0$. Let us cancel the ψ_{n+1} term first, then proceed down the ladder to $n = 0$.

Suppose $v = v_n(x,t)\psi_n(y)$,

then $$u = u_{n+1}(x,t)\psi_{n+1}(y) + u_{n-1}(x,t)\psi_{n-1}(y)$$
$$p = u_{n+1}(x,t)\psi_{n+1}(y) - u_{n-1}(x,t)\psi_{n-1}(y),$$

where u_{n+1} satisfies

$$\frac{\partial}{\partial t}\left[\frac{\partial^2}{\partial t^2} - \frac{\partial^2}{\partial x^2}\right]u_{n+1} + \left[(2n+1)\frac{\partial}{\partial t} - \frac{\partial}{\partial x}\right]u_{n+1} = 0.$$

Taking the Laplace Transform we have

$$s\left(s^2 - \frac{\partial^2}{\partial x^2}\right)\bar{u}_{n+1} + \left[(2n+1)s - \frac{\partial}{\partial x}\right]\bar{u}_{n+1} = 0,$$

where $$\bar{u}_{n+1} = \mathcal{L}\{u_{n+1}(x,t)\} \equiv \int_0^\infty e^{-st}\, u_{n+1}(x,t)\, dt.$$

The solution to the above equation is of the form

$$\bar{u}_{n+1} = \bar{F}(s)e^{kx}$$

Substituting this into the equation yields

$$k^2 + \frac{k}{s} - (2n+1) - s^2 = 0$$
$$k = -\frac{1}{2s} \pm \sqrt{s^2 + (2n+1) + \frac{1}{4s^2}}$$

We take the lower sign so that the solution remains bounded as $x \longrightarrow \infty$:

$$\bar{u}_{n+1} = \bar{F}(s)e^{-\frac{x}{2s} - x\sqrt{s^2 + (2n+1) + \frac{1}{4s^2}}}.$$

We want $\bar{u}_{n+1}$ to cancel the ψ_{n+1} term in the forced problem at $x = 0$; so

$$\bar{F}(s) = \mathcal{L}\left\{\frac{\sqrt{n}}{2n+1}\left[t - \frac{\sin\sqrt{2n+1}\,t}{\sqrt{2n+1}}\right]\sqrt{\frac{n+1}{2}}\,\psi_{n+1}\right\}.$$

The inverse transform is

$$u_{n+1}(x,t) = \mathcal{L}^{-1}\{\bar{u}_{n+1}\} \equiv \frac{1}{2\pi i}\int_{c-i\infty}^{c+i\infty} \bar{F}(s)e^{st - \frac{x}{2s} - x\sqrt{\left(s - \frac{1}{2s}\right)^2 + 2(n+1)}}\, ds,\ c > 0.$$

There are four branch points on the imaginary axis at

$$s = \pm i\sqrt{\frac{n+1}{2}} \pm i\sqrt{\frac{n}{2}}.$$

We place the two branch cuts between the upper pair and between the lower pair. The term in the exponent can be rewritten as

$$s(-x+t) + x\left[s - \frac{1}{2s} - \sqrt{\left(s - \frac{1}{2s}\right)^2 + 2(n+1)}\right]$$

As $s \longrightarrow \infty$, the term in the brackets goes to zero; so if $x > t$, we can close the contour in the RHP and

$$u_{n+1}(x,t) = 0, \quad x > t.$$

Nothing propagates to the right faster than the gravity wave speed. If $x < t$, we close the contour in the LHP and from $F(s)$ we get a term which basically cancels the inertial oscillations.

Proceeding in the same manner, we cancel the lower order terms.

Discussion

Stern: Shouldn't one take the undercurrent into consideration when doing the problem?

Moore: The undercurrent does not affect the barotropic or first baroclinic modes because the phase speeds are too high. The interaction occurs at the second baroclinic mode.

References

Lighthill, M.J. 1969 Dynamic Response of the Indian Ocean to the Onset of Southwest Monsoon. PTRSL A 265: 45-92.

Yoshida, Kozo 1959 A Theory of the Cromwell Current and of the Equatorial Upwelling. J.Oceanogr.Soc.Japan 15: 154-170.

Notes submitted by
Robert E. Hall

TOPOGRAPHIC AND PLANETARY WAVES: LINEAR THEORY

Peter B. Rhines

In this lecture we discuss the linear theory of ocean waves with frequencies $\omega < f \equiv 2\Omega \sin(\text{latitude})$ (i.e. periods $\gtrsim 1$ pendulum day). We consider waves whose horizontal scale is of the order of 2π times the Rossby radius of deformation (~ 250 km). A study of these waves is important since the kinetic energy is known to be dominated by mesoscale waves and eddies with time scales of many days. Motions on these scales are also thought to have significant interactions with the mean flow and to be important for understanding the spin-up of the oceans.

We now consider the simplest accepatble model: f-plane approximation, small, uniform, plane bottom slope, uniform stratification ($N^2(z) \equiv -g\bar{\rho}^{-1}\partial\bar{\rho}/\partial z =$ constant), Boussinesq fluid. The governing equations are non-dimensionalized using a characteristic horizontal velocity, U, for the horizontal velocities (u,v), characteristic horizontal and vertical lengths L and H for the horizontal (x,y) and vertical (z) coordinates respectively, UH/L for the vertical velocity (w), $\rho_0 f U L$ for the pressure, f^{-1} for the time and $\rho_0 f U L/(gH)$ for the density. Let

$$B = \frac{NH}{fL}$$

The model considered is shown in the following diagram:

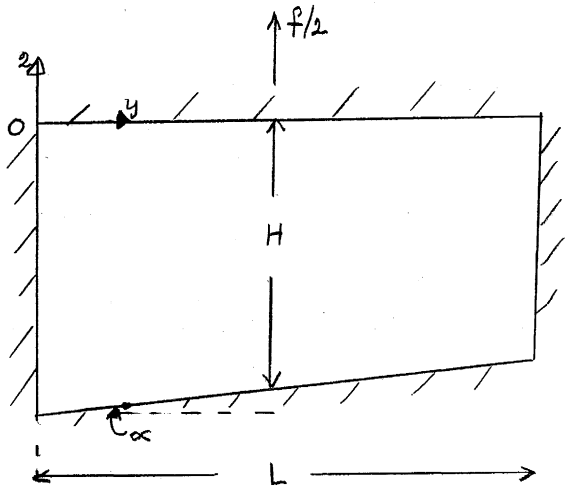

We linearize the equations and look for motions $\propto e^{-i\omega t}$, giving:

$$\left.\begin{aligned} -i\omega u - v &= -p_x \,, \\ -i\omega v + u &= -p_y \,, \\ -i\omega (H/L)^2 w &= -p_z - \rho \,, \\ -i\omega\rho - B^2 w &= 0 \\ u_x + v_y + w_z &= 0 \end{aligned}\right\} \qquad (1)$$

We assume that the bottom slope, α, is small, with

$$\delta \equiv \frac{\alpha L}{H} << 1.$$

Then the (linearized) boundary conditions are

$$w\big|_{z=0} = 0 \qquad w\big|_{z=0} = 0, \qquad \frac{w}{v}\Big|_{z=-1+\delta(y-1/2)} = \delta.$$

u, v, w, ω, p and ρ are expanded in the form:

$$\psi = \psi^{(0)} + \delta\,\psi^{(1)} + O(\delta^2).$$

The zero-order state is assumed to be steady ($\omega^{(0)} = 0$) and is in geostrophic balance: $u^{(0)} = p_y^{(0)}$, $v^{(0)} = p_x^{(0)}$, $w^{(0)} = 0$, $\rho^{(0)} = -p_z^{(0)}$.

The $O(\delta)$ terms give

$$\left.\begin{aligned} v^{(1)} - p_x^{(1)} &= -i\omega^{(1)} p_y^{(0)}, \\ u^{(1)} + p_y^{(1)} &= i\omega^{(1)} p_x^{(0)}, \\ p_z^{(1)} + \rho^{(1)} &= 0, \\ w^{(1)} &= iB^{-2}\omega^{(1)} p_z^{(0)}, \\ u_x^{(1)} + v_y^{(1)} + w_z^{(1)} &= 0, \end{aligned}\right\} \qquad (2)$$

with the boundary conditions

$$w^{(1)}\Big|_{z=0} = 0, \qquad w^{(1)}\Big|_{z=1} = v^{(0)}.$$

Since the above perturbation scheme is used only to find the slow evolution of the zero-order field, it may therefore be valid even if the first order quantities are not small, provided they change sufficiently slowly. From (2) we obtain

$$i\omega^{(1)}\left(\nabla_2^2 p^{(0)} + B^{-2} p_{zz}^{(0)}\right) = 0 \quad \text{where } \nabla_2^2 \equiv \partial_x^2 + \partial_y^2 \qquad (3)$$

with the boundary conditions

$$p_z^{(0)}\Big|_{z=0} = 0, \quad i\omega^{(1)} B^{-2} p_z^{(0)} = p_x^{(0)} \text{ at } z = -1.$$

This is an eigenvalue problem for $\omega^{(1)}$ and has the horizontally plane wave solutions:

$$\left.\begin{aligned} p^{(0)} &= \text{constant} \times e^{i(kx+ly)} \cosh \mu z, \quad \mu^2 = B^2(k^2+l^2), \\ \omega^{(1)} &= -\frac{kB^2}{\mu \tanh \mu} \end{aligned}\right\} \qquad (4)$$

(4) provides the dispersion relation. We consider first the two limits $\mu \ll 1$ and $\mu \gg 1$ which correspond to wavelengths that are respectively long and small compared with $2\pi\times$ (Rossby radius of deformation).

(1) Long wave limit ($\mu \ll 1$) : From (4), the dimensional frequency is

$$\sigma \sim -\frac{f\alpha}{H}\frac{k}{k^2+l^2}$$

The quantity $f\alpha/H$ corresponds to the β in the dispersion relation for Rossby waves on a β-plane. The vertical structure is nearly uniform, as would be expected from the Taylor-Proudman theorem, with a small shear that increases with depth.

(2) Short wave limit $(\mu \gg 1)$: From (4), the dimensional frequency is

$$\sigma \sim - \alpha N \sin\phi$$

where ϕ is defined as the angle between $\underset{\sim}{k} = (k, \ell, 0)$ and the y-direction. For a slope of finite amplitude the frequency becomes

$$\sigma = - \sin \alpha N \sin\phi .$$

In this case the frequency depends only on the direction of $\underset{\sim}{k}$ and not on its magnitude and so the group velocity is perpendicular to $\underset{\sim}{k}$ in the horizontal plane. This is similar to the dispersion of internal gravity waves for which ϕ is the angle between $\underset{\sim}{k}$ and the vertical. The vertical structure is $\sim e^{-\mu z}$, so that the waves are exponentially trapped at the bottom, with an e-folding depth of $f^2/(N^2 |\underset{\sim}{k}|^2)$. This behavior resembles that of Kelvin waves and Lamb waves near boundaries.

The dispersion relation (4) can be visualized by plotting the lines of constant frequency in the wavenumber space, as shown in the following diagram:

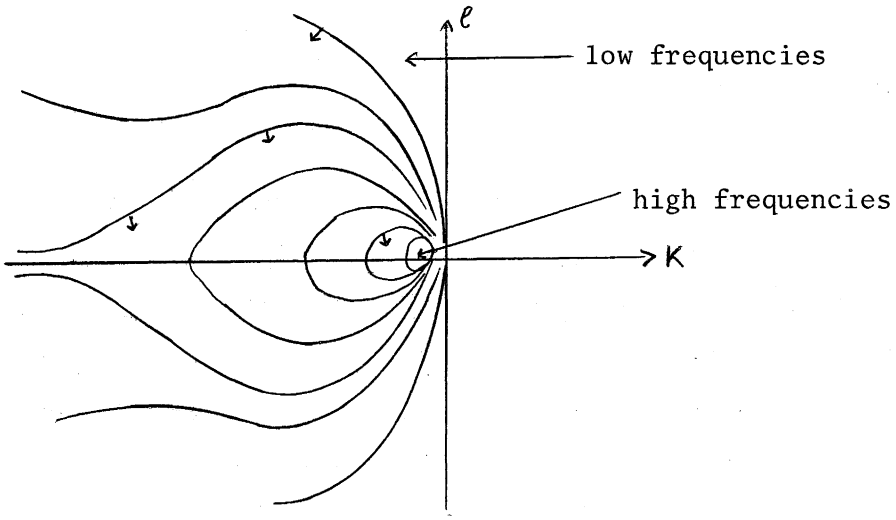

The arrows point in the direction of the group velocity, $\underset{\sim}{c}_g$. It is interesting to note that $\underset{\sim}{c}_g$ remains finite as $\omega \to 0$. One might therefore use the concept of group velocity for energy flow or region-of-influence considerations even in steady flows.

The above may be generalized to the case of arbitrary stratifications, N(z). If one is interested mainly in the dispersion relation rather than the details of the vertical structure, one can find $\omega^{(1)}$ by a Rayleigh-Ritz technique, observing that

$$\omega^{(1)} = \min_{P} \frac{-K|P|^2_{z=-1}}{\int_{-1}^{0} \left[|\underset{\sim}{K}|^2 |P|^2 + B(z)^{-2} P_z^2\right] dz}, \tag{5}$$

since the minimum of the functional of P on the right-hand side of (5) occurs when P(z) is a solution of the eigenvalue problem corresponding to (3).

The solution of an initial value problem for constant stratification is found by inspection to have Fourier components given by

$$P^{(0)} = e^{i(kx+ly)} F(z,t)$$

where

$$F(z,t) = F(z,0) + F(-1,0)\ \frac{\cosh \mu z}{\cosh \mu}\left(e^{-i\omega t} - 1\right),\quad \mu^2 = B^{-2}(k^2+l^2). \tag{6}$$

We now consider waves on a β-plane. We let $f = f_0(1 + Ly/R)$ where $R = R_{\text{earth}} \tan(\text{latitude})$, so that (3) is replaced by

$$-i\omega^{(1)}\left[\nabla_2^2 P^{(0)} + B^{-2} P_{zz}^{(0)}\right] + \frac{L}{\delta R} P_x^{(0)} = 0 \tag{7}$$

For solutions $\propto e^{i(kx+ly)}$, there are both barotropic modes varying like $\cosh \mu z$ and baroclinic modes varying like $\cos m z$ with the dispersion relation:

$$\omega^{(1)} = -\frac{KL/(\delta R)}{k^2 + l^2 + B^{-2} m^2} \tag{8}$$

where m is given by

$$m \tan m = -\frac{\delta R}{L}\left[(k^2+l^2)B^2 + m^2\right] \tag{9}$$

(9) is a transcendental equation for m from which m is determined by the interaction of $m \tan m$ with a parabola. As illustrated in the following diagram for the lowest internal mode, the current reverses direction in the limit $\delta \longrightarrow 0$ whereas it decreases monotonically with depth for large δ. For large δ the phase velocity of the waves is about four times the value for small δ and so the effect of the slope is to speed up the waves and thus the baroclinic adjustment.

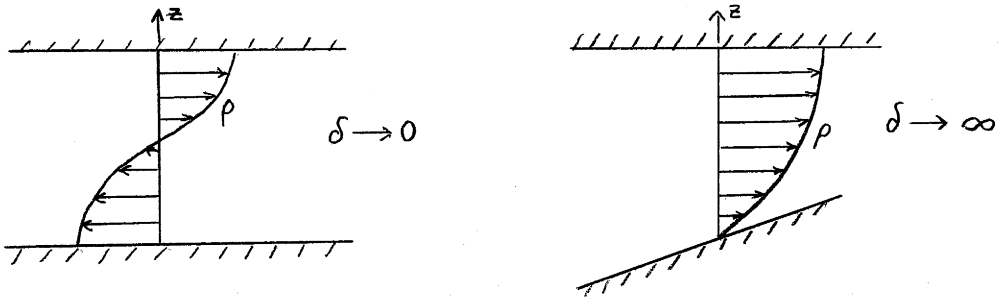

Notes submitted by
Rosemary G. Kennett
and Jürgen Willebrand

TOPOGRAPHIC AND PLANETARY WAVES: NONLINEAR THEORY

Peter B. Rhines

In the last lecture linear theories for planetary waves were discussed. The problem now is to prove the waves indeed occur in the ocean. One approach is to prove from observations that the derived dispersion relations hold. This, however, is difficult to do even with simple gravity waves.

Rory Thompson and J.R.Luyten (unpublished, 1974) did try to observe short, topographically controlled waves, whose theoretical dispersion relation is $\omega = -N\alpha \sin\phi$

(where N = buoyancy frequency
α = bottom slope
ϕ = angle between the horizontal wave number vector and gradient of the bottom topography).

To this end, they considered data from site D, a current meter and temperature sensor mooring located about 50 km south of the continental shelf, and north of where the separated Gulf Stream travels. The relevant periods are in the range of 4 to 15 days. The records at 2500 m depth, or about 100 m above the bottom, were considered. They plot the principal axes of the band-passed vector velocities for each frequency interval. The anisotropy of the dispersion relation is thereby exhibited.

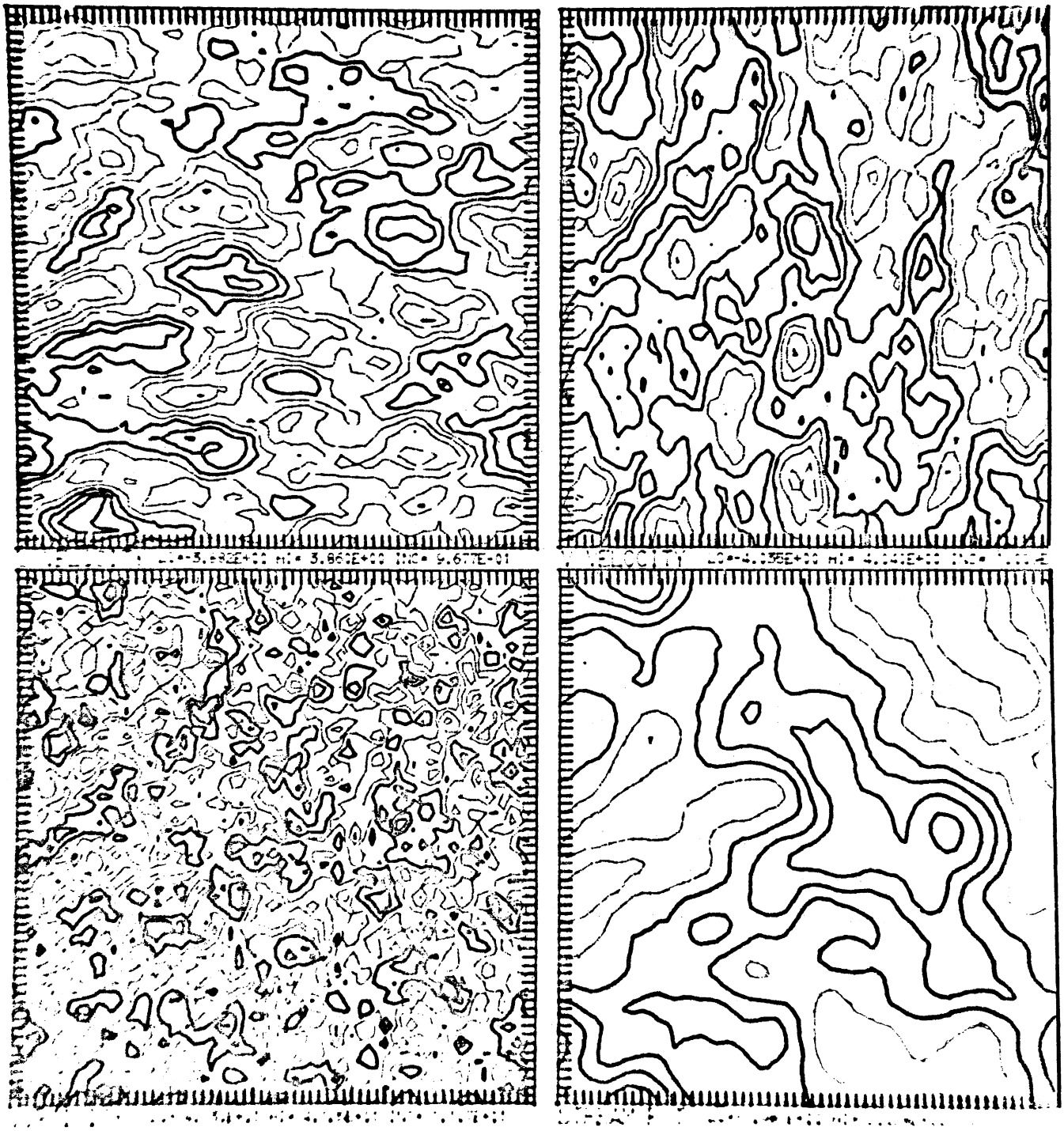

A reminder of the disparity in apparent length scales among various related fields: lower right: stream function, ψ, or pressure; upper right: corresponding v-velocity, $\partial\psi/\partial x$; upper left: u-velocity, $-\partial\psi/\partial y$; lower left: vorticity, $\nabla^2\psi$. The (isotropic) wavenumber spectrum of the velocities is $E(k) = 1.0$ for $k \leq 5$, $E = (k/5)^{-3}$ for $k > 5$. Note how the velocities are better correlated ('larger scale') downstream than across-stream.

Another observational approach is that of Munk, Brown, Snodgrass, Mofjeld, Zetler (submitted to J.Phys.Oc., for publication, 1974), in which bottom pressures were measured in the MODE region. This is motivated by the relation:

$$\frac{\nabla p}{\rho_0} \cong -f \times \underline{u}$$

for quasi-geostrophic flows. It is argued (see included illustrations of flow fields) that integration smoothes, and that differentiation roughens. Since velocities are obtained by differentiating pressure, it is expected that the pressure field be "smoother", i.e., coherent over a larger scale, than the velocity field. This seems to be in agreement with the data, which indicates coherence over at least 700 km. The data display large-scale coherence at periods 5 - 20 days, while the velocity data show smaller scales dominating at longer periods (60 - 200 days). This gives qualitative agreement with the Rossby wave-type dispersion relation,

$$\omega \sim -\frac{\beta}{k},$$

as opposed to a turbulence-type relation,

$$\omega \sim |\underline{k}|$$

At this point a movie was shown of Rossby and Webb's neutrally buoyant floats, taken during the MODE experiment, demonstrating mesoscale oceanic flows at 1500 m depth.

Now, we begin to look at the heart of the lecture, Rhines' studies of two-dimensional turbulent flows. To do this, he considers a two-layer model, solved with cyclical boundary conditions, and satisfying the vorticity equations that Phillips used for the atmosphere:

$$\frac{d_1}{dt}\left[\nabla^2\psi_1 + \varepsilon_1(\psi_2 - \psi_1) + \beta y\right] = 0$$

$$\frac{d_2}{dt}\left[\nabla^2\psi_2 + \varepsilon_2(\psi_1 - \psi_2) + \beta y\right] = 0$$

where

$$\varepsilon_i = \frac{f^2}{\left(g\frac{\Delta\rho}{\rho} H_i\right)}$$

and

$$\frac{d_i}{dt} = \frac{\partial}{\partial t} + J$$

for $i = 1$ or 2, for the upper and lower layers, respectively. The H_i represents the mean depths of layers. No bottom topography is included. There are two important horizontal scales corresponding to:

k_ρ^{-1} = internal Rossby radius $\cong$ 50 km for the ocean.

$$\left[k_\rho^2 = \frac{f^2}{g\frac{\Delta\rho}{\rho}}\left(\frac{1}{H_1}+\frac{1}{H_2}\right)\right]$$

$$k_\beta^{-1} = \left(\frac{2U}{\beta}\right)^{1/2},$$

where U is an R.M.S. particle speed.

First, consider the strongly stratified fluid on an f-plane ($\beta = 0$). Initially the scale of the motions is much smaller than the Rossby radius of deformation. Both layers start with random, unrelated, velocity fields, and then cascade independently toward larger scales of motion. When the scale of motion nears the Rossby radius of deformation, upper and lower layer motions become coupled (roughly like the atmospheric process of occlusion), and the fluid behaves barotropically, continuing to progress toward larger scales of motion. Nonlinearities of the mathematical form $\underline{u}\cdot\nabla\underline{u}$ are very important in this cascade process.

Nonlinearity of the types $\underline{v}\cdot\nabla\eta$ (η = deflection from mean of the interface height) is also demonstrated. The starting state is a nearly pure baroclinic Rossby wave, of large scale. The wave is unstable, and cascades its energy to wavenumber k_ρ, then the fluid 'occludes' (eddies at different depths locking together), tending toward a barotropic state. Next, the barotropic eddies act like 2-d turbulence, clustering toward larger scales until reaching k_β where the field (now barotropic Rossby waves of steepness unity) equilibrates. This complex history (cascade from large scale to small, then back toward large, cascade from potential energy to kinetic) is roughly analogous to the index cycle in the atmosphere. But here, without a maintained zonal flow, the 'jet-sharpening' role of atmospheric eddies is not found, and the late stages involve simply a field of weakly interacting Rossby waves. The scale of motion grows, and the fluid tends toward a barotropic state, and the cascade to small wavenumbers is stopped whan the scale is of order k_β.

Notes submitted by
Kenneth H. Brink
and Laurence D. Armi.

RAY THEORY

Joseph B. Keller

Ray theory is a method of reducing a partial differential equation (PDE), to a set of ordinary differential equations (ODE's). It is based on the assumption that it is easier to solve ODE's than it is to solve PDE's. For a first order PDE, ray theory is just the method of characteristics.

1) Let us begin with a simple ODE.

$$\frac{dA}{d\sigma} + f(\sigma)A = g(\sigma) \tag{1}$$

The initial condition is $A(\sigma_0) = A_0$.

The solution to (1) with the initial condition is:

$$A(\sigma) = A_0 \exp\left[-\int_{\sigma_0}^{\sigma} f(\sigma')\,d\sigma'\right] + \int_{\sigma_0}^{\sigma} \exp\left[-\int_{\sigma'}^{\sigma} f(\sigma'')\,d\sigma''\right] g(\sigma')\,d\sigma' \tag{2}$$

This result can be used to solve a linear, first order PDE, as we shall now show.

2) Take a partial differential equation of the form:

$$K_1 \partial_{x_1} A + \cdots + K_n \partial_{x_n} A + f A = g \tag{3}$$

We define a curve $x_1(\sigma), \ldots, x_n(\sigma)$ such that:

$$\frac{dx_1}{d\sigma} = K_1, \ldots, \frac{dx_n}{d\sigma} = K_n \tag{4}$$

with initial conditions:

$$x_1(\sigma_0) = x_1^0, \ldots, x_n(\sigma_0) = x_n^0$$

This curve is a ray, or characteristic curve of the PDE (3). Equations (4) form a system of ODE's.

Next we write

$$A\left[x_1(\sigma), \ldots, x_n(\sigma)\right] = A(\sigma)$$

so that

$$\frac{dA}{d\sigma} = \frac{\partial A}{\partial x_1}\frac{dx_1}{d\sigma} + \cdots + \frac{\partial A}{\partial x_n}\frac{\partial x_n}{\partial \sigma}$$

$$= A_{x_1} K_1 + \cdots + A_{x_n} K_n \tag{5}$$

By substituting this into the original PDE, Eqn.(3), we get:

$$\frac{dA}{d\sigma} + fA = g \tag{6}$$

which is exactly the same as Eqn.(1).

It is now necessary to look at the initial conditions for Eqn.(3) before we solve (6). Assume that there is some k-dimensional manifold (point, curve, . . .) Γ given parametrically by

$$x_1 = x_1^0(t_1, \ldots, t_k)$$
$$x_n = x_n^0(t_1, \ldots, t_k) \tag{7}$$

Here k is an integer in the range $0 \leq k \leq n-1$. On this manifold Γ we give the initial value of A in the form

$$A(x_1^0(t_1, \ldots, t_k), \ldots, x_n^0(t_1, \ldots, t_k)) = A_0(t_1, \ldots, t_k) \tag{8}$$

To find A at points off Γ, we take a point on Γ and solve for the ray through it. Then we solve (6) along this ray with the initial value $A_0 = A(\sigma_0)$ given by (8). The solution gives the solution of (3) in the region covered by the rays.

3) Now let us look at nonlinear first order PDE's. Take a general equation of the form:

$$F(x, s, p) = 0 \tag{9}$$

Here $x = (x_1, \ldots, x_n)$ and $p = (p_1, \ldots, p_n)$ where $p_i = \frac{\partial s}{\partial x_i}$. The initial conditions are $s = s_0$ on Γ. Introduce rays or characteristics

$$x = x(\sigma), \quad s = s(\sigma), \quad p = p(\sigma)$$

The system of ODE's for these rays is:

$$\frac{dx}{d\sigma} = F_p; \quad \frac{dp}{d\sigma} = -F_x - p F_s, \quad \frac{ds}{d\sigma} = p \cdot F_p \tag{10}$$

This is a set of 2n + 1 equations for 2n + 1 functions. The method of arriving at these equations will not be given here. Instead it will be shown that they enable us to solve (9) for s.

To solve these 2n + 1 equations, 2n + 1 initial conditions must be specified. The requirement that a ray start at a particular point x^0 of Γ yields n conditions. The fact that $s(x^0) = s^0$ is another condition. Then the equation (9) yields a condition on the initial value p^0 of p:

$$F(x^0, s^0, p^0) = 0 \tag{11}$$

To obtain further conditions we write the initial condition on S in the form:

$$S\left[x^0(t_1, \cdots, t_K)\right] = s^0(t_1, \cdots t_k) \tag{12}$$

When this is differentiated with respect to t_j the following results:

$$\partial_{x_1} s \frac{\partial x_1^0}{\partial t_j} + \cdots + \partial_{x_n} s \frac{\partial x_n^0}{\partial t_j} = \frac{\partial s^0}{\partial t_j}, \; j = 1, \cdots, K$$

or

$$p^0 \cdot \frac{\partial x^0}{\partial t_j} = \frac{\partial s^0}{\partial t_j}; \; j = 1, \cdots, k \tag{13}$$

This gives k more restrictions on the initial values, for a total of n+k+2 restrictions. Thus there are (2n+1) - (n+k+2) = n-k-1 parameters free in the choice of p^0 at each point.

By construction the initial conditions satisfy F = 0 at $\sigma = \sigma_0$. Furthermore we have

$$\frac{dF}{d\sigma} = F_x \frac{dx}{d\sigma} + F_s \frac{ds}{d\sigma} + F_p \frac{dp}{d\sigma}$$

Substitution from (10) gives

$$\frac{dF}{d\sigma} = F_x F_p + F_s (p \cdot F_p) + F_p (-F_x - p f_s) = 0$$

Combining this result with Eqn. (11) gives $F(x, s, p) = 0$ along each characteristic. Thus each solution of (10), satisfying the initial conditions, yields the solution s of (9) along one ray issuing from Γ.

On Γ there is a k parameter family of points and n-(k+1) characteristics issue from each point. Thus there is an (n-1) parameter family of characteristics. Each characteristic has a one-parameter family of points so in all we have an n-parameter family of points. Thus in general the characteristics cover an n-dimensional neighborhood of Γ, and yield the solution s there.

Now for an example of how to use this technique, we consider the eiconal equation

$$(\nabla s)^2 = 1 \tag{14}$$

In the form we are using, this is

$$F = p^2 - 1 = 0$$

The ray equations (10) now give

$$\frac{dx}{d\sigma} = 2p \quad \Rightarrow \quad x = x^0 + 2p\sigma \tag{15}$$

$$\frac{dp}{d\sigma} = 0 \quad \Rightarrow \quad p = p^0 \tag{16}$$

$$\frac{ds}{d\sigma} = 2p^2 \quad \Rightarrow \quad s = s^0 + 2p^2\sigma \tag{17}$$

We will now try several choices of initial condition to find x^o, s^o and p^o. First we take the initial surface to be zero dimensional, i.e., $k = 0$. Thus s has a given value s^o at a point x^o. From Eqn.(11)

$$p^{o2} = 1 \tag{18}$$

Hence p^o lies on a unit sphere with centre x^o. Now (15) - (18) provide a parametric form of the solution s(x). From (15) and (18)

$$(x-x_o)^2 = 4p^{o2}\sigma^2 = 4\sigma^2$$
$$\Rightarrow \quad \sigma = \pm \frac{|x-x_o|}{2}$$

This and (17) yield $s = s^o + 2p^2\sigma$

$$= s^o \pm |x-x_o| = s^o \pm r \tag{19}$$

Here $r = |x-x_o|$.

Now we look at the case $k = 1$. Here Γ is a curve

$$x = x^o(t)$$
$$s = s^o(t)$$

In addition to condition (18), we now have from Eqn.(13):

$$p^o \frac{\partial x^o}{\partial t} = \frac{\partial s^o}{\partial t} \tag{20}$$

This is the equation of a plane perpendicular to the tangent vector to the curve Γ .

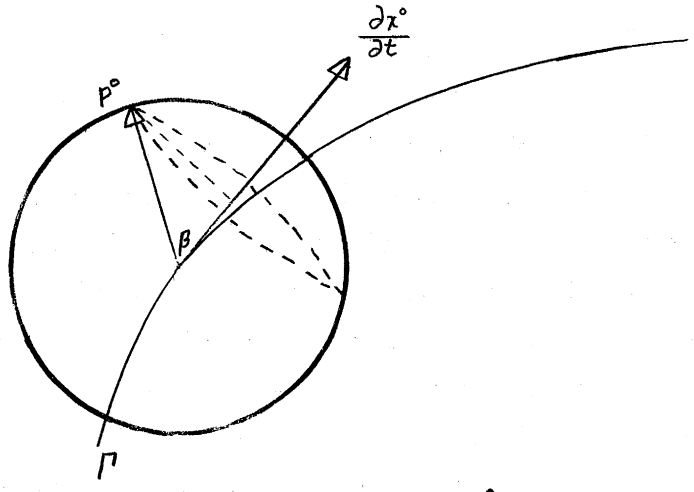

The intersection of this plane with the sphere $(p^o)^2 = 1$ yields either no solution (no intersection), one solution (tangential intersection) or many solutions (a cone in the sphere, called the Monge cone) for p^o .

The half angle of the cone is

$$\cos\beta = \frac{\partial s^o}{\partial t} \Big/ \left|\frac{\partial x^o}{\partial t}\right| \tag{21}$$

Another example is the Hamilton-Jacobi equation of classical mechanics. To define it, we let s depend upon x and the time t, and write

$$F(t, x, s, s_t, p) = 0$$

Suppose that we solve (22) for s_t and write

$$s_t + H[x, p] = 0$$

Then H is called the Hamiltonian, and (23) is the Hamilton-Jacobi equation. It is possible to get more than one Hamiltonian from (22), one for each solution for s_t. In classical mechanics and in wave propagation H is usually independent of s and in conservative mechanical systems it is independent of t also. Then (23) becomes

$$s_t + H[x, p] = 0$$

4) Now let us look at ray theory as applied to wave propagation. Call s(x,t) the phase function. It is convenient to call

$s_x = k$, the wave vector

$s_t = -\omega$, the angular frequency

There is a dispersion relation

$$F(x, t, k, \omega) = 0$$

or

$$\omega = H(x, t, k).$$

This is a first order PDE for s. Here the different values of the Hamiltonian correspond to different modes of propagation.

What happens when a wave hits a boundary? Assume that we know the form of the incident wave and a boundary condition (for example, $s_i = s_r$, the incident phase equals the reflected phase on the boundary). Then we can find the reflected rays and the reflected phase by the methods described above.

When the incident wave hits a vertex or corner on the boundary, then the condition on s is known only at a point. Therefore the rays emerge from it in all directions. They are called corner diffracted rays. If the incident wave hits an edge of the surface then each point produces a cone of emerging rays. They are called edge diffracted rays.

What happens when a ray is tangential to the reflecting surface? It travels along the surface of the body and leaves tangentially. Experiments have been done to show this. One such experiment involves bouncing radar

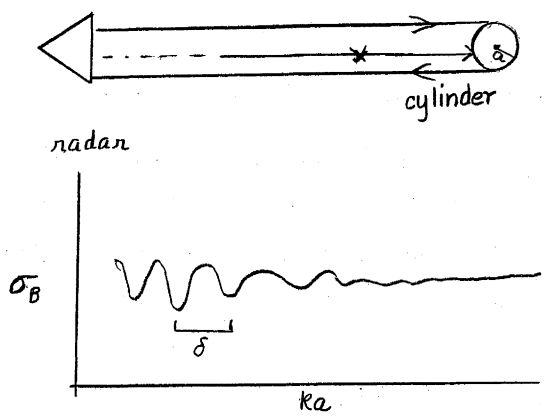

waves off a cylinder. The phase difference at the receiver between a ray reflected off the front of the cylinder and one that passes around the cylinder is $k(a + \pi a + a)$ .There will be interference between the reflected and diffracted fields with a period δka determined by equating this phase difference to 2π . Thus

$$\delta ka(1+\pi+1) = 2\pi \quad \text{or} \quad \delta ka = \frac{2\pi}{2+\pi}$$

This is what is observed.

5) An example of ray treatment of a "wave" equation. (Really a diffusion equation.)

$$u_t = \epsilon u_{xx}\,, \quad u(x,0) = \delta(x) \tag{25}$$

Let

$$u = e^{\frac{1}{\epsilon}s(x,t)} A(x,t,\epsilon) \tag{25a}$$

Therefore

$$\frac{\partial u}{\partial t} = \frac{s}{\epsilon} t\, e^{s/\epsilon} A + e^{s/\epsilon} A_t \tag{26}$$

$$\frac{\partial^2 u}{\partial x^2} = e^{s/\epsilon}\left\{ \frac{s_x^2}{\epsilon^2} A + \frac{2 s_x A_x}{\epsilon} + \frac{s_{xx} A}{\epsilon} + A_{xx} \right\} \tag{27}$$

Putting (26) and (27) into (25) gives:

$$\frac{1}{\epsilon}\left[s_t - s_x^2\right] A + \epsilon^0 \left[A_t - 2 s_x A_x - s_{xx} A\right] - \epsilon A_{xx} = 0 \tag{28}$$

Let now $$A = \sum_{n=0}^{\infty} A_n(x,t)\,\epsilon^n$$

and substitute it into (28) and equate powers of ϵ .

$$\left[s_t - s_x^2\right] A_n + \left[A_{n-1,t} - 2 s_x A_{n-1,x} - s_{xx} A_{n-1}\right] - A_{n-2,xx} = 0 \tag{29}$$

Starting with $n=0$; $A_{-n}=0$, $n<0$ we get either $A_0=0$ or,

$$S_t - S_x^2 = 0 \tag{30}$$

This is the dispersion equation for S . For $n=1$ we get

$$A_{0_t} - 2S_x A_{0_x} - S_{xx} A_0 = 0 \tag{31}$$

This is a linear first order PDE in A_0 . The initial conditions on s are s = 0 at x,t = 0 since the source of k is the delta function at x = 0 at t = 0.

We now make the substitution $p = S_x$, $\omega = S_t$. Then (30) becomes

$$\omega - p^2 = 0. \tag{32}$$

Applying the equations (10) to (32) we get

$$\frac{dx}{d\sigma} = -2p \implies x = x^0 - 2p\sigma = -2p^0\sigma,\ x^0 = 0 \tag{33}$$

$$\frac{dt}{d\sigma} = 1 \implies t = t^0 + \sigma = \sigma,\ t^0 = 0 \tag{34}$$

$$\frac{dp}{d\sigma} = 0 \implies p - p^0 \tag{35}$$

$$\frac{d\omega}{d\sigma} = 0 \implies \omega - \omega^0 = p^{0^2} \tag{36}$$

$$\frac{ds}{d\sigma} = \omega - 2p^2 \implies s = s^0 + (\omega - 2p^2)\sigma = -p^{0^2}\sigma \tag{37}$$

From (35) $$p^{0^2} = \frac{x^2}{4\sigma^2} = \frac{x^2}{4t^2} \tag{38}$$

From (37) $$p^{0^2} = \frac{-s}{t} \tag{39}$$

Now (38) and (39) yield the solution

$$s = \frac{-x^2}{4t} \tag{40}$$

Next we calculate

$$S_x = \frac{-x}{2t};\quad S_{xx} = -\frac{1}{2t}$$

Putting these into Eqn.(31) yields:

$$\frac{dA_0}{dt} = -\frac{A_0}{2t} \tag{41}$$

which is solved by $A_0 = \frac{c}{\sqrt{t}}$.

Finally, using this result for A_0 and (40) for s in Eqn.(25a) gives the solution

$$u(x,t,\epsilon) = \frac{c}{\sqrt{t}} \exp\left(-x^2/4t\epsilon\right) \tag{42}$$

The only remaining problem is to determine the constant c. This cannot be determined from the theory as developed so far here, since the origin, where the initial conditions are specified, is a caustic. It can be found, but we shall not find it.

The preceding procedure can be applied to any nonlinear PDE of any order, or any system of PDE's.

Notes submitted by
Joseph R. Buckley
and Mark Koenigsberg.

ABSTRACTS

MINI-MAX PRINCIPLES FOR LINEAR SYSTEMS (abstract)

James L. Anderson

A number of physical systems are governed by a linear, inhomogeneous integral equation of the form

$$X(t) = f(t)Q(t) - \alpha\int_a^b F(t,t')Q(t')dt' \equiv H[Q]$$

where $X(t)$ and $f(t)$ are given functions of t, α is a parameter, $F(t,t')$ is a symmetric, semi-definite (positive or negative) kernal and $Q(t)$ is the unknown. Three examples of such systems are given: (a) Knudson flow through a channel, where $Q(t)$ is the number of molecules hitting the wall of the channel at t per unit area and unit time; (b) radiative transfer through a plane-parallel atmosphere, where $Q(t)$ is the density of radiation as a function of optical depth and (c) transport in a gas where $Q(t)$ is related to the deviation of the distribution function from that for local thermodynamic equilibrium. In many instances one is not so much concerned with the details of the full solution as with some weighted average of Q. More specifically one is often intereated in the quantity

$$T = (X,Q)$$

where in general $(A,B) \equiv \int A(t)B(t)dt$. In case (a) T is number of molecules leaving the channel per unit time, in (b) it is the integrated reflected flux, and in (c) it is proportional to a transport coefficient.

By constructing a variational principle for the integral equation it is possible to find a variety of upper and lower bounds on the quantity T. Assuming, for definiteness, that F(t,t') is semi-positive definite, it follows from the Schwartz inequality that, for any trial function U(t)

$$T \geq (U,X)^2/(U,H[U]).$$

Using the method of reciprocal variational principles one can obtain both improved lower and upper bounds on T.[1] Thus, for case (b), for an optical depth of 0.1 one obtains a simple lower bound of .084159 while an improved lower bound gives .084292 and an upper bound of .084337. Systematic procedures for improving the bounds are also discussed.

NUMERICAL SIMULATION OF LAKE ONTARIO
(abstract)

John R. Bennett

The circulation of Lake Ontario during July, 1972 has been simulated with two numerical models. One of the models is a 12-level cross section model with a horizontal grid resolution of 3 km and the other is a 7-level three-dimensional model with a 5 km grid. In both the hydrostatic, Boussinesq, f-plane and rigid lid approximations are used, and advection of momentum is neglected. The cross section model was used to estimate preliminary values of the empirical parameters and to isolate some of the physical processes operating in the three-dimensional model. The chief difference between the two models is that the three-dimensional model allows longshore propagation and advection.

Turbulent diffusion is parameterized with a vertical coefficient of turbulent diffusion which depends on wind stress and Richardson number diffusivity.

---

[1] H.H.Jensen, H.Smith and J.W.Wilkens, Phys.Rev. 185: 323 (1969).

The input data for the models consists of objectively analyzed fields of winds and air temperature at hourly increments. Both Canadian and United States IFYGL stations were used. For most of the cases a constant drag coefficient was used to estimate the surface stress but for some cases the coefficient was made dependent on the air lake temperature difference.

The mean north-south temperature gradient due to upwelling on the north shore, the thermocline depth and the monthly mean circulation compare favorably with the analyses of R. L. Pickett and F. Richards. It is shown that the cyclonic circulation is due to both the variation of stratification across the lake as well as the geostrophic flow due to shore zones being warmer than mid-lake.

The most important propagation mechanism is shown to be topographic stretching. At several times in the month, after periods of relatively strong winds, two large counter-rotating gyres rotate counterclockwise around the lake. To a good approximation the period corresponds to that of a topographic or "second class" mode. Propagation of baroclinic Kelvin waves, and longshore advection of temperature are less important.

A REVIEW OF NUMERICAL MODELS OF THE OCEAN CIRCULATION (abstract)

Kirk Bryan

The first numerical models were intended to explore the response of a homogeneous fluid on the β-plane to simple wind-stress patterns. For the purposes of this discussion we can interpret these models as representing the shallow upper layer of a two-layer ocean with a rigid interface between the layers. In this case the lower layer is at rest, and the interface is horizontal. Numerical models have been useful for studying time-dependent and nonlinear versions of earlier analytic models of homogeneous, wind-driven oceans. Spin-up of the system from a state of rest takes place through the excitation of Rossby waves which propagate energy to the western boundary. The final solution depends very much on the lateral boundary conditions imposed at the walls. For free-slip boundary conditions the solution tends

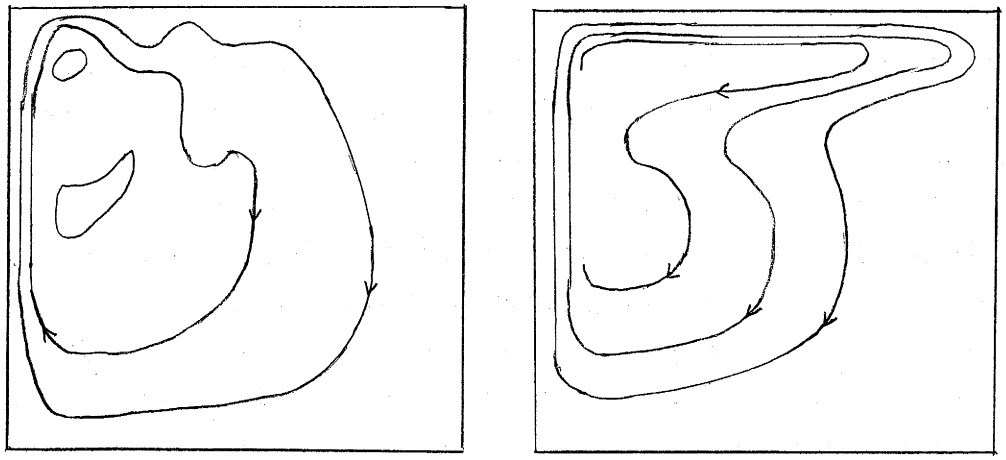

Fig.1

to a steady state with a circulation much stronger than that given by linear theory. For non-slip boundary conditions there is very little downstream transport of vorticity in the western boundary current as shown by R. Stewart. As a result vorticity generated by the boundary current must be dissipated locally. For low Ekman numbers the western boundary current becomes unstable, and a series of vortices form which are carried downstream. The free-slip and non-slip cases are shown in Fig.1, as computed by Blandford. In both cases the dissipative mechanism is by the lateral diffusion of vorticity.

Surprisingly the free-slip case shown in Fig.1 has almost the same pattern as found in earlier calculations for another model investigated by Veronis in which dissipation is entirely due to bottom friction.

Recently, interesting results have been obtained by Lin and Holland for similar models in which the interface between the two layers is free to respond, and there is motion in both layers. The initial response of the system is barotropic, but later the spin-up process deforms the interface and the motion tends to be confined to the upper layer. For the case of free-slip boundary conditions a large depression of the thermocline forms in the upper gyre shown in Fig.1(b). Eventually baroclinic eddies form on the lower part of the gyre. The upper branches of the current adjacent to the western and northern walls are stable. The effect of the eddies is to excite motion in

the lower layer and arrest the baroclinic spin-up process. In the two-layer case with no-slip boundary conditions the flow pattern in the upper layer is like that of Fig.1a, and baroclinic instability does not take place in the same parameter range.

The simplicity of the two-layer model makes it an ideal tool for studying mechanism involved in the interaction of baroclinic instability and the ocean circulation. Studies should be made on a two-layer model to see if parameterization of baroclinic eddies is possible. More detailed treatment of vertical variations of velocity and temperature can be kept in reserve for more detailed simulations with an aim to comparing results with observed data.

A MODEL FOR A CONVECTION DRIVE GEODYNAMO
(abstract)

Friedrich H. Busse

It has become generally accepted that the earth's magnetic field is generated by motions in the earth's liquid core. The process by which motions in an electrically conducting fluid generate a magnetic field is called the dynamo process. It is governed by the dynamo equation for the magnetic field $\underset{\sim}{B}$.

$$\left(\frac{\partial}{\partial t} + \underset{\sim}{v}\cdot\nabla\right)\underset{\sim}{B} - \eta\nabla^2\underset{\sim}{B} = \underset{\sim}{B}\cdot\nabla\underset{\sim}{v} \qquad (1)$$

where η is the magnetic diffusivity $\eta = (\sigma\mu)^{-1}$. There are two candidates for the energy source of the geodynamo, convection and precession induced motions (Bullard, Proc.Roy.Soc. A197: 433, 1946; Malkus, Science 160: 259, 1968). Fortunately, the convection rolls in the core (illustrated in Fig.1) and the Rossby waves induced by precession are similar in character owing to dominating influence of the Taylor-Proudman Theorem. Hence we shall restrict ourselves to the case of convection assuming that the dynamo process will be similar in the case of precession induced motions.

The complete system of equations to be solved consists of the Navier-Stokes equations of motions in a rotating system, the heat equation for the temperature field, and Eq.(1). Our approach is based on the assumption that

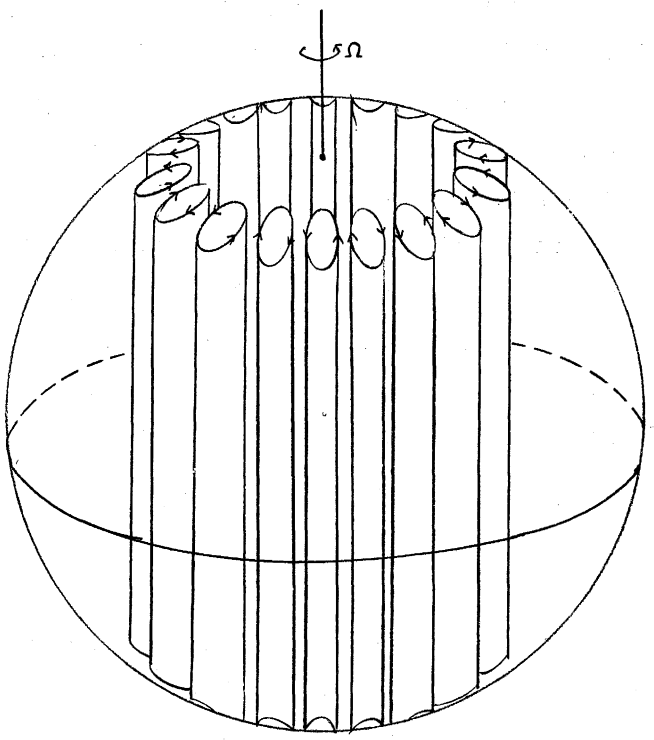

Fig.1. Qualitative sketch of the marginally unstable convective motions in an internally heated rotating sphere.

the geostrophic balance governs the motions in first approximation even if the magnetic field is present. This requires that the toroidal magnetic field in the earth is at best one order of magnitude larger than the poloidal field instead of two orders as has been sometimes assumed. The analysis proceeds by first solving the hydrodynamic problem without magnetic field (Busse, J.Fluid Mech. 44: 441, 1970). Then the kinematic dynamo problem represented by (1) is solved. Then we modify the problem slightly by considering a cylindrical annulus with parabolic instead of spherical top and bottom. This will not change the qualitative conclusions, however. Finally, the equilibrium amplitude of the magnetic field can be calculated by considering the Lorentz forces. This part has not been completed yet. The results will be similar, however, to a simpler case treated earlier (Busse, J.Fluid Mech. 57: 529, 1973).

It is found that the field corresponding to the lowest magnetic Reynolds number $R_m \equiv U r_o/\eta$ is predominantly dipolar outside the conducting fluid

with the axis parallel to axis of rotation. The field is stationary and the toroidal component is of the same order as the poloidal component since differential rotation is assumed to be negligible. The known features of the earth's magnetic field agree with the basic properties of the model if the secular variation is regarded as a secondary phenomenon. The model does not exhibit reversals. These do not contradict the property of stationarity since they occur on a much longer time scale than the diffusive time scale of the geodynamo.

PATTERN OF CONVECTION IN SPHERICAL SHELLS
(abstract)

Friedrich H. Busse

The problem to which this work is addressed can be simply formulated by the question: "What is the analogue to hexagonal convection cells in the case of a spherical geometry?" The problem of convection in a spherical shell with spherically symmetric gravity and temperature gradient has a long history mainly motivated by the possibility of convection in the earth's mantle. Chandrasekhar's monograph "Hydrodynamic and Hydromagnetic Stability" has a long chapter on this topic.

The general three-dimensional problem of convection in a spherical shell has been treated only in the linear approximation which yields a degenerate eigen value R_o for the Rayleigh number. Since R_o depends only on the order ℓ of the spherical harmonic

$$Y_\ell^m \equiv P_\ell^m(\cos\theta)\, e^{im\varphi} \qquad (1)$$

and not m, the multiplicity of the eigen value R_o is $2\ell + 1$. In order to determine which superposition of the $2\ell + 1$ independent spherical harmonics (1) is preferred, the nonlinear problem has to be considered. In the analogous problem of a plane convection layer it can be shown (Busse, J.Fluid Mech. 30: 625, 1967) that hexagonal convection patterns are preferred if the properties of the layer are sufficiently asymmetric. The importance of asymmetries between top and bottom part of the layer is emphasized by the geometrical inhomogeneity in the case of the sphere. In addition it should

be noticed that in the application to the earth mantle and stellar convection zones the basic neutrally stable state has generally inhomogeneous material properties owing to the adiabatic temperature gradient, while the neutral state under laboratory conditions is isothermal. This has consequences also for high Rayleigh number convection when the neutral state is approached in the interior of the convection layer.

We use the property that

$$\mathcal{R}(w) \equiv \frac{\langle w(x\cdot y)^3\rangle}{\langle w(x\cdot y^2)\rangle^{3/2}}$$

is an extremum for hexagons in the plane case when x,y represent the horizontal coordinates and $\langle . \; . \; . \rangle$ indicates the average. In the spherical case we assume that $w = w_\ell$ is given as a linear superposition of $2\ell+1$ modes of the form (1). Since $\langle w_\ell^3 \rangle$ vanishes for odd ℓ, modes with even ℓ are preferred since they can adjust to the asymmetric properties of the layer. No general solution of the extremum problem (2) seems to exist in the spherical case. For $\ell=2$ we find that $w_2 = Y_2^0$ extremalizes the functional $\mathcal{R}$. In the case of $\ell=4$ the extremalizing solution exhibits the symmetry of an octahedron or a cube, depending on whether we identify the primary or secondary maxima of vertical flow with the corners of the polyhedra. In the case $\ell=6$ the solution shows the symmetry of the icosahedron or the dodecahedron. No relationship to the problem of convection in the earth mantle has yet been found. Because of the continental cratons the boundary conditions seem to deviate too strongly from spherical symmetry for the theory to be directly applicable.

"WHAT IS POTENTIAL VORTICITY?"
(abstract)

Louis N. Howard

Ertel's theorem states that in any flow of an inviscid compressible fluid subject to a conservative body force per unit mass the quantity $\rho^{-1}\nabla\times\underline{u}\cdot\nabla\lambda$ is constant following particles, provided that λ is similarly constant, and, if $\nabla p\times\nabla\rho\neq 0$, is a function of p and ρ. For a gas which does not conduct heat, the entropy per unit mass is a function λ of this kind.

Nonlinear shallow water theory is mathematically analogous to two-dimensional compressible isentropic flow with $p=C\rho^2$ ("$\gamma=2$") in which the "density" is proportional to the depth h, bottom to free surface, of the water. Since the analogous gas flow here has $\nabla p\times\nabla\rho=0$, λ may be anything constant following particles, and a good candidate is the position variable z, absolutely constant since the analog flow is two-dimensional. Thus for nonlinear shallow water theory $\frac{1}{h}(\nabla\times\underline{u})\cdot\underline{k}$ is constant following particles. This quantity is commonly called potential vorticity in nonlinear shallow water theory. Evidently the quantity referred to in Ertel's theorem gives a generalization of this concept appropriate for stratified compressible flow with any conservative body force field.

Because of its constancy following particles, potential vorticity is often useful in qualitative discussions of, e.g., flow of shallow rotating fluids over topography. However the fundamental significance of this temporally invariant field for the whole initial value problem is most explicitly appreciated by considering linearized shallow water theory, or the linearization of a compressible stratified flow about a basic state of rigid rotation and hydrostatic equilibrium. In these linear problems, the solution to the initial value problem can be described as a superposition of a steady part and of an oscillatory part. For rotating stratified flow the possibilities for the steady part are frequently very numerous - the normal modes of frequency zero ("geostrophic normal modes") make up an infinite dimensional space. However it turns out that the way this steady part is determined by the initial data can be described in considerable detail even in a very

general case, by making use of certain quantities closely related to the "potential vorticity" of Ertel's theorem. These quantities are defined slightly differently so that they are constant in time at a fixed place rather than following particles, which is more convenient in the linearized theory. They can be calculated from the initial data, and then determine the steady part of the solution to the initial value problem.

When dissipative effects, viscosity and heat conduction, are taken into consideration the potential vorticity (or related quantities) is no longer constant, but with small dissipation varies slowly. The way this slow variation occurs can be described approximately by studying the boundary layers, and in this way motions such as spin-up which are long time-scale variations of nearly geostrophic flows can be investigated in considerable generality; in particular the equation of state, the gravitational field, and the basic stratification may be quite arbitrary.

(This lecture is primarily an exposition of material published in pp.121-137, "Mathematical Problems in the Geophysical Sciences", Vol.13 of Lectures in Applied Mathematics, American Mathematical Society, 1971.)

SOME COMMENTS ON THE METHOD OF MATCHED ASYMPTOTIC EXPANSIONS (WITH APPLICATION TO THE THEORY OF LAPLACE'S TIDAL EQUATIONS.) (abstract)

Vladmir M. Kamenkovitch

A situation that is found very often in many problems of geophysical fluid dynamics is: an asymptotic expansion of the solution $y(x)$ of a certain problem in $0 \leq x \leq 1$ (outer expansion) is proved to be not valid in the vicinity of some point (say $x=0$). Usually it implies that in the vicinity of $x=0$ the solution, $y(x)$, has an alternative asymptotic expansion (inner expansion). As a rule it appears that the regions of validity of both expansions overlap. This essential fact is the real basis for deriving so-called matching conditions without which usually it is impossible to find both outer and inner expansion. A discussion of the subject is given in several review papers of Lagerstrom, in M. Van-Dyke's book, J. Cole's book, etc. The recipes which will be discussed in this lecture are based on a recent paper of Ilyin *et al.*[1]

Consider for example a simple case: let ε = a small positive parameter, $\sum_0^\infty \varepsilon^k u_k(x)$ is an outer expansion of y(x), and $\sum_0^\infty \varepsilon^k v_k(\zeta)$, $\zeta = x/\varepsilon$ is an inner expansion of y(x). Then for given accuracy $O(\varepsilon^n)$ and boundary $b = \varepsilon^\nu$, $0 < \nu < 1$ it is always possible to find numbers, N_e and N_i, so that

$$y(x) - \sum_0^{N_e} \varepsilon^k u_k(x) = O(\varepsilon^n), \quad b \le x \le 1$$

$$y(x) - \sum_0^{N_i} \varepsilon^k v_k\left(\frac{x}{\varepsilon}\right) = O(\varepsilon^n), \quad 0 \le x \le b$$

Therefore

$$\sum_0^{N_e} \varepsilon^k u_k(b) - \sum_0^{N_i} \varepsilon^k v_k\left(\frac{b}{\varepsilon}\right) = O(\varepsilon^n); \quad b = \varepsilon^\nu, \quad 0 < \nu < 1 \quad (*)$$

From this relation it follows that asymptotics of functions $u_k(x)$ at $x \to 0$ and asymptotics of function $v_k(\zeta)$ at $\zeta \to \infty$ are related to each other. For example, in simple cases $u_0(0) = v_0(\infty)$.

A straightforward application of basic relation (*) is hardly possible because it is difficult to find N_e, N_i for given accuracy $O(\varepsilon^n)$ and ν. However it is possible to offer the following procedures which will be sufficient for validity of this relation:

<u>First procedure</u> 1) Consider $\sum_0^N \varepsilon^k u_k(\varepsilon\zeta)$ with fixed N and ζ.
2) Expand it in an asymptotic sequence $\{\varepsilon^k\}$ to yield $\sum_0^N \varepsilon^k C_k^{(N)}(\zeta)$.
Then starting with sufficiently large N functions $C_K^{(N)}(\zeta)$ will be correspondingly asymptotics for functions $v_k(\zeta)$ at $\zeta \to \infty$.

<u>Second procedure</u> 1) Consider $\sum_0^N \varepsilon^k v_k\left(\frac{x}{\varepsilon}\right)$ with fixed N and x.
2) Expand it in an asymptotic sequence $\{\varepsilon^k\}$ to yield $\sum_0^N \varepsilon^k d_k^{(N)}(x)$.
Then starting with sufficiently large N functions $d_k^{(N)}(x)$ will be correspondingly asymptotics for functions $u_k(x)$ at $x \to 0$.

The choice of a procedure depends on the problem. Several illustrative examples are considered. In conclusion short wave asymptotics are found for eigen functions of Laplace's tidal equation and corresponding dispersion relations.

<u>Reference</u>

1) A.M.Ilyin *et al.*, 1974. <u>Dokldy Acad.Nauk</u>. S.S.S.R.

WAVE PATTERNS OF NON-THIN OR FULL-BODIED SHIPS
(abstract)

Joseph B. Keller

A method is presented for determining the wave pattern produced by the motion of a non-thin or full-bodied ship. It is based upon the assumption that the Froude number $F = U^2gL$ is small, where U is the ship speed, L is the ship length and g is the acceleration of gravity. In this case the wavelength of the resulting waves is small compared to L. Therefore, the waves can be described by a theory like geometrical optics, in which rays, a phase function and an amplitude function play a role. The waves are superposed on the double body flow, which is the potential flow about the ship and its image in the undisturbed free surface. They are produced at the bow and stern, and travel outward and rearward from these points along curved rays which become straight far from the ship. In addition some waves from the bow travel along the surface at the waterline and leave it tangentially toward the rear along similar rays. Thus the ship wave pattern consists primarily of the waves from two sources, one at the bow and one at the stern. The results are confirmed by comparison with the small F asymptotic evaluation of Michell's solution for thin ships.

TOPOGRAPHIC ROSSBY WAVES - A CAUTIONARY TALE
(abstract)

James R. Luyten

The dynamics of linear barotropic topographic Rossby waves are discussed for various forms of the underlying topography, with particular reference to the "paradox" of the energy flux of simple wave groups. The usual perturbation scheme is developed assuming that the fractional change in depth, $\Delta h/h$, is small with respect to unity. For an exponential bottom profile, it is found that the flux of energy, the pressure-velocity correlation, is precisely equal to the product of the mean kinetic energy and the group velocity, in accordance with intuition. For a uniformly sloping bottom, energy

flux contains, in addition to the product of the mean energy and group velocity, a term arising from the turning of the wave fronts as the wave progresses up the slope. Energy is conserved since this additional flux of energy is balanced by corresponding terms arising from the gradients of the envelope or the pressure fields of the wave packet.

FLOWS DUE TO ARBITRARY BODY FORCES IN A ROTATING FLUID (abstract)

Willem V.R. Malkus

The linear solution for forced flow in a homogeneous fluid is given by H. P. Greenspan (1968, Eqs. 2.13.7-8) in terms of an expansion in the free modes of the system. However, the free modes can be found explicitly only in a few simple geometries and even in these geometries summation of the expansion which determines the flow may be impractical. An alternative direct determination of flow for steady forcing was first given by J. B. Taylor (1963) in a study of the conditions which Lorentz forces must satisfy so that steady inviscid hydromagnetic solutions may exist. More complete reformulations of Taylor's work have been needed in recent geodynamo studies. The (unpublished) presentation of A. M. Soward (1972) is used as the framework of this discussion.

It is concluded that the only restriction on the arbitrary body forces for an inviscid solution to exist is that the integral of that force vanish over any geostrophic cylinder. The forced flow is then directly given by the curl of a partial integral of the body force along the rotation axis plus the gradient of a pressure also determined by the body force. Special consideration must be given to points or contours on which $\hat{N}_T \times \hat{N}_B = 0$, where the $\hat{N}$ are vectors normal to the top and bottom surfaces respectively.

The general conclusions reached may prove useful in a number of oceanic or other geophysical contexts. They are used here to determine the flow resulting in a rotating spheroid from Lorentz forces of a growing

magnetic field. It is shown (Malkus and Proctor, 1974) that the resulting flow can stabilize the magnetic field and that the novel eigenvalue problem which arises requires geostrophic "eigenflows" of scale amplitude as a solvability condition.

References

Greenspan, H.P. 1968 "Theory of Rotating Fluids", Cambridge Univ. Press.

Taylor, J.B. 1963 Proc.Roy.Soc. A274: 274.

Malkus, W.V.R. and M.R.E.Proctor 1974 J.Fluid Mech. (in press)

AN ANALYTICAL MODEL FOR THE OCEANIC RESPONSE TO ATMOSPHERIC COLD FRONTS (abstract)

Christopher N. K. Mooers

The basic hypotheses of this model are: (1) an appreciable fraction of the turbulence in the ocean is wind-induced; (2) this component of turbulence can be adequately synthesized from a linear response model; (3) atmospheric events, e.g., cold fronts, have well-defined space-time structures; (4) such events may not contribute significantly to the mean wind stress on a monthly or a longer time scale, but they contribute significantly to energizing the ocean in an r.m.s. sense; indeed, their r.m.s. values may exceed monthly mean values by an order of magnitude; (5) when coastal topography is introduced, the consequent wave reflection and trapping phenomena for incident radiation lead to definite spatial structure to the mean square response fields; and (6) a divergent Reynolds stress field emerges, providing a mechanism for driving or damping a mean circulation. The model was first motivated by examination of some contemporary observations indicating energetic oscillations (40 to 80 cm sec^{-1}) of horizontal currents and thermal fields on a continental shelf occurring on a weekly time scale, i.e., the time scale of the seasonal succession of atmospheric cold fronts. Though the oscillations appeared to be largely barotropic, there was no escaping the existence of baroclinic aspects to the response signatures. The second motivational element was provided by considering the magnitude and form for the surface

expression of a hypotehtical atmospheric cold front, whose features were at least consistent with observed and textbook values. The model cold front had the following features: (1) a traveling disturbance (propagation velocity $\sim$10 m sec^{-1}) of constant form; (2) two predominant scales - the $\left\{\begin{matrix}\text{time} \sim 5 \text{ days} \\ \text{distance} \sim 4{,}000 \text{ km}\end{matrix}\right\}$ between successive fronts and the $\left\{\begin{matrix}\text{time} \sim \frac{1}{\pm} \text{ day} \\ \text{distance} \sim 800 \text{ km}\end{matrix}\right\}$ over which the front was most intense; (3) the front had strong pressure ($\sim \pm 10$ mb), sensible heat flux ($\sim -7 \times 10^{-3}$ g cal $cm^{-2} sec^{-1}$), wind stress ($\sim \pm 6$ dynes cm^{-2}), wind stress curl ($\sim \pm 1 \times 10^{-7}$ dynes cm^{-3}), and wind stress divergence ($\sim \pm 1 \times 10^{-7}$ dynes cm^{-3}) forcing signatures. We will account for four meteorological forces: (1F, 2F) = $\frac{1}{\rho_o} (\tau^{(x)}, \tau^{(y)})$, the wind stress; 3F = $\frac{1}{\rho_o} P_a$, the atmospheric pressure; and 4F $\doteq$ B, the buoyancy flux.

We can thus model each of the four meteorological forces, ${}_i\mathcal{F}$, $(i = 1(1)4)$ as a sum of propagating Fourier components:

$$ {}_i\mathcal{F} = \sum_m {}_i F_m e^{i K_m (Ct - x \cos\theta - y \sin\theta)} , $$

where C and θ are the propagation speed and direction of the disturbance, respectively; $K_m = \frac{m\pi}{2L}$, $(m = 1, 2, \ldots)$, the m^{th} wave number of the disturbance; L is the half-distance between disturbances; and ${}_i F_m$ is the m^{th} complex Fourier amplitude of the disturbance. Typically, the Fourier amplitudes have the following form:

$$ {}_i F_m \propto \frac{n}{\pi} \frac{\sin(\pi m/n)}{(n^2 - m^2)}, \; (m \neq n) \text{ and } \frac{1}{2n}, \; (m = n); $$

where L/n is the half-width of the zone of intense forcing. Thus, the amplitude distribution over wave numbers is fairly uniform between the fundamental and the n^{th} harmonic and then falls off rapidly with increasing n. In the atmospheric cold front case, the forcing is approximately broad band between periods of one and five days; therefore, near-inertial forcing must be considered.

Ultimately, the mean circulation produced by the divergence in the time-averaged wind-induced Reynolds stress is to be considered. We content ourselves here with outlining the oceanic response, with coastal boundaries included, from which the Reynolds stress and its divergence are to be computed. We assume that the fluid is Boussinesq and inviscid; we consider dynamics on

the f-plane and an infinitely-long, straight coastline; we neglect the effects of the mean flow on the fluctuations and treat linearized dynamics; we idealize the forcing as traveling, periodic disturbances incident upon the coastline at an arbitrary angle, θ_I ; we treat the momentum and buoyancy flux from the sea surface as body forces which decay linearly from the surface to zero at some depth d, neglecting the details of the dynamics and thermodynamics of the surface mixed layer; and we initially treat the case of uniform depth, returning briefly to the case of uniformly sloping bottom at the end.

The momentum, continuity, and buoyancy equations are then

$$(1)\quad \partial_t u - fv = -\frac{1}{\rho_0}\partial_x p + \frac{1}{\rho_0}\partial_z \tau^{(x)},$$

$$(2)\quad \partial_t v + fu = -\frac{1}{\rho_0}\partial_y p + \frac{1}{\rho_0}\partial_z \tau^{(y)},$$

$$(3)\quad \partial_t w = -\frac{1}{\rho_0}\partial_z p + b,$$

$$(4)\quad \partial_x u + \partial_y v + \partial_z w = 0 \text{ and}$$

$$(5)\quad \partial_t b + N^2 w = \partial_z B.$$

From (1) - (5), a governing equation for the vertical velocity, w, is derived:

$$(6)\quad \mathcal{D}_1^2 \nabla_H^2 w + \mathcal{D}_2^2 w_{zz} = -\frac{1}{\rho_0}\partial_{zz}^2\left[\partial_t \nabla_H \cdot \vec{\tau} + f(\nabla \times \vec{\tau})_z\right] + \partial_z \nabla_H^2 B$$

where $\mathcal{D}_1^2( ) \equiv \partial_{tt}^2( ) + N^2$, $\mathcal{D}_2^2( ) \equiv \partial_{tt}^2( ) + f^2$, and the other notation is conventional. With (6) to examine, and disregarding vertical derivatives for the moment, it is then clear that the interior forcing of w is provided by f times the wind stress curl, the time rate of change of the wind stress divergence (which can be important, especially for time scales of the order of f^{-1} or smaller, as in an atmospheric cold front), and the horizontal Laplacian of the buoyancy flux. For the case of a flat bottom, at $z = -\mathcal{D}$,

(7) $w(-\mathcal{D}) = 0$. The linearized dynamic boundary condition at the free surface (z = 0) is $\partial_t p - g w = \partial_t p_a$, or

$$g \nabla_H^2 w(0) - \partial_z \mathcal{D}_2^2 w(0) = -\frac{1}{\rho_0}\partial_t \nabla_H^2 p_a + \frac{1}{\rho_0}\partial_z\left[\partial_t \nabla_H \cdot \vec{\tau} + f(\nabla \times \vec{\tau})_z\right]_D \qquad (8)$$

Solutions are then obtained for each Fourier component of the forcing individually. The problem to be solved in the vertical reduces to the following form:

$$K^2(N^2-\sigma^2)z + (\sigma^2-f^2)z'' = F(z) \tag{6'}$$

$$z(-D)=0, \text{ and } (8')\ K^2 g\, z(0) - (\sigma^2-f^2)z'(0) = G_0\,, \tag{7'}$$

where $\sigma \equiv KC$ and the subscript of the space-time harmonic has been dropped for convenience. The solution for z is found in terms of the modal solutions, $\{\phi_m$'s$\}$, to the corresponding homogeneous problem:

$$z = \sum A_m \phi_m\,, \text{ where}$$

$$A_m = \frac{B_m + C_m}{(K^2-K_m^2)(\phi_m,\phi_m)}\,,$$

$$B_m = \int_{-d}^{0} F\phi_m\, dz\,,$$

$$C_m = G_0\,\phi_m(0),$$

$$(\phi_m,\phi_m) = \int_{-D}^{0} (N^2-\sigma^2)\phi_m\,\phi_m\, dz + g\,\phi_m(0)\,\phi_m(0),$$

and K_m is the eigenvalue corresponding to the eigenfunction ϕ_m. The formula for A_m exhibits an expected tendency for spatial resonance where K tends to K_m; also, a direct response occurs for $|K| > K_m$ and an indirect response for $|K| < K_m$.

Now that the directly forced part of the solution has been obtained, we turn to the coastal boundary where the normal velocity must vanish, i.e., $u=0$ at $x=0$, say. From (1) and (2), that is equivalent to requiring

$$-\partial_{tx}^2 p - f\partial_y p + \partial_z\left[\partial_t \tau^{(x)} + f\tau^{(y)}\right] = 0, \text{ at } x=0.$$

Clearly, a "free, reflected or trapped wave" will be forced by this boundary condition. Such waves are solutions to the homogeneous problem with horizontal wave numbers $K_R(\cos\theta_R, \sin\theta_R)$. It must be true that

$$K_R \sin\theta_R = K_I \sin\theta_I \tag{9}$$

and

$$ {}_nK_R^2 = \lambda^2 \left(\frac{n\pi}{D}\right)^2, \quad \left(\lambda^2 \equiv (\sigma^2 - f^2)/(N^2 - \sigma^2)\right) , \tag{10} $$

for the n^{th} vertical mode in the case of constant N. If $\sigma > N$ or $\sigma < f$, ${}_nK_R$ will be imaginary, i.e., a trapped, Kelvin-like wave will be generated. Combining (9) and (10) for $f < \sigma < N$, it follows that

$$ \tan {}_n\theta_R = \sin\theta_I \Big/ \left[(\lambda n\pi/DK_I)^2 - \sin^2\theta_I\right]^{1/2} \tag{11} $$

If $|\theta_I| > {}_n\theta_C \equiv \arcsin(\lambda n\pi/DK_I)$, ${}_n\theta_R$ and, thus, ${}_nK_R$, is imaginary, and again a Kelvin-like wave is generated. Otherwise, a Poincaré wave will be generated which will propagate away from the boundary. Such leakage is favored by a small angle of incidence, θ_I; or, for a fixed θ_I, by high frequency, high vertical mode number, shallow depth, and long incident wavelength.

If we add a continental shelf with variable depth to our model coastline, we can anticipate from (11) that some of the reflected (Poincaré) wave energy will be refracted and thus trapped on the continental shelf. If we also add a continental slope in any form, say a topographic step, it is clear that some of the incident wave energy can be trapped as Kelvin-like waves at the step; other portions of the energy will be reflected back into the ocean, and a pattern of incident and back-reflected or trapped motions will be established on the shelf, too. More generally, the case of sloping topography must be treated. With a uniformly sloping bottom ($z = -D_o + rx$), the kinematic bottom boundary condition yields the reflection law for $f < \sigma < N$:

$$ k_R = \frac{(\lambda^2 + r^2)\,k_I + 2r\lambda(\ell^2 + k_I^2)^{1/2}}{(\lambda^2 - r^2)} \tag{12} $$

where the incident 3-D wave number is

$$ \vec{K}_I = (k_I, \ell, m_I), \text{ with } m_I = (\ell^2 + k_I^2)^{1/2}/\lambda , $$

and the reflected wave number is $\vec{K}_R = (k_R, \ell, m_R)$, with $m_R = (\ell^2 + k_R^2)^{1/2}/\lambda$.

Three limiting cases are noted:

(i) $(r=0)$, $k_R = k_I$: simple forward reflection from a flat bottom;

(ii) $(\ell=0),\ k_R = \frac{(\lambda+r)}{(\lambda-r)} k_I$: normal incidence and $\left\{\begin{matrix}\text{forward}\\ \text{backward}\end{matrix}\right\}$ reflection if $\lambda \left\{\begin{matrix}\geq r\\ < r\end{matrix}\right\}$; and

(iii) $(k_I=0),\ k_R = \frac{2r\lambda\ell}{(\lambda^2-r^2)}$; $(r \text{ and } \ell>0)$: tangential incidence and strong refraction if $\lambda \sim r$.

For $\sigma < f$ or $\sigma > N$, replace λ by $i\mu$, then (12) becomes

$$k_R = \frac{(\mu^2-r^2)k_I - i2r\mu(\ell^2+k_I^2)^{1/2}}{(\mu^2+r^2)} \qquad (13)$$

i.e., the reflected wave has a complex wave number unless $r=0$. Thus, the mechanism of bottom-trapping comes into play.

All of the principles have been outlined; what remains to be done is to work out the details, including the partial scattering and trapping over variable topography. In the final analysis, the divergence of the time-averaged Reynolds stress will involve terms such as the following:

with $u = R_e \sum_n \sum_m u_{nm} \left[e^{-iK_m \cos\theta x} - e^{ik_{mn}x}\right] \phi'_n(z) \cdot e^{iK_m(ct - y\sin\theta)}$,

Then

$$\overline{uu} = \tfrac{1}{2} \sum_m \sum_p \sum_q u_{pm} u_{qm} \phi'_p(z) \phi'_q(z) \left[1 + \cos((k_{mq} - k_{mp})x) - \right.$$
$$\left. - \cos((K_m\cos\theta - k_{mq})x) - \cos((K_m\cos\theta - k_{mp})x)\right].$$

For simplicity, we also average over depth to take advantage of the orthogonality of the ϕ'_n's,

$$\overline{\overline{uu}} = \sum_m \sum_p u^2_{pm} \left[1 - \cos((K_m\cos\theta - k_{mp})x)\right].$$

Finally,

$$\partial_x(\overline{\overline{uu}}) = \sum_m \sum_p u^2_{pm} (K_m\cos\theta - k_{mp}) \sin((K_m\cos\theta - k_{mp})x) \qquad (14)$$

which lays bare the results to be expected from the general procedure. At the coastline, (14) vanishes; due to topographic trapping, it will generally vanish at infinity, too. Therefore, it will have at least one extremum over the topography, and a driving mechanism for a mean circulation will be provided. Since this is work in progress, no quantitative results are presented. It is hoped to provide an accounting for a

$$\partial_x(\rho_0 \overline{uu}) \sim \rho_0 \frac{(50\,\mathrm{cm\,sec^{-1}})^2}{250\,\mathrm{km}} = 1 \times 10^{-4}\,\mathrm{dynes\ cm^{-3}}$$

which would have an effect equivalent to a mean wind stress $\overline{\tau}_w = 1$ dyne cm^{-2} applied to a water column of depth $D \sim 100$ m. We can estimate the effect of a wind stress disturbance to be:

$$\partial_x(\rho_0 \overline{\overline{uu}} \sim \frac{1}{\rho_0} \frac{D\overline{\tau}^2_w}{d^2 f^2} K.$$

Hence, the mean squared wind stress with effect equivalent to a mean wind stress is estimated by

$$\overline{\tau^2_w}/\overline{\tau}_w \sim \rho_0 d^2 f^2/DK \sim 10,$$

where $d = 10^3$cm, $D = 10^4$cm, $f = 10^{-4}$sec^{-1}, and $K = 10^{-7}$cm^{-1}. As a final remark, the calculations should be extended to account for various mechanisms, e.g., bottom roughness, which will make the incident and reflected forced waves partially coherent and which will contribute to making such terms as $(\overline{w})_y \neq 0$.

A TWO-LAYER MODEL FOR THE SEPARATION OF INERTIAL BOUNDARY CURRENTS (Abstract)

Dennis W. Moore

An unforced, inviscid two-layer model is used to examine the separation of inertial boundary layers. The Bernoulli taken as linear in the stream function ψ and the potential vorticity of the upper moving layer is everywhere constant. The lower layer is at rest. In the interior of the basin, the flow is a slow westward drift, and the depth of the moving layer increases linearly with latitude. Let ε be the Rossby number for this interior flow.

This flow hits the western boundary and is deflected to the north as an intense, narrow inertial boundary current. The width of the current is $O(\varepsilon^{1/2})$ and the northward velocity is $O(\varepsilon^{-1/2})$. The depth of the moving layer on the western coast decreases to the north, and the interface surface near an apparent separation latitude $f = f_c$. ($f = 1+y$ is the Coriolis parameter). At this latitude, the jet leaves this coast but remains

coherent with cross-stream width of $O(\varepsilon^{1/2})$. It leaves the coast going nearly parallel to it, with an initial deflection through an angle which is $O(\varepsilon^{3/10})$. The free jet meanders to the east, while oscillating about the latitude $f = f_c$ with an $O(\varepsilon^{1/4})$ amplitude and $O(\varepsilon^{1/4})$ downstream wavelength.

Reference

Moore, Dennis W. and Pearn P. Niiler 1974 A Two-Layer Model for the Separation of Inertial Boundary Currents, J.Mar.Res., 32(#3).

EMPIRICAL ORTHOGONAL FUNCTIONS -- A NON-STATISTICAL VIEW (Abstract)

Dennis W. Moore

The method of empirical orthogonal functions is being used to analize various segments of the MODE-I data. The purpose of this note is to explain the basis of the method in simple terms, without statistical jargon. In this analysis we make no distinction between signal and noise. We simply take the data as given and treat a deterministic problem. The distinction between signal and noise, and the process of obtaining corresponding error estimates, are important for interpreting the empirical orthogonal functions once they have been found, but are not important to the process of actually finding the empirical orthogonal functions.

Consider a discrete set of real data which depends on two variables. We denote the elements of the data set by f_{ij}, and the total data set by the matrix

$$F = (f_{ij})_{I \times J} .$$

The independent variables i and j can refer to anything we want. For example, if we are looking at a time series of XBT soundings at a fixed location, the data might be the depth of selected isotherms from each sounding. Then i would refer to the specific sounding and j to the specific isotherm.

We assume that i ranges from 1 to I and j from 1 to J, and that there is no missing data (i.e., all of the elements of F are known). We ask the following question: How well can we represent the given data and

the product of a single function of i times a single function of j ? Specifically, we wish to choose a column vector

$$G = (g_i)_{I \times 1}$$

and a row vector $H = (h_j)_{1 \times J}$ such that the quantity

$$R = \sum_{i=1}^{I} \sum_{j=1}^{J} (f_{ij} - g_i h_j)^2$$

is minimized. Since multiplying each element of G by a constant and dividing each element of H by the same constant does not change the product GH, we may assume that H is normalized. We take

$$\sum_{j=1}^{J} h_j^2 = 1,$$

which in vector form is $HH^T = 1$. The superscript T indicates the transpose matrix, so $H^T = (h_j)_{J \times 1}$ is a column vector.

We incorporate this constraint in the minimumization by means of a Lagrange multiplier, so we actually minimize

$$R' = \sum_{i=1}^{I} \sum_{j=1}^{J} (f_{ij} - g_i h_j)^2 + \Lambda \left(\sum_{j=1}^{J} h_j^2 - 1 \right).$$

Variation of R' with respect to each element of G (i.e., set $\frac{\partial R'}{\partial g_K} = 0$ for each $K = 1, \ldots I$) gives the condition

$$G = FH^T. \tag{1}$$

Variation of R' with respect to each element of H gives

$$\lambda H = G^T F, \tag{2}$$

where

$$\lambda = \Lambda + G^T G = \Lambda + \sum_{i=1}^{I} g_i^2 . \tag{3}$$

From Eq.(1) we see that $G^T = HF^T$, and substitution into Eq.(2) gives

$$\lambda H = HF^T F . \tag{4}$$

Therefore λ is an eigenvalue and H a left eigenvector of the symmetric matrix $F^T F$. The transpose of Eq.(4) is

$$\lambda H^T = F^T F H^T, \tag{5}$$

so H^T is a right eigenvector of $F^T F$. From Eq.(2) we find $\lambda H^T = F^T G$. We multiply Eq.(1) by λ and substitute for λH^T to obtain

$$\lambda G = FF^T G . \tag{6}$$

Therefore G is a right eigenvector of FF^T with the same eigenvalue λ. Now right multiply both sides of Eq.(4) by H^T to obtain

$$\lambda = \lambda HH^T = HF^TFH^T = G^TG.$$

Therefore the eigenvalue λ is non-negative.

From Eq.(3) we find that the Lagrange multiplier Λ is zero. Furthermore, direct computation gives

$$R = \sum_{i=1}^{I}\sum_{j=1}^{J}(f_{ij} - g_i h_j)^2 = \sum_{i=1}^{I}\sum_{j=1}^{J} f_{ij}^2 - \lambda \qquad (7)$$

Therefore R is minimized by taking λ to be that largest eigenvalue of F^TF.

Denote the J real eigenvalues λ in decreasing order by λ^K, so that

$$\lambda^1 \geq \lambda^2 \geq \lambda^3 \geq \ldots \geq \lambda^J \geq 0.$$

Denote the corresponding eigenvectors by G^K and H^K. The eigenvectors are orthogonal, so that

$$H^K H^{\ell T} = \delta_{K\ell}. \qquad (8)$$

The corresponding eigenvectors G^K are given by $G^K = FH^{KT}$, so we find

$$G^{KT}G^{\ell} = H^K F^T F H^{\ell T} = \lambda^K H^K H^{\ell T} = \lambda^K \delta_{K\ell}. \qquad (9)$$

So the eigenvectors G^K are also orthogonal.

Subtract the matrix $G'H'$ from the original data matrix F to obtain a new data matrix F' given by

$$F' = F - G'H'.$$

Now we repeat the entire process. Note that

$$F'^TF' = F^TF - H'^TH'F^TF.$$

Therefore we find

$$H'F'^TF' = H'F^TF - H'H'^TH'F^TF = 0$$

since $H'H'^T = 1$. So H' is a left eigenvector of F'^TF' with zero eigenvalue. Next we compute $H^KF'^TF'$ with $K \neq 1$. We find

$$H^KF'^TF' = H^KF^TF - H^KH'^TH'F^TF = \lambda^K H^K, \qquad (10)$$

since $H^KH'^T = 0$. Therefore H^K is a left eigenvector of $F'F'^T$ with eigenvalue λ^K. The sum of squares of the elements of $F' - GH$ is minimized by choosing $H = H^2$, $G = G^2$. Now we form

$$F^2 = F^1 - G^1 H^1 = F - G^1 H^1 - G^2 H^2$$

and so on. At each step the total variance $\sum_{i=1}^{I}\sum_{j=1}^{J} f_{ij}^2$ is reduced by λ^K. Since $\sum_{i=1}^{I}\sum_{j=1}^{J} f_{ij}^2$ is the trace of F^TF, it is equal to the sum $\sum_{K=1}^{J} \lambda^K$. Therefore by repeating this process J times we obtain the identity

$$F \equiv \sum_{K=1}^{J} G^K H^K \qquad (11)$$

The vectors G^K and H^K are the empirical orthogonal functions. The K^{th} term in the sum in Eq.(11) contributes an amount λ^K to the total trace of F^TF. The decomposition of the original data set into the form given in Eq.(11) is an identity. The usefulness of the representation depends on how much of the total variance $\sum_{i,j} f_{ij}^2$ is accounted for by the first few terms of the sum over K. If a few of the eigenvalues of F^TF are much bigger than the others, this representation is very informative. On the other hand, if all the λ^K are nearly equal nothing particular has been gained.

Recall from Eqs.(4) and (6) that for each left eigenvector H of F^TF, the corresponding $G = FH^T$ was a right eigenvector of FF^T. But F^TF is a $J \times J$ matrix, and FF^T is an $I \times I$ matrix. Say J is greater than I. Then F^TF has more eigenvalues than FF^T. Say λ is an eigenvalue of F^TF which is not an eigenvalue of FF^T. Let H be the corresponding eigenvector from Eq.(4). Then $G = FH^T$ must be zero, since λ is not an eigenvalue of FF^T. Finally, we still have $\lambda = G^TG$, so $\lambda = 0$. Therefore F^TF has at least $J-I$ zero eigenvalues. So if $J > I$ the sum in Eq.(11) will have at most I non-zero terms. That is to say, the total number of terms contributing to the sum in Eq.(11) is $\min(I, J)$. So in practice, we might as well find the eigenvalues from the smaller of the two matrices FF^T and F^TF.

ADVECTIVE-DIFFUSIVE BALANCE FOR THE MEDITERRANEAN SALINITY ANOMALY (Abstract)

George T. Needler

In recent years a series of theoretical models have been developed that can describe the general features of the distribution of mass in the main anticyclone gyres below the mixed layer. An important feature of these "thermocline" models is that the density fields are relatively insensitive to moderate diffusion of mass. On the other hand, it is clear that even though the mass balance may be advective (that is, non-diffusive), there are first order diffusive changes in the temperature and salinity along streamlines in such features as the Mediterranean salinity anomaly. Assuming that the diffusion of mass, temperature and salinity may be described by the same Austauch coefficients, the Mediterranean salinity anomaly has been analyzed to determine whether the advective-diffusive balance in the anomaly implies significant diffusive effects in the mass balance for the main pycnocline in the North Atlantic anticyclonic gyre.

The high-salinity anomaly due to the Mediterranean has been separated from the background salinity gradient by determining the difference from a linear T-S gradient. The resulting anomaly, which must satisfy the same conservation equations as T and S, exhibits a "tongue-like" distribution. The vertical and horizontal scales of this tongue have been determined as functions of the distance along its axis from the available station data. Vertical and horizontal Austauch coefficients have been computed through the use of a simple model including three-dimensional diffusion, constant advection, and an upstream Gaussian distribution. Upon taking the mean velocity to be .2 to .4 cm sec^{-1} along the tongue, the resulting vertical and horizontal Austauch coefficients are .35 to .7 cm sec^{-1} and 1.5 to $3x10^{7}$ cm sec^{-1} respectively. The diffusion in the tongue is found to be principally in the "horizontal" direction and diffusion along the axis of the tongue is of first order importance. Because of the scatter in the available data, no distinction has been made between diffusion along isopycnals and in the true horizontal direction.

From the values obtained for the Austauch coefficients, one can show that in the main pycnocline diffusion is unimportant in either the vertical

or horizontal directions for the first order mass balance. Thus, it is not inconsistent to use a non-diffusive model for the main pycnocline in the North Atlantic anticyclonic gyre even though the distributions of T and S show first order diffusive effects. The results are suggestive that the principal diffusion of T and S takes place along isopycnals.

SEASONAL VARIABILITY IN THE OCEAN
(Abstract)

Pearn P. Niiler

The theory of large-scale seasonal variations of temperature, salinity, sea level, velocity, etc. in the ocean is considered herein. Regions near the boundaries and within 15^{o} of the equator are excluded. It is found that, for the scales considered, the heat input is mainly stored locally and horizontal advection by the mean flow is not particularly important. Effects of vertical advection and of seasonal changes of horizontal advection in the Ekman layers are calculated for 5^{o} squares in the North Atlantic and North Pacific and also found to be relatively minor. Observational evidence is discussed.

Contributions to sea-level changes are calculated for each season for 5^{o} squares in the North Atlantic and North Pacific. First, there is a response to changes in atmospheric pressure which is particularly important (a few cm) at high latitudes. This response is, however, dynamically uninteresting as temperature, velocity, etc. are hardly changed. Second, there is the barotropic response to changes in the wind stress. This produces small changes (a few mm) in sea level on the scales considered, and corresponding changes of bottom pressure. Velocity amplitudes increase to about 3 mm sec^{-1} in the west, corresponding to horizontal displacements of 15 km. Although these values seem small, the associated transports, spread over 20^{o} of latitude, are considerable ($30 \times 10^{6} m^{3} sec^{-1}$). However, since topographic effects are so important for barotropic motions, the large transports are confined to deep water regions and would not, for instance, be expected to contribute much to seasonal changes of transport through the

Florida Straits. Because the changes in bottom pressure are small, the sea-level changes are approximately isostatic, as concluded from observational studies. On the other hand, there is reason to believe that large barotropic changes will be found in regions of closed contours of H cosecϕ, where H is the depth and ϕ the latitude.

Thirdly, there are steric changes in sea level. The major change (a few cm) is produced by expansion and contraction of the water column above the seasonal thermocline due to changing fluxes of heat and water across the surface. Currents of a few mm sec^{-1} are produced above the seasonal thermocline by the changes in density field, but the transport over 20^{o} latitude is under $10^{6} m^{3} sec^{-1}$. There are other, less important, steric changes (usually less than 10%) due to movements induced by the changing wind stress, and these effects have been explicitly calculated by season for the North Atlantic and North Pacific. The changes involve (1) changes in the mixed layer due to convergences of heat and salt produced by Ekman fluxes, and (2) changes produced by Ekman pumping which displace the main thermocline up or down by a few metres. The latter change represents the baroclinic response which increases in strength towards the equator, although even at 15^{o} (where the analysis breaks down), currents are only about 1 mm sec^{-1}. The baroclinic response dominates the barotropic response at low latitudes, while the reverse is true at high latitudes. The two responses are comparable at 30^{o}. Fourthly, there is a tidal component, Sa (Doodson, 1921; Wunsch, 1967) with a period of one year and an amplitude of a few mm which will not be discussed herein.

Large-scale anomalies in the surface temperature of the ocean are discussed qualitatively, although these are not seasonal changes. It is suggested that the main changes are simply due to changes in the heat flux through the surface, and changes in the convergence of heat in the Ekman layer, the latter becoming significant at low latitudes. Simple ways of modelling the changes can be employed for regions not too close to the equator.

---

*This abstract appeared in "The theory of the seasonal variability in the ocean" by A.E.Gill and P.P.Niiler, Deep-Sea Res., 1973 20: 141-177.

ROLE OF WESTERN BOUNDARY CURRENTS IN OCEAN CIRCULATION
(Abstract)

Pearn P. Niiler

The boundary currents which flow along eastern coasts of the major continents are observable regions of largest vorticity gradients and in models of ocean circulation are regions in which wind-induced vorticity is transferred from the interior of the ocean basin to its solid boundaries. Measurements of the velocity and density structure of the Florida Current along the eastern United States seaboard are used to map out the vorticity and potential vorticity fields within this western boundary current. There is a persistent increase of the potential vorticity of a water column within the cyclonic shear zone of the Florida Current. Vorticity and potential vorticity of positive sign is transferred into the subtropical gyre along this seaboard; the sign of this transfer is consistent with the convergence of eddy vorticity flux; however, its magnitude is an order of magnitude smaller than the rate at which the surface wind induces into the gyre, or the rate at which the boundary current advects vorticity to the north.

The Florida Current is seen to be an inertial advective current; its role in the general circulation of the North Atlantic is to advect mass and heat from the equatorial regions to the northerly latitudes. Its southernmost extension, the Guiana Current off the northeast coast of South America, advects planetary vorticity of positive sign into the North Atlantic across the boundary of the zero of the wind-stress curl at 8^{o}N latitude, which serves to balance the negative flux from the wind. It is postulated that in the region of the northerly extension of the Florida Current, the Gulf Stream, strong lateral vorticity transfer from the subtropical circulation pattern must take place by eddy process in the open ocean.

THE ONSET OF BIOCONVECTION
(Abstract)

Edward A. Spiegel

In the proceedings of last year's course W. S. Childress[1] described how certain cultures of free-swimming microorganisms produce regular patterns as a result of their tendency to swim upwards and in spite of the fact that they are denser than the ambient medium. At that time, this work, carried out in collaboration with M. Levandowsky, had been developed to the point where critical conditions for the onset of bioconvection had been computed; the form of some nonlinear solutions had also been found. The results occasioned some discussion, because at the critical conditions for the onset of bioconvection, the critical horizontal wavelength of patterns is infinite whereas patterns are evidently first seen with a finite horizontal scale. The boundary conditions appropriate here are just those corresponding to fixed flux in ordinary Boussinesq convection, and they are known to give a vanishing critical wavenumber in that case[2]. The question that then comes up is: Why do patterns first appear with finite size? While this is difficult to answer definitively, it seems that a relevant aspect is the dependence of growthrate on horizontal scale, and I should like to discuss that here.

For a general description including references I refer you to Childress' discussion in the proceedings of last year. Briefly, we are interested in swimming protozoa of size $\sim 10\mu$ which tend to swim upward or, as the biologists say, are negatively geotactic. Of course, these organisms may also have a random component to their swimming, which we shall allow for. We shall describe the suspension of organisms as a single Newtonian fluid. Let n be the number of organisms/unit volume and v_o be the mean volume per organisms. Let ρ be the density of the ambient fluid in the absence of organisms and ρ_o be the volume of an individual organism. Then the density of the suspension is

$$\rho\,(1-n v_o) + \rho_o\,(n v_o).$$

Let

$$c = n v_o\,; \quad \alpha = \rho_o/\rho - 1.$$

Then the density of the suspension is, in a felicitous form,

$$\rho(1+\alpha c),$$

The equation of motion of the suspension is then

$$\rho\left(\frac{\partial \underset{\sim}{u}}{\partial t} + \underset{\sim}{u}\cdot\nabla\underset{\sim}{u}\right) = -\nabla p - g\rho(1+\alpha c)\hat{\underset{\sim}{k}} + \mu\nabla^2\underset{\sim}{u} \qquad (2)$$

where $\underset{\sim}{u}$ is the suspension velocity and μ is the viscosity. For typical organisms, $\alpha = 0.1$ and we are interested in cases with $c \approx 10^{-2}$. For this reason, we have ρ as the coefficient on the left-hand side of (2), since the Boussinesq approximation is good and we assume that

$$\nabla\cdot\underset{\sim}{u} = 0 \qquad (3)$$

In suspensions whose depths are mms, patterns form in minutes. So the organisms cannot change their numbers on the time scale of pattern formation and we may write

$$\frac{\partial c}{\partial t} + \nabla\cdot\underset{\sim}{J} = 0 \qquad (4)$$

where $\underset{\sim}{J}$ is the organism flux which we take to be

$$\underset{\sim}{J} = c\,\underset{\sim}{u} + c\,\underset{\sim}{V} - \chi\nabla c. \qquad (5)$$

The first term in (5) represents the flow due to fluid dragging organisms, the second term represents directed swimming with respect to the fluid, and the third "describes" random swimming (here taken to be isotropic for brevity). A simple model is given by the choice

$$\underset{\sim}{V} = V\hat{\underset{\sim}{k}}, \qquad (6)$$

in which the directed swimming is purely due to negative geotaxy with no photo-, chemo-, or baro- taxes, though any of these might occur in given circumstances. Of course, U and χ are generally functions of c and the distance from boundaries, hence z, but we shall assume that

$\frac{\chi}{V}$ is independent of z.

The boundary conditions are

$$w = J_3 = 0 \quad \text{on} \quad z = 0, -H \qquad (7)$$

where $w = \hat{\underset{\sim}{k}}\cdot\underset{\sim}{u}$, $J_3 = \hat{\underset{\sim}{k}}\cdot J$ and

$$\frac{\partial w}{\partial z} \text{ or } \frac{\partial^2 w}{\partial z^2} = 0 \quad \text{on} \quad z = 0, -H \qquad (8)$$

according as the surface is rigid or free.

This system admits static solutions with no horizontal structure and with a vertical distribution $c = K(z)$, defined implicitly by

$$z = \int_{K(0)}^{K(z)} \frac{v\,dc}{\chi} \tag{9}$$

Evidently, for χ/v = const., K is an exponential, and all the profiles of interest have K decreasing downward.

If we set $c = K + \phi$, where ϕ is small, and treat $\underset{\sim}{u}$ also as small, we obtain a set of linear equations in the usual way. These have solutions of the form

$$\begin{pmatrix} \phi \\ w \end{pmatrix} = \begin{pmatrix} \Phi(z) \\ W(z) \end{pmatrix} f(x,y)\, e^{\gamma t}, \quad \nabla_1^2 f = -a^2 f, \tag{10}$$

in conventional convective notation. The linear theory, with $h = (\chi/v)_{z=0}$ as unit of length, $(v)_{z=0}$ as unit of speed, and $K(0)$ as unit of c, is

$$\frac{\gamma}{\sigma}(D^2 - a^2)W - (D^2 - a^2)^2 W = R a^2 \Phi \tag{11}$$

$$\gamma\Phi + WDK + DF + \chi a^2 \Phi = 0 \tag{12}$$

$$F = -\chi (DK) D[\Phi/(D\chi)] \tag{13}$$

with

$$W = F = 0, \quad z = 0, -\lambda \tag{14}$$

and

$$DW \text{ or } D^2 W = 0, \quad z = 0, -\lambda \tag{15}$$

where

$$R = \frac{g\alpha K(0) d^3}{\chi_0 \nu}, \quad \sigma = \nu/\chi_0, \quad \lambda = H/h \tag{16}$$

and

$$\chi_0 = \chi_{z=0}, \quad \nu = \mu/\rho.$$

It is not difficult to show that γ is real for all λ and a, for any combination of rigid and free conditions. Moreover it appears that when $\gamma = 0$ the eigenvalues of R (for the gravest mode) increase monotonically from a finite value at a = 0. That is, the critical wavenumber for the onset of bioconvection is zero. Indeed as $\lambda \to 0$ the present system reduces to that of ordinary convection with $\lambda^4 R$ playing the role of the Rayleigh number. However, for most cases that arise in the laboratory, λ is appreciably greater than unity and we shall confine our attention to that case.

For large λ the linear problem can be treated by matched asymptotic expansions and an asymptotic sequence for γ can be developed. The appropriate parameters in this case are $\tilde{a}=\lambda a$, $\tilde{\gamma}=\lambda^2\gamma$ and $\tilde{R}=\lambda R$, all of which remain finite as $\lambda\to\infty$. The asymptotics show that the interesting mode (appropriate branch of $\tilde{\gamma}$) always has $\tilde{\gamma}=0$ for $\tilde{a}=0$. For $\tilde{R}\leq 4$, $\tilde{\gamma}<0$ for $a\neq 0$. For $R>4$, $\tilde{\gamma}>0$ for a band of positive $\tilde{a}$, and $\tilde{\gamma}$ has a single maximum as a function of $\tilde{a}$. The approximate values of these maxima are:

$\tilde{R}$	4	5	6	7.5	10
$\tilde{\gamma}_{max}$	0	.18	.8	2	5
$\tilde{a}_{max}$	0	1.4	1.8	2.4	3

When we recall that $\tilde{a}$ is the horizontal wavenumber scaled on the total layer thickness, we see that in fact linear theory does not really imply that we should see infinite horizontal scale first. The very large horizontal scales when they are unstable, grow so slowly that it would require a very careful experiment to detect them. The values of $\tilde{a}_{max}$ computed from linear theory are in reasonable agreement with observed pattern sizes, and that is the point of this footnote to Childress' remarks.

References

1. Childress, S., G.F.D. Summer Program, W.H.O.I., Notes of 1973.
2. Hurle, D.T.J., E. Jakeman and E.R.Pike, PRS.A, 296:469, 1967.

INTERACTION OF INERTIA GRAVITY WAVES WITH A GEOSTROPHIC CURRENT (Abstract)

Melvin E. Stern

We compute the reflected and transmitted waves when an inertia gravity wave is obliquely incident on a barotropic shear layer in a uniformly stratified fluid bounded by horizontal walls. If the incident phase speed vector is in the opposite sense to the basic lateral shear then a transmitted wave always occurs, and we find a net divergence of wave energy from the shear layer. The kinetic energy of the basic flow decreases with time. If the incident wave

propagates in the same sense as the basic lateral shear then the wave either supplies energy to the basic flow or is perfectly reflected, depending on the angle of incidence. The calculation of the "absorption and emission" coefficients has only been done for the rather artificial model in which the geostrophic shear is confined to a vortex sheet. But a maximum in the absorbtion coefficient is found for waves very near the inertial frequency, when the current jump across the barotropic shear layer is small (compared to the Väisälä frequency times the channel depth). Therefore it is suggested that the large scale geostrophic eddies in the ocean "leak" energy to the inertia gravity wave field. A preferred horizontal wavelength emerges from this calculation, but the significance of the result must await a calculation for the case of a more realistic basic geostrophic flow.

"MODONS"
(Abstract)

Melvin E. Stern

An isolated barotropic eddy on the β-plane can be in equilibrium only if it is composed of a coupled cyclone-anticyclone system, only if it is separated by a vorticity discontinuity (free streamline) from the surrounding fluid, and only if its rms vorticity exceeds $\beta R/\sqrt{2}$, where R is the radius of the free streamline. The eddy having this minimum vorticity is called a "modon", and a close-packed array of non-overlapping modons is also an equilibrium solution. The latter is called a "modon-sea" and its rms velocity is $\beta R^2/7.6$. Although the equilibrium modon-sea is probably dynamically unstable, so that nonlinear Rossby waves will develop, the total energy is invariant and related to the modon area by the previous relation. The variational principle on which the equilibrium theory is based has also been generalized so that some baroclinic effects can be examined in future work. It is suggested that some of the statistical properties of mid-ocean eddies can be interrelated through the use of the "modon-sea" model.

RECENT EXPERIMENTS IN DOUBLE-DIFFUSIVE CONVECTION
(Abstract)

J. Stewart Turner

The early experiments in double-diffusive convection were all one-dimensional in character. They were concerned either with the production of layers from a hydrostatically stable gradient of one property using a destabilizing flux of a second, or the measurement of the coupled fluxes across horizontal interfaces separating two well-mixed layers. This work was reviewed, and the limitations of such experiments discussed. In many oceanographically important situations there are initially two smooth vertical gradients of properties (heat and salt) having opposing effects on the vertical density gradient, and often there are nearly compensating horizontal gradients as well, across a frontal surface separating two water masses. The sugar-salt model of the salt-heat system has been used to explore various motions which can arise in such cases.

Two problems of particular interest have been the mechanism of formation of layers near an intruding water-mass with different T-S properties from its surroundings, and the nature of the motion in the layers once they have formed. When a small source of sugar solution is released into uniform salt solution of the same density, there is a strong diffusive separation, leading to vigorous vertical convection above and below the source. Eventually this can set up a stable, layered density stratification. A sugar source released in a uniform salt gradient causes similar convection plumes locally, which then spread out horizontally at several levels. The next stage of complication is to release sources with anomalous T-S properties at their own density level into opposing gradients of two properties. The rate of extension of the system of layers both horizontally and vertically is greater, particularly in the "finger" case where the number of layers below the source level is increased dramatically. A systematic shearing and overturning motion is observed in each of the layers as it extends, and they all have an upward or downward tilt, the sense of which can be related to the properties of the input. It has been found possible to set up a system of layers in which quasi-steady shearing motions are sustained by

supplying the driving fluxes at opposite corners of the experimental tank. In the finger case, the horizontal gradients set up in this way produce strong shears and eventual overturning of an initially smooth gradient region, to give tilted convecting layers which behave in a similar way. Each of these processes was illustrated using shadowgraph photography and time-lapse movies.

STRATIFIED SPIN-UP
(Abstract)

George Veronis

The response of a contained rotating fluid to a small, abrupt change in the rotation rate is analyzed by multi-scaling methods. The procedure used in this paper makes use of the fact that three different physical processes (inertial oscillations, spin-up response, diffusion) give rise to three different time scales. Since the flow is known to have a boundary-layer character, the variables are divided into interior and boundary-layer parts. The pertinent parameter separating the magnitudes of the amplitudes and the different time scales is the square root of the Ekman number, $E^{\frac{1}{2}}$, so an expansion in powers of $E^{\frac{1}{2}}$ is used. The solution for a homogeneous fluid is derived first and is shown to be consistent with the solution of Greenspan and Howard (1963). The results are given in two forms: one is a direct deduction of the expansion method and is valid to $0(E)$ and the other is obtained by regrouping the terms to derive a form apparently valid for indefinitely long times.

When the fluid is stratified, the physical structure of the system is substantially more complicated and so is the analysis. Exact results can be obtained for the case where the buoyancy (N) and the rotational (Ω) frequencies are the same. For the general case where $F = N/\Omega \neq 1$, results valid for $t >> 1$ can be obtained. In both cases the exact lowest-order solution for the interior can be derived since it is independent of short time (t). For the stratified fluid the elementary spin-up solution of Holton (1965) is part of the solution at $0(E^{\frac{1}{2}})$. The remaining part includes

the long-time behavior toward which the system tends as diffusive processes become dominant. The formulation of the long-time problem is complete at O(E) but parts of it emerge from the analysis at lower order and it is necessary to treat the lower-order system in order to obtain a consistent formulation at O(E). In particular it is possible to show that the thermal boundary condition, which does not affect the elementary spin-up solution, should be satisfied only by the long-time part of the problem. The complete, lowest-order response of the system includes a diffusive part which is quantitatively significant even for times of the order of one spin-up time. It is suggested here that the diffusive contribution may be responsible for part of the discrepancy between elementary spin-up theory and recent experiments.

ANALYTIC OCEAN - ATMOSPHERE MODEL
(Abstract)

Pierre Welander

In existing analytical theories of the oceanic circulation the wind-stress field $\vec{\tau}^{\omega}$ and the normal surface heat flux q_0, or the surface temperature T_0 are prescribed. This thermal condition is not satisfactory as it does not represent a proper external forcing. The specification of the heat flux by a Newtonian law (heat flux proportional to the difference between the atmospheric temperature T_a at a standard height and the ocean surface temperature T_0) is a better condition. Still, it leaves out the feedback link through the atmosphere which involves the dependence of T_a on T_0, the subsequent dependence of $\vec{\tau}^{\omega}$ on T_a, and finally the dependence of T_0 on $\vec{\tau}^{\omega}$ (the T_0-distribution to a main part is determined by advection from wind-driven currents). It seems important to consider completely analytical models of the ocean-atmosphere system, where the solar radiation is the only external forcing. These models must necessarily be drastically simplified, and may be far removed from reality. However, the understanding of such simple models, and in particular finding the time scales and amplification factors of feedback links such as the one described may be of help to understand the real and much more complex system.

The study of a quasi-linear oceanic model[1] reveals that T_o reacts to $\vec{\tau}^{\omega}$ mainly through the advection in the western boundary current. Important is that only a small amount of a mechanical wind stress work is needed to rearrange large amounts of differential heat in the ocean; even if only a small percentage of this differential heat is utilized to change the atmospheric flow, a strong feedback arises.

An attempt has been made to add a simple atmospheric model to the quasi-linear oceanic one, coupling these models by the requirements of continuity in heat flux and stress. Specifically, the model considered is an annulus filled with a Boussinesq fluid on top of periodically repeated underlying boxes (no continents, only thin meridional walls between the boxes) containing a heavier Boussinesq fluid. The system, of course, rotates. There is a prescribed amount of radiative heat Q absorbed per unit time in the ocean surface layer, a part proportional to $T_o - T_a$ goes to the atmosphere, while the rest diffuses downward into the ocean. Both the ocean and the atmosphere are (strongly) diffusive, with the nonlinear advection terms considered as corrections. Difficulties arise when one tries to obtain a realistic surface stress distribution in an atmosphere with continually increasing temperature from pole to equator. The attempt to apply the dynamics of a laminar model is not very satisfactory. Still, it is felt that an underatanding of the laminar model, which possibly could be realized in a laboratory experiment, should come first. The preliminary study of the laminar coupled model shows noticeable feedback through the western boundary current with very short characteristic time (few weeks to few months), when scaled realistically. In this case the atmosphere has been assumed in a quasi-balanced state at every moment. The calculations will be repeated after some deficiencies in the atmospheric model (pointed out by the Geophysical Fluid Dynamics audience) have been taken care of. Calculations using a turbulent atmospheric model seem far off, as no existing analytical model predicts the dependence of the turbulence on T_a etc. The formulation of such a model, following earlier ideas by Charney, Green and others, seems to be a critical task.

---

[1] M.Rattray and P.Welander, "A Quasi-linear Model of the Combined Wind-driven and Thermohaline Circulations in Rectangular β-plan Ocean", (submitted to J.Phys.Oceanog.)

THE INERTIAL ROTATIONAL BALANCE OF STRAITS AND SILL FLOWS
(Abstract)

John A. Whitehead

Theoretical and laboratory models of certain types of rotating strait and sill flows were discussed. Specifically, a two-layer rotating fluid was considered in which the upper layer is at rest and the lower layer flows from one large basin to another via a connecting channel. The flow was assumed to be principally in a down-channel direction. The cross-channel balance was therefore geostrophic and the Bernoulli and potential vorticity equations were simplified. Use of the usual non-rotating hydraulic principle of maximum transport in flow over a weir - here the end of the channel - was then used to calculate relations between transport, rotation rate, and upstream interface height.

The results were that volume transport was proportional to the parameter group $g' h_u^2 / 2f$ in the limit of $b^2 \geq 2 g' h_u / f^2$ and volume transport was proportional to $(2/3)^{3/2} b\, g'^{1/2} (h_u - f^2 b^2 / 8 g')^{3/2}$ otherwise, where g' is reduced gravity, h_u is upstream height, b is width of the channel, and f is two times the angular rotation of the system.

Experiments were described which tested these relations favorably. A nonsteady decaying flow in the same system was analyzed similarly and also compared well with experiment, as does a flow in both layers driven by an initial density imbalance. The resulting formulae were used to predict flows through the Denmark Straits, the Straits of Gibraltar, the Anegada-Jungfern passage, and the mouth of Spencer Gulf, South Australia, and the results compared favorably with observations in the literature.